UNIVERSITY OF CALIFORNIA
RIVERSIDE

Ameliorating Auditory Hyperactivity and Improving Auditory Temporal Processing in a Mouse Model of Fragile X Syndrome by Targeting Serotonin-1A Post-Synaptic Receptors

A Dissertation submitted in partial satisfaction
of the requirements for the degree of

Doctor of Philosophy

in

Neuroscience

by

Xin Tao

June 2024

Dissertation Committee:
Dr. Khaleel A. Razak, Chairperson
Dr. Iryna M. Ethell
Dr. Edward W. Zagha

The Dissertation of Xin Tao is approved:

_____

_____

_____

Committee Chairperson

University of California, Riverside

Acknowledgements

I would like to express my profound gratitude to my PhD advisor, Dr. Khaleel Razak, for his tremendous mentorship over the past six years. Arriving in his lab as a naïve undergraduate with limited research experience, Dr. Razak exhibited immense patience and consistently inspired and challenged me to think differently. He celebrated each milestone of my PhD journey and provided encouragement during challenging times. I am also deeply thankful to my committee members, Dr. Edward Zagha and Dr. Iryna Ethell, for their invaluable support and encouragement throughout my studies.

My heartfelt thanks go to all past and present members of the Razak lab, who created a supportive and enjoyable work environment. A special thanks to Dr. Jamiela Kokash, who provided extensive guidance when I first joined the lab; to Dr. Katilynne Croom, who expertly taught me EEG surgeries and analysis techniques; to Stephen W. Brookshire and Phoebe Hsu for their assistance in cFos study. I am grateful to Dr. Michael Erickson, Dr. Melina Acosta, and Teresa Ubina for their assistance with data analysis, imaging, and RNAscope experiments, respectively.

I extend my deepest appreciation to my parents and spouse for their unconditional support over these six years. Their belief in my potential and their optimism, even when I doubted myself, have been a constant source of strength. Thank you to all the friends I made over the past six years; you all made this journey not just bearable but joyously memorable. You made me laugh even on the most challenging days.

Thank you all for being part of my story.

This dissertation is dedicated to my spouse, who always sees the best in me and inspires me to be resilient.

ABSTRACT OF THE DISSERTATION

Ameliorating Auditory Hyperactivity and Improving Auditory Temporal Processing in a Mouse Model of Fragile X Syndrome by Targeting Serotonin-1A Post-Synaptic Receptors

by

Xin Tao

Doctor of Philosophy, Graduate Program in Neuroscience
University of California, Riverside, June 2024
Dr. Khaleel A. Razak, Chairperson

Autism spectrum disorder (ASD) is a developmental condition characterized by symptoms: intellectual difficulties, motor, and language impairment, altered sensory processing, social impediments, and repetitive behaviors. Only 10-20% ASD have clear genetic causes, and fragile X syndrome (FXS) is one of them. FXS is caused by the lack of fragile X messenger ribonucleoprotein (FMRP) whose expression is transcriptionally silenced due to *Frm1* gene hypermethylation. Altered sensory processing across all sensory domains has been widely described in humans with FXS. Most noticeable alterations in auditory processing are auditory hyperactivity and impaired temporal processing. The *Fmr1* knockout (KO) mouse is a well characterized animal model for FXS studies which also shows signs of auditory hypersensitivity and impaired temporal processing: increased evoked and induced auditory responses, susceptible to audiogenic seizures (AGS), and reduced phase-locking to temporally modulated sound. The consistent manifestations of auditory hyperactivity and impaired temporal processing

between human FXS individuals and *Frm1* KO make it possible to evaluate potential FXS treatment with *Frm1* KO mice. Previous studies by others implied that enhancing serotonin signaling ameliorated auditory hyperactivity, yet they failed to pinpoint the specific serotonin receptor subtypes involved. With a more specific and highly selective post-synaptic serotonin-1A (5-HT_{1A}) receptor agonist, NLX-101, we found the AGS susceptibility in developing *Frm1* KO mice is significantly reduced, suggesting enhancing 5-HT_{1A} signaling is effective in reducing auditory hyperactivity at the behavioral level in *Frm1* KO mice. Electroencephalography (EEG) data acquired from *Frm1* KO mice following NLX-101 treatment showed that enhancing 5-HT_{1A} signaling not only reduced auditory hyperactivity at the network level but also improved temporal processing by increasing consistency of the auditory responses to temporally modulated stimuli. RNAscope results showed mRNA transcripts of 5-HT_{1A} receptors are predominately associated with non-GAD cells, implying NLX-101 may reduce auditory hyperactivity in *Frm1* KO mice by hyperpolarizing excitatory neurons through 5-HT_{1A} receptor activation.

Table of Contents

Chapter 1: Introduction

Autism spectrum disorder (ASD) is a developmental condition, characterized by symptoms including but not limited to intellectual difficulties, motor and language impairment, altered sensory processing, social impediments as well as repetitive behaviors (Lai et al., 2014). So far diagnosis for ASD is largely dependent on behavioral evaluation with only 10-20% of them having clear genetic causes (Lai et al., 2014). Fragile X syndrome (FXS) is one of them (Niu et al., 2017).

FXS is caused by lack of fragile X messenger ribonucleoprotein (FMRP) and affects approximately 1 in 4000 males and 1 in 8000 females (Hunter et al., 2014). FMRP is encoded by *Fmr1* gene, at the promotor region of which are trinucleotide CGG repeats. Normally the copy number is under 45. Full mutation is seen when the copy number exceeds 200, which leads to hypermethylation and a transcriptional silencing of the *Fmr1* gene, eventually resulting in partial or total loss of FMRP (Pieretti et al., 1991).

FMRP is an RNA binding protein (Ashley et al., 1993) and actively regulates mRNA translation (Khandjian et al., 2004). FMRP is abundant in many brain regions and interacts with various mRNAs (Brown et al., 2001). In addition to acting as translational regulator, FMRP also involves in RNA editing (Shamay-Ramot et al., 2015) and pre-mRNA splicing (Zhou et al., 2017). Loss of FMRP affects synaptogenesis by disrupting mRNA transportation and synthesis in dendritic regions, further resulting in dysregulated plasticity in response to stimuli (Dictenberg et al., 2008). More recently, FMRP was found to directly interact with ion channels and regulate their gating through translation-independent mechanism (Brown et al., 2010; Deng et al., 2013). BK channels are voltage-gated, and calcium activated potassium channels and are needed to repolarize the

membrane potential after depolarization (McManus, 1991). Lack of FMRP causes reduced calcium sensitivity in BK channels, which leads to non-fully opened channels and prolonged duration of action potential, resulting in increased neurotransmitter release (Deng et al., 2013).

Given important roles above that FMRP plays in the central nervous system, loss of FMRP leads to multiple developmental deficits (Freund et al., 1993; Maes et al., 2000; Merenstein et al., 1996). Lowest IQ was seen in human males having full mutation and full methylation of *Fmr1* compared with full mutation but partial methylation as well as those with mosaic patterns (Merenstein et al., 1996). Delayed speech and motor development has been reported and was used for one of items on the FXS early diagnosis checklist (Maes et al., 2000). Hyperactivity, anxiety, and social deficits were found to be associated with FXS in young females (Freund et al., 1993). Autistic like behaviors such as hand flapping, poor eye contact, and hand biting were also frequently seen in FXS humans (Garber et al., 2008; Kaufmann et al., 2004). Indeed, about 21%-50% of humans diagnosed with FXS have autism (Lai et al., 2014). Except for developmental deficits mentioned above, altered sensory processing in FXS has been intensively studied.

Altered sensory processing across multiple sensory modalities has been widely reported in FXS human individuals (Ethridge et al., 2016, 2019; Miller et al., 1999; Rigoulot et al., 2017; Rogers et al., 2003; D. C. Rojas et al., 2001; Van der Molen et al., 2012a, 2012b). With electrodermal responses (EDR), (Miller et al., 1999) examined evoked responses by olfactory, visual, auditory, somatosensory, and vestibular stimuli. They found FXS individuals overreact to sensory stimuli, characterized by greater

magnitude of EDR, more EDR per stimulation, longer duration of EDR and reduced habituation of EDR (Miller et al., 1999). They further pointed out responses in one sensory modality was able to predict responses in other modalities, and EDR responses are correlated with FMRP levels in individuals, which further confirmed the critical roles of FMRP in the nervous systems. Magnetoencephalography (MEG) data marked increased N100m amplitude in FXS individuals compared with typically developing controls (TDC) in response to pure tone, indicating more neurons are activated by auditory stimulus which is indictive of hyperactive auditory system (Rojas et al., 2001). Similar finding was replicated with electroencephalography (EEG). In the auditory oddball task, where a deviant sound was mixed in standard sounds, FXS individuals exhibited enhanced N1 amplitude in contrast with TDC (Van der Molen et al., 2012a). Except for enhanced responses toward auditory stimuli, FXS individuals also failed to habituate to repeated sound stimulation (Ethridge et al., 2016, 2019; Van der Molen et al., 2012b). When presented with four consecutive and identical tones, FXS individuals consistently showed elevated N1 amplitudes (Ethridge et al., 2016, 2019). Like findings in the auditory system, visual system in FXS individuals is also hyperactive (Rigoulot et al., 2017; Van der Molen et al., 2012a). In the visual oddball task where a deviant image was mixed among standard stimuli, enhanced N1 amplitude was observed in FXS individuals in comparison to TDC (Van der Molen et al., 2012a).Reduced habituation to repeated visual stimuli was also found in FXS population (Rigoulot et al., 2017). N170 is a human face sensitive component of ERP, (Rigoulot et al., 2017) found N170 component

remained high in FXS individuals when they were exposed to the identical images twice, which suggested hyperactive visual system (Rigoulot et al., 2017).

In addition to hypersensitivity across sensory modalities, increased trial-by-trial variability in sensory processing is another hallmark in humans with ASD, including FXS. Neural variability was found to be higher in young individuals and it seems to be beneficial as it is correlated with enhanced learning and expiration (Dinstein et al., 2015). However, excessive neural variability in adults instead suggests cognitive malfunction (Dinstein et al., 2015). Increased variability in sensory responses in ASD humans has been intensively studied (Dinstein et al., 2012; Haigh et al., 2016; Kovarski et al., 2019; Latinus, 2019; Milne, 2011). By applying functional magnetic resonance imaging (fMRI), (Dinstein et al., 2012) examined response reliability in ASD by testing the same individual for multiple sensory evoked responses (visual, somatosensory, and auditory) and found signal-to-noise ratio was significantly weaker in ASD compared with TDC (Dinstein et al., 2012). Similar finding was made with EEG techniques. Reduced consistency of visual evoked potentials in ASD group toward reverse pattern checkerboard was revealed by increased inter-trial variability in P100 component latencies (Kovarski et al., 2019). In auditory system, higher intra-individual variability in response to auditory stimuli was also found, marked by reduced inter-trial consistency (Ethridge et al., 2016, 2019; Latinus, 2019).

To better understand the pathology of FXS in humans, *Fmr1* KO animal models were produced by knocking out *Fmr1* gene globally. Among them, *Fmr1* KO mice are one of the most widely used models. Despite the different mechanisms that cause loss of

FMRP (in humans it is caused by transcriptional silencing, whereas in mouse it is due to missing *Fmr1* gene) (Dahlhaus, 2018), *Fmr1* KO mice successfully captured the major FXS features that have been established in humans, particularly in the sensory domains.

Fmr1 KO mice showed lager representation in the barrel cortex upon whisker deflection (Arnett et al., 2014; Juczewski et al., 2016) and lager excitatory postsynaptic potentials (EPSP) amplitudes in the primary somatosensory cortex (S1) layer 2/3 in response to hind paw tactile stimulation (Bhaskaran et al., 2023), indicating hyperactive somatosensory system. The elevated visual responses were also reported in *Fmr1* KO mice: there were significantly reduced percentage of orientation selective pyramidal neurons in the primary visual cortex (V1) layer 2/3 and they have broader tuning (Goel et al., 2018), which marked hyperactive visual cortex in *Fmr1* KO mice. Besides, *Fmr1* KO mice also showed deficits in tactile-dependent learning (Arnett et al., 2014; Juczewski et al., 2016), and exhibited delayed learning on visual discrimination task (Goel et al., 2018), suggesting altered sensory processing potentially impairs the sensory-related learning. The hyperactivity in auditory system has been studied from both single unit level (Nguyen et al., 2020; Rotschafer & Razak, 2013) and network level (Croom et al., 2023; Wen et al., 2019). At the single unit level, broadened tuning and hyper-responsiveness toward auditory stimuli were found in both auditory cortex (AC) neurons (Rotschafer & Razak, 2013) and inferior colliculus (IC) neurons ((Nguyen et al., 2020a). At the network level, hyperactivity in the auditory system was manifested by increased N1 amplitudes in event-related potentials (ERP) toward broad band noise (Croom et al., 2023; Wen et al., 2019), as well as increased non-phased locked single trial power (STP)

during silent sessions between stimulation (Jonak et al., 2020; Lovelace et al., 2018, 2020; Rais et al., 2022).

Like findings in humans with ASD, increased variability in sensory responses were also found in *Fmr1* KO mice. The whole cell recording in S1 layer 2/3 revealed increased variability in EPSP amplitudes evoked by hind paw tactile stimulation, and it correlated with variability in restring membrane potentials right before stimulation in *Fmr1* KO mice (Bhaskaran et al., 2023). In the AC, at the single unit level, increased variability was also observed regarding first spike latency in *Fmr1* KO mice (Rotschafer & Razak, 2013). At the network level, the consistency in auditory processing was evaluated by measuring inter-trial phase coherence (ITPC) in response to temporally modulated sound stimuli. Reduced ITPC has been consistently reported in *Fmr1* KO mice (Croom et al., 2023; Lovelace et al., 2018).

Consistent behavioral outputs largely rely on reliable sensory perception. Abnormal sensory processing can therefore contribute to sensory-related cognitive function (Haigh, 2018). Altered sensory processing, including sensory hyperactivity and increased variability in sensory responses, has been consistently seen in both humans with FXS and *Fmr1* KO mice. So far there is no treatment for either of them.

Serotonin singling has been suggested to be involved in ASD and FXS (Boccuto et al., 2013; Chugani, 2002; Cook & Leventhal, 1996; Hanson & Hagerman, 2014). Elevated blood serotonin level in autism was found decades ago and was regarded one of the ASD biomarkers, which was caused by elevated platelet serotonin transporter (Cook

& Leventhal, 1996). Impaired tryptophan metabolism was reported in ASD patients with or without FXS (Boccuto et al., 2013), suggesting an altered serotonin signaling in ASD because tryptophan is a precursor of serotonin. Gene analysis revealed impaired tryptophan metabolism was due to reduced expression of tryptophan transporters and tryptophan hydroxylase (an enzyme required for serotonin synthesis) (Boccuto et al., 2013). Serotonin plays critical roles in development (Gaspar et al., 2003). Indeed, humans undergo a period of high brain serotonin synthesis capacity during childhood, specifically before age 5, and that this developmental process is disrupted in autistic children (Chugani et al., 1999). So far, there has been at least 15 serotonin receptor subtypes reported, suggesting serotonin exerts various functions during different developmental stages by activating different receptor subtypes (Gaspar et al., 2003). Early disturbance of serotonin homeostasis can lead to circuit miswiring and eventually lead to severe consequences in adulthood (Gross et al., 2002). Mouse work showed that expression of serotonin-1A (5-HT_{1A}) receptor during early development, rather than adulthood, is necessary to establish normal anxiety behavior in adulthood (Gross et al., 2002). Findings in human and animal models above prompt serotonin intervention during early development in FXS or ASD generally (Hanson & Hagerman, 2014).

Indeed, administration of FDA approved selective serotonin reuptake inhibitor (SSRI) in young children with ASD and/ or FXS has shown various improvement (Greiss Hess et al., 2016a; Indah Winarni et al., 2012; Winarni et al., 2012). In two case studies, two young children with FXS were treated with a combination of three medications: Memantine (to reduce glutamatergic signaling), Sertraline (to enhance serotonin

signaling), and Minocycline (to reduce MMP-9). Together with intensive education at early age, significant improvement on cognitive test was seen in both young children with FXS (Winarni et al., 2012). In a retrospective review chart study (not strict clinical trial and administration method differs among groups), (Indah Winarni et al., 2012) found low dose of Sertraline treatment in young children with FXS (< 5 yrs. old) is beneficial in both expressive and receptive language development. Such potential benefits of Sertraline were further characterized by a controlled clinical trial (Greiss Hess et al., 2016). Contradictory to the finding by (Indah Winarni et al., 2012), long-term administration of Sertraline in young children with FXS showed no significant effect on expressive language improvement (Greiss Hess et al., 2016). However, long-term Sertraline treatment showed improvement in motor, visual processing as well as social ability (Greiss Hess et al., 2016). Another randomized and controlled clinic trial probed the potential beneficial effects of Sertraline in young children with ASD but no FXS and found no benefits in language ability, visual or motor perception (Potter et al., 2019). The discrepancies can be explained by at least two possibilities: 1) it is possible that Sertraline treatment is specific to FXS but no other ASD; 2) Sertraline, as an SSRI, increases serotonin level in the system nonselective, and long-term exposure of exogenous serotonin may induce down regulation of targeted serotonin receptors.

Given the mixed results in human studies with SSRI, the potential benefits of boosting serotonin signaling has been explored with mouse models. One of the most robust expressions of auditory hyperactivity is audiogenic seizures (AGS), a generalized convulsive seizure evoked by loud sound, in *Fmr1* KO mice (Chen & Toth, 2001;

Musumeci et al., 2000). Whether humans with FXS display AGS has not been directly tested, however, FXS individuals do show spontaneous seizures (Berry-Kravis, 2007), which marked the hyperactive cortical network in FXS. In the previous literature, it has been shown that enhancing serotonin signaling by SSRI [Fluoxetine: (Tupal & Faingold, 2006); Sertraline: (Heydari & Davoudi, 2017)] or by manipulating serotonergic neurons (Buchanan et al., 2014; Zhang et al., 2018) significantly increased seizure threshold in various animal models. Despite of exciting results, none of above was able to narrow down the serotonin receptor subtype(s) involved. A more direct effect of serotonin in *Fmr1* KO mice was done by (Armstrong et al., 2020). They found by activating 5-HT_{1A}R eceptors with a partial agonist FPT ((S)-5-(2′-Fluorophenyl)-N,N-dimethyl-1,2,3,4-tetrahydronaphthalen2-amine) significantly reduced AGS-induced death rate (Armstrong et al., 2020). However, FPT also activates 5-HT_{2C} and 5-HT_7 receptor (Armstrong et al., 2020), leaving it unresolved that which serotonin receptor subtype is the major player in reducing auditory hyperactivity in *Fmr1* KO.

A discovery of a novel 5-HT_{1A}R eceptor agonist, NLX-101 gives an opportunity to overcome the difficulty. NLX-101, also known as F15599, is a highly selective and post-synaptic 5-HT_{1A} receptor agonist with selectivity much higher than 8-OH DPAT (a widely used 5-HT_{1A} receptor agonist) (Newman-Tancredi et al., 2009).

By employing NLX-101, I explored the potential functions of 5-HT_{1A} receptor signaling in AGS in *Fmr1* KO mice in Chapter 2 (Acute and Repeated Administration of NLX-101, a Selective Serotonin-1A Receptor Biased Agonist, Reduces Audiogenic

Seizures in Developing *Fmr1* Knockout Mice). Briefly, I found acute and repeated application of NLX-101 in juvenile *Fmr1* KO mice effectively protected them from having AGS. Such effect was not affected by repeated exposures. Besides, we also found females *Fmr1* KO mice were less susceptible to AGS compared with male counterparts, and they benefit from NLX-101 at lower dosage of NLX-101. These two observations suggest a potential sex difference following NLX-101 treatment.

According to the finding of (Hurley, 2007), application of 8-OH DAPT impacted firing patterns in IC neurons by shortening the response window: at the population level, neurons with longer latencies are suppressed; for an individual neuron, the later spikes are more suppressed than initial spikes (Hurley, 2007). Such finding suggests 5-HT_{1A} modulation may be involved in temporal processing. So far, it has not been reported whether serotonin treatment, or specifically 5-HT_{1A} targeted treatment will improve temporal processing. In Chapter 3 (Acute Administration of Serotonin 1A Receptor Agonist NLX-101 Improves Auditory) I explored if NLX-101 treatment can normalize abnormal EEG phenotypes (increased evoked N1 amplitude in response to broad band noise, increased STP during silent session between stimuli, and reduced ITPC toward temporally modulated sound) seen in *Fmr1* KO mice. Briefly, I found acute and systemic administration of NLX-101 at both P21 and P30 improved temporal processing in *Fmr1* KO mice. I also found a significant reduction in STP but only at P30 not P21. Such finding suggests there might be an age-dependent effect of NLX-101 treatment.

Given the observed sex and age differences following NLX-101 treatment in Chapter 2 and 3 respectively, In Chapter 4, I investigated if these differences can be

traced back to different expression levels of 5-HT_{1A} receptor mRNA in the AC and IC across sex and age by performing RNAscope. Briefly, I did not find any sex effect on the expression level of 5-HT_{1A} receptor mRNA. However, the expression level of 5-HT_{1A} receptor mRNA is significantly higher at P30 than P21 in all examined AC layers. Plus, KO surprisingly showed higher expression level of 5-HT_{1A} receptor mRNA than WT in the AC layer2/3.

References

Armstrong, J. L., Casey, A. B., Saraf, T. S., Mukherjee, M., Booth, R. G., & Canal, C. E. (2020). (*S*)-5-(2′-Fluorophenyl)- *N* , *N* -dimethyl-1,2,3,4-tetrahydronaphthalen-2-amine, a Serotonin Receptor Modulator, Possesses Anticonvulsant, Prosocial, and Anxiolytic-like Properties in an *Fmr1* Knockout Mouse Model of Fragile X Syndrome and Autism Spectrum Disorder. *ACS Pharmacology & Translational Science*, *3*(3), 509–523. https://doi.org/10.1021/acsptsci.9b00101

Arnett, M. T., Herman, D. H., & McGee, A. W. (2014). Deficits in Tactile Learning in a Mouse Model of Fragile X Syndrome. *PLoS ONE*, *9*(10), e109116. https://doi.org/10.1371/journal.pone.0109116

Ashley, C. T., Wilkinson, K. D., Reines, D., & Warren, S. T. (1993). FMR1 Protein: Conserved RNP Family Domains and Selective RNA Binding. *Science*, *262*(5133), 563–566. https://doi.org/10.1126/science.7692601

Berry-Kravis, E. (2007). Epilepsy in fragile X syndrome. *Developmental Medicine & Child Neurology*, *44*(11), 724–728. https://doi.org/10.1111/j.1469-8749.2002.tb00277.x

Bhaskaran, A. A., Gauvrit, T., Vyas, Y., Bony, G., Ginger, M., & Frick, A. (2023). Endogenous noise of neocortical neurons correlates with atypical sensory response variability in the Fmr1−/y mouse model of autism. *Nature Communications*, *14*(1), 7905. https://doi.org/10.1038/s41467-023-43777-z

Boccuto, L., Chen, C.-F., Pittman, A. R., Skinner, C. D., McCartney, H. J., Jones, K., Bochner, B. R., Stevenson, R. E., & Schwartz, C. E. (2013). Decreased

tryptophan metabolism in patients with autism spectrum disorders. *Molecular Autism*, *4*(1), 16. https://doi.org/10.1186/2040-2392-4-16

Brown, M. R., Kronengold, J., Gazula, V.-R., Chen, Y., Strumbos, J. G., Sigworth, F. J., Navaratnam, D., & Kaczmarek, L. K. (2010). Fragile X mental retardation protein controls gating of the sodium-activated potassium channel Slack. *Nature Neuroscience*, *13*(7), 819–821. https://doi.org/10.1038/nn.2563

Brown, V., Jin, P., Ceman, S., Darnell, J. C., O'Donnell, W. T., Tenenbaum, S. A., Jin, X., Feng, Y., Wilkinson, K. D., Keene, J. D., Darnell, R. B., & Warren, S. T. (2001). Microarray Identification of FMRP-Associated Brain mRNAs and Altered mRNA Translational Profiles in Fragile X Syndrome. *Cell*, *107*(4), 477–487. https://doi.org/10.1016/S0092-8674(01)00568-2

Buchanan, G. F., Murray, N. M., Hajek, M. A., & Richerson, G. B. (2014). Serotonin neurones have anti-convulsant effects and reduce seizure-induced mortality. *The Journal of Physiology*, *592*(19), 4395–4410. https://doi.org/10.1113/jphysiol.2014.277574

Chen, L., & Toth, M. (2001). Fragile X mice develop sensory hyperreactivity to auditory stimuli. *Neuroscience*, *103*(4), 1043–1050. https://doi.org/10.1016/S0306-4522(01)00036-7

Chugani, D. C. (2002). Role of altered brain serotonin mechanisms in autism. *Molecular Psychiatry*, *7*(S2), S16–S17. https://doi.org/10.1038/sj.mp.4001167

Chugani, D. C., Muzik, O., Behen, M., Rothermel, R., Janisse, J. J., Lee, J., & Chugani, H. T. (1999). Developmental changes in brain serotonin synthesis capacity in

autistic and nonautistic children. *Annals of Neurology*, *45*(3), 287–295. https://doi.org/10.1002/1531-8249(199903)45:3<287::AID-ANA3>3.0.CO;2-9

Cook, E. H., & Leventhal, B. L. (1996). *The serotonin system in autism*. Current opinion in pediatrics.

Croom, K., Rumschlag, J. A., Erickson, M. A., Binder, D. K., & Razak, K. A. (2023). Developmental delays in cortical auditory temporal processing in a mouse model of Fragile X syndrome. *Journal of Neurodevelopmental Disorders*, *15*(1), 23. https://doi.org/10.1186/s11689-023-09496-8

Dahlhaus, R. (2018). Of Men and Mice: Modeling the Fragile X Syndrome. *Frontiers in Molecular Neuroscience*, *11*, 41. https://doi.org/10.3389/fnmol.2018.00041

Deng, P.-Y., Rotman, Z., Blundon, J. A., Cho, Y., Cui, J., Cavalli, V., Zakharenko, S. S., & Klyachko, V. A. (2013). FMRP Regulates Neurotransmitter Release and Synaptic Information Transmission by Modulating Action Potential Duration via BK Channels. *Neuron*, *77*(4), 696–711. https://doi.org/10.1016/j.neuron.2012.12.018

Dictenberg, J. B., Swanger, S. A., Antar, L. N., Singer, R. H., & Bassell, G. J. (2008). A Direct Role for FMRP in Activity-Dependent Dendritic mRNA Transport Links Filopodial-Spine Morphogenesis to Fragile X Syndrome. *Developmental Cell*, *14*(6), 926–939. https://doi.org/10.1016/j.devcel.2008.04.003

Dinstein, I., Heeger, D. J., & Behrmann, M. (2015). Neural variability: Friend or foe? *Trends in Cognitive Sciences*, *19*(6), 322–328. https://doi.org/10.1016/j.tics.2015.04.005

Dinstein, I., Heeger, D. J., Lorenzi, L., Minshew, N. J., Malach, R., & Behrmann, M. (2012). Unreliable Evoked Responses in Autism. *Neuron*, *75*(6), 981–991. https://doi.org/10.1016/j.neuron.2012.07.026

Ethridge, L. E., De Stefano, L. A., Schmitt, L. M., Woodruff, N. E., Brown, K. L., Tran, M., Wang, J., Pedapati, E. V., Erickson, C. A., & Sweeney, J. A. (2019). Auditory EEG Biomarkers in Fragile X Syndrome: Clinical Relevance. *Frontiers in Integrative Neuroscience*, *13*, 60. https://doi.org/10.3389/fnint.2019.00060

Ethridge, L. E., White, S. P., Mosconi, M. W., Wang, J., Byerly, M. J., & Sweeney, J. A. (2016). Reduced habituation of auditory evoked potentials indicate cortical hyper-excitability in Fragile X Syndrome. *Translational Psychiatry*, *6*(4), e787–e787. https://doi.org/10.1038/tp.2016.48

Freund, L. S., Reiss, A. L., & Abrams, M. T. (1993). Psychiatric disorders associated with fragile X in the young female. *Pediatrics*, *91*(2), 321–329.

Garber, K. B., Visootsak, J., & Warren, S. T. (2008). Fragile X syndrome. *European Journal of Human Genetics*, *16*(6), 666–672. https://doi.org/10.1038/ejhg.2008.61

Gaspar, P., Cases, O., & Maroteaux, L. (2003). The developmental role of serotonin: News from mouse molecular genetics. *Nature Reviews Neuroscience*, *4*(12), 1002–1012. https://doi.org/10.1038/nrn1256

Goel, A., Cantu, D. A., Guilfoyle, J., Chaudhari, G. R., Newadkar, A., Todisco, B., de Alba, D., Kourdougli, N., Schmitt, L. M., Pedapati, E., Erickson, C. A., & Portera-Cailliau, C. (2018). Impaired perceptual learning in a mouse model of Fragile X syndrome is mediated by parvalbumin neuron dysfunction and is

reversible. *Nature Neuroscience*, *21*(10), 1404–1411. https://doi.org/10.1038/s41593-018-0231-0

Greiss Hess, L., Fitzpatrick, S. E., Nguyen, D. V., Chen, Y., Gaul, K. N., Schneider, A., Lemons Chitwood, K., Eldeeb, M. A. A. A., Polussa, J., Hessl, D., Rivera, S., & Hagerman, R. J. (2016). A Randomized, Double-Blind, Placebo-Controlled Trial of Low-Dose Sertraline in Young Children With Fragile X Syndrome. *Journal of Developmental & Behavioral Pediatrics*, *37*(8), 619–628. https://doi.org/10.1097/DBP.0000000000000334

Gross, C., Zhuang, X., Stark, K., Ramboz, S., Oosting, R., Kirby, L., Santarelli, L., Beck, S., & Hen, R. (2002). Serotonin1A receptor acts during development to establish normal anxiety-like behaviour in the adult. *Nature*, *416*(6879), 396–400. https://doi.org/10.1038/416396a

Haigh, S. M. (2018). Variable sensory perception in autism. *European Journal of Neuroscience*, *47*(6), 602–609. https://doi.org/10.1111/ejn.13601

Haigh, S. M., Minshew, N., Heeger, D. J., Dinstein, I., & Behrmann, M. (2016). Over-Responsiveness and Greater Variability in Roughness Perception in Autism. *Autism Research*, *9*(3), 393–402. https://doi.org/10.1002/aur.1505

Hanson, A. C., & Hagerman, R. J. (2014). Serotonin dysregulation in Fragile X Syndrome: Implications for treatment. *Intractable & Rare Diseases Research*, *3*(4), 110–117. https://doi.org/10.5582/irdr.2014.01027

Heydari, A., & Davoudi, S. (2017). The effect of sertraline and 8-OH-DPAT on the PTZ_induced seizure threshold: Role of the nitrergic system. *Seizure*, *45*, 119–124. https://doi.org/10.1016/j.seizure.2016.12.005

Holley, A. J., Shedd, A., Boggs, A., Lovelace, J., Erickson, C., Gross, C., Jankovic, M., Razak, K., Huber, K., & Gibson, J. R. (2022). A sound-driven cortical phase-locking change in the Fmr1 KO mouse requires Fmr1 deletion in a subpopulation of brainstem neurons. *Neurobiology of Disease*, *170*, 105767. https://doi.org/10.1016/j.nbd.2022.105767

Hunter, J., Rivero-Arias, O., Angelov, A., Kim, E., Fotheringham, I., & Leal, J. (2014). Epidemiology of fragile X syndrome: A systematic review and meta-analysis. *American Journal of Medical Genetics Part A*, *164*(7), 1648–1658. https://doi.org/10.1002/ajmg.a.36511

Hurley, L. M. (2007). Activation of the serotonin 1A receptor alters the temporal characteristics of auditory responses in the inferior colliculus. *Brain Research*, *1181*, 21–29. https://doi.org/10.1016/j.brainres.2007.08.053

Indah Winarni, T., Chonchaiya, W., Adams, E., Au, J., Mu, Y., Rivera, S. M., Nguyen, D. V., & Hagerman, R. J. (2012). Sertraline May Improve Language Developmental Trajectory in Young Children with Fragile X Syndrome: A Retrospective Chart Review. *Autism Research and Treatment*, *2012*, 1–8. https://doi.org/10.1155/2012/104317

Jonak, C. R., Lovelace, J. W., Ethell, I. M., Razak, K. A., & Binder, D. K. (2020). Multielectrode array analysis of EEG biomarkers in a mouse model of Fragile X

Syndrome. *Neurobiology of Disease*, *138*, 104794. https://doi.org/10.1016/j.nbd.2020.104794

Juczewski, K., von Richthofen, H., Bagni, C., Celikel, T., Fisone, G., & Krieger, P. (2016). Somatosensory map expansion and altered processing of tactile inputs in a mouse model of fragile X syndrome. *Neurobiology of Disease*, *96*, 201–215. https://doi.org/10.1016/j.nbd.2016.09.007

Kaufmann, W. E., Cortell, R., Kau, A. S. M., Bukelis, I., Tierney, E., Gray, R. M., Cox, C., Capone, G. T., & Stanard, P. (2004). Autism spectrum disorder in fragile X syndrome: Communication, social interaction, and specific behaviors. *American Journal of Medical Genetics Part A*, *129A*(3), 225–234. https://doi.org/10.1002/ajmg.a.30229

Khandjian, E. W., Huot, M.-E., Tremblay, S., Davidovic, L., Mazroui, R., & Bardoni, B. (2004). Biochemical evidence for the association of fragile X mental retardation protein with brain polyribosomal ribonucleoparticles. *Proceedings of the National Academy of Sciences*, *101*(36), 13357–13362. https://doi.org/10.1073/pnas.0405398101

Kovarski, K., Malvy, J., Khanna, R. K., Arsène, S., Batty, M., & Latinus, M. (2019). Reduced visual evoked potential amplitude in autism spectrum disorder, a variability effect? *Translational Psychiatry*, *9*(1), 341. https://doi.org/10.1038/s41398-019-0672-6

Lai, M.-C., Lombardo, M. V., & Baron-Cohen, S. (2014). Autism. *The Lancet*, *383*(9920), 896–910. https://doi.org/10.1016/S0140-6736(13)61539-1

Latinus, M. (2019). Atypical Sound Perception in ASD Explained by Inter-Trial (In)consistency in EEG. *Frontiers in Psychology*, *10*.

Lovelace, J. W., Ethell, I. M., Binder, D. K., & Razak, K. A. (2018). Translation-relevant EEG phenotypes in a mouse model of Fragile X Syndrome. *Neurobiology of Disease*, *115*, 39–48. https://doi.org/10.1016/j.nbd.2018.03.012

Lovelace, J. W., Rais, M., Palacios, A. R., Shuai, X. S., Bishay, S., Popa, O., Pirbhoy, P. S., Binder, D. K., Nelson, D. L., Ethell, I. M., & Razak, K. A. (2020). Deletion of Fmr1 from Forebrain Excitatory Neurons Triggers Abnormal Cellular, EEG, and Behavioral Phenotypes in the Auditory Cortex of a Mouse Model of Fragile X Syndrome. *Cerebral Cortex*, *30*(3), 969–988. https://doi.org/10.1093/cercor/bhz141

Maes, B., Fryns, J. P., Ghesquière, P., & Borghgraef, M. (2000). Phenotypic Checklist to Screen for Fragile X Syndrome in People With Mental Retardation. *Mental Retardation*, *38*(3), 207–215. https://doi.org/10.1352/0047-6765(2000)038<0207:PCTSFF>2.0.CO;2

McManus, O. B. (1991). Calcium-activated potassium channels: Regulation by calcium. *Journal of Bioenergetics and Biomembranes*, *23*(4), 537–560. https://doi.org/10.1007/BF00785810

Merenstein, S. A., Sobesky, W. E., Taylor, A. K., Riddle, J. E., Tran, H. X., & Hagerman, R. J. (1996). Molecular-clinical correlations in males with an expanded FMR1 mutation. *American Journal of Medical Genetics*, *64*(2), 388–394.

https://doi.org/10.1002/(SICI)1096-8628(19960809)64:2<388::AID-AJMG31>3.0.CO;2-9

Miller, L. J., McIntosh, D. N., McGrath, J., Shyu, V., Lampe, M., Taylor, A. K., Tassone, F., Neitzel, K., Stackhouse, T., & Hagerman, R. J. (1999). Electrodermal responses to sensory stimuli in individuals with fragile X syndrome: A preliminary report. *American Journal of Medical Genetics*, *83*(4), 268–279. https://doi.org/10.1002/(SICI)1096-8628(19990402)83:4<268::AID-AJMG7>3.0.CO;2-K

Milne, E. (2011). Increased Intra-Participant Variability in Children with Autistic Spectrum Disorders: Evidence from Single-Trial Analysis of Evoked EEG. *Frontiers in Psychology*, *2*. https://doi.org/10.3389/fpsyg.2011.00051

Musumeci, S. A., Bosco, P., Calabrese, G., Bakker, C., De Sarro, G. B., Elia, M., Ferri, R., & Oostra, B. A. (2000). Audiogenic Seizures Susceptibility in Transgenic Mice with Fragile X Syndrome. *Epilepsia*, *41*(1), 19–23. https://doi.org/10.1111/j.1528-1157.2000.tb01499.x

Newman-Tancredi, A., Martel, J.-C., Assié, M.-B., Buritova, J., Lauressergues, E., Cosi, C., Heusler, P., Bruins Slot, L., Colpaert, F., Vacher, B., & Cussac, D. (2009). Signal transduction and functional selectivity of F15599, a preferential post-synaptic 5-HT $_{1A}$ receptor agonist. *British Journal of Pharmacology*, *156*(2), 338–353. https://doi.org/10.1111/j.1476-5381.2008.00001.x

Nguyen, A. O., Binder, D. K., Ethell, I. M., & Razak, K. A. (2020). Abnormal development of auditory responses in the inferior colliculus of a mouse model of

Fragile X Syndrome. *Journal of Neurophysiology*, *123*(6), 2101–2121. https://doi.org/10.1152/jn.00706.2019

Niu, M., Han, Y., Dy, A. B. C., Du, J., Jin, H., Qin, J., Zhang, J., Li, Q., & Hagerman, R. J. (2017). Autism Symptoms in Fragile X Syndrome. *Journal of Child Neurology*, *32*(10), 903–909. https://doi.org/10.1177/0883073817712875

Pieretti, M., Zhang, F., Fu, Y.-H., Warren, S. T., Oostra, B. A., Caskey, C. T., & Nelson, D. L. (1991). Absence of expression of the *FMR-1* gene in fragile X syndrome. *Cell*, *66*(4), 817–822. https://doi.org/10.1016/0092-8674(91)90125-I

Potter, L. A., Scholze, D. A., Biag, H. M. B., Schneider, A., Chen, Y., Nguyen, D. V., Rajaratnam, A., Rivera, S. M., Dwyer, P. S., Tassone, F., Al Olaby, R. R., Choudhary, N. S., Salcedo-Arellano, M. J., & Hagerman, R. J. (2019). A Randomized Controlled Trial of Sertraline in Young Children With Autism Spectrum Disorder. *Frontiers in Psychiatry*, *10*, 810. https://doi.org/10.3389/fpsyt.2019.00810

Rais, M., Lovelace, J. W., Shuai, X. S., Woodard, W., Bishay, S., Estrada, L., Sharma, A. R., Nguy, A., Kulinich, A., Pirbhoy, P. S., Palacios, A. R., Nelson, D. L., Razak, K. A., & Ethell, I. M. (2022). Functional consequences of postnatal interventions in a mouse model of Fragile X syndrome. *Neurobiology of Disease*, *162*, 105577. https://doi.org/10.1016/j.nbd.2021.105577

Rigoulot, S., Knoth, I. S., Lafontaine, M., Vannasing, P., Major, P., Jacquemont, S., Michaud, J. L., Jerbi, K., & Lippé, S. (2017). Altered visual repetition suppression in Fragile X Syndrome: New evidence from ERPs and oscillatory activity.

International Journal of Developmental Neuroscience, *59*(1), 52–59. https://doi.org/10.1016/j.ijdevneu.2017.03.008

Rogers, S. J., Hepburn, S., & Wehner, E. (2003). Parent Reports of Sensory Symptoms in Toddlers with Autism and Those with Other Developmental Disorders. *Journal of Autism and Developmental Disorders*, *33*(6), 631–642. https://doi.org/10.1023/B:JADD.0000006000.38991.a7

Rojas, D. C., Benkers, T. L., Rogers, S. J., Teale, P. D., & Reite, M. L. (2001). *Auditory evoked magnetic Æelds in adults with fragile X syndrome*. 4.

Rotschafer, S., & Razak, K. (2013). Altered auditory processing in a mouse model of fragile X syndrome. *Brain Research*, *1506*, 12–24. https://doi.org/10.1016/j.brainres.2013.02.038

Shamay-Ramot, A., Khermesh, K., Porath, H. T., Barak, M., Pinto, Y., Wachtel, C., Zilberberg, A., Lerer-Goldshtein, T., Efroni, S., Levanon, E. Y., & Appelbaum, L. (2015). Fmrp Interacts with Adar and Regulates RNA Editing, Synaptic Density and Locomotor Activity in Zebrafish. *PLOS Genetics*, *11*(12), e1005702. https://doi.org/10.1371/journal.pgen.1005702

Tupal, S., & Faingold, C. L. (2006). Evidence Supporting a Role of Serotonin in Modulation of Sudden Death Induced by Seizures in DBA/2 Mice. *Epilepsia*, *47*(1), 21–26. https://doi.org/10.1111/j.1528-1167.2006.00365.x

Van der Molen, M. J. W., Van der Molen, M. W., Ridderinkhof, K. R., Hamel, B. C. J., Curfs, L. M. G., & Ramakers, G. J. A. (2012a). Auditory and visual cortical activity during selective attention in fragile X syndrome: A cascade of processing

deficiencies. *Clinical Neurophysiology*, *123*(4), 720–729. https://doi.org/10.1016/j.clinph.2011.08.023

Van der Molen, M. J. W., Van der Molen, M. W., Ridderinkhof, K. R., Hamel, B. C. J., Curfs, L. M. G., & Ramakers, G. J. A. (2012b). Auditory change detection in fragile X syndrome males: A brain potential study. *Clinical Neurophysiology*, *123*(7), 1309–1318. https://doi.org/10.1016/j.clinph.2011.11.039

Wen, T. H., Lovelace, J. W., Ethell, I. M., Binder, D. K., & Razak, K. A. (2019). Developmental Changes in EEG Phenotypes in a Mouse Model of Fragile X Syndrome. *Neuroscience*, *398*, 126–143. https://doi.org/10.1016/j.neuroscience.2018.11.047

Winarni, T. I., Schneider, A., Borodyanskara, M., & Hagerman, R. J. (2012). Early Intervention Combined with Targeted Treatment Promotes Cognitive and Behavioral Improvements in Young Children with Fragile X Syndrome. *Case Reports in Genetics*, *2012*, 1–4. https://doi.org/10.1155/2012/280813

Zhang, H., Zhao, H., Zeng, C., Van Dort, C., Faingold, C. L., Taylor, N. E., Solt, K., & Feng, H.-J. (2018). Optogenetic activation of 5-HT neurons in the dorsal raphe suppresses seizure-induced respiratory arrest and produces anticonvulsant effect in the DBA/1 mouse SUDEP model. *Neurobiology of Disease*, *110*, 47–58. https://doi.org/10.1016/j.nbd.2017.11.003

Zhou, L.-T., Ye, S.-H., Yang, H.-X., Zhou, Y.-T., Zhao, Q.-H., Sun, W.-W., Gao, M.-M., Yi, Y.-H., & Long, Y.-S. (2017). A novel role of fragile X mental retardation

protein in pre-mRNA alternative splicing through RNA-binding protein 14. *Neuroscience*, *349*, 64–75. https://doi.org/10.1016/j.neuroscience.2017.02.044

Chapter 2: Acute and Repeated Administration of NLX-101, a Selective Serotonin-1A Receptor Biased Agonist, Reduces Audiogenic Seizures in Developing *Fmr1* Knockout Mice

Abstract

Fragile X syndrome (FXS) is caused by the lack of fragile X messenger ribonucleoprotein (FMRP) and is a leading known genetic cause of autism spectrum disorders (ASD) and intellectual disability. One of the most debilitating phenotypes of FXS is sensory hypersensitivity that manifests strongly in the auditory domain and may lead to delayed language and high anxiety. The mouse model of FXS, the *Fmr1* KO mouse, also shows auditory hypersensitivity, an extreme form of which is seen as audiogenic seizures (AGS). AGS are general convulsive seizures induced by loud sound that led to lethality. Previous studies have shown the midbrain inferior colliculus (IC) is critically involved in generating AGS and IC neurons are hyperactive in developing *Fmr1* KO mice. Serotonin receptor-1A (5-HT_{1A}) activation reduces IC neuronal activity. Therefore, we tested whether 5-HT_{1A} activation is sufficient to reduce AGS in *Fmr1* KO mice. A selective and post-synaptic 5-HT_{1A} receptor biased agonist, NLX-101 (0.6, 1.2, 1.8 or 2.4 mg/kg, i.p.) was administered to *Fmr1* KO mice 15 mins before AGS induction. Whereas the 0.6 mg/kg dose was ineffective in reducing AGS, the 1.2, 1.8 and 2.4 mg/kg doses of NLX-101 dose-dependently and dramatically reduced seizures and increased mouse survival probability from AGS. Treatment with a combination of NLX-101 and 5-HT_{1A} antagonists prevented the protective effects of NLX-101, indicating that NLX-101 acts selectively through 5-HT_{1A} receptor to reduce AGS. NLX-101 (1.8 mg/kg IP) was still strongly effective in reducing AGS even after repeated administration over 5 days, suggesting a lack of tachyphylaxis to the effects of the compound. Our data also indicates sex differences in AGS susceptibility and dose-dependent response

characteristics of NLX-101. Together, these studies point to a promising treatment option specifically targeting post-synaptic 5-HT_{1A} receptor to reduce auditory hypersensitivity, and potentially other forms of sensory deficits in FXS.

2.1 Introduction

Fragile X Syndrome (FXS) is an inherited autism spectrum disorder (ASD) caused by the lack of fragile X messenger ribonucleoprotein (FMRP) and affects approximately 1 in 4000 males and 1 in 8000 females (Dombrowski et al., 2002; Rousseau et al., 1995). FMRP is expressed from the *Fmr1* gene, at the promotor region of which are several CGG trinucleotide repeats. The full mutation occurs when the CGG repeat number exceeds 200, leading to transcriptional silencing of the *Fmr1* gene and the loss of FMRP (Goodlin-Jones et al., 2004). Children with FXS show cognitive deficits, anxiety, hyperactivity, intellectual disabilities, seizure susceptibility and sensory hypersensitivity (Greiss Hess et al. 2016; Hagerman and Hagerman 2002). Strong and consistent auditory hypersensitivity impairs daily functioning and may lead to delayed language, high anxiety and social impairments in FXS. Currently, there are no effective treatments to reduce sensory hypersensitivity in FXS, or other forms of ASD.

The *Fmr1* knockout (KO) mouse satisfies multiple validity requirements to serve as a useful animal model of FXS. Importantly, *Fmr1* KO mice also show auditory hypersensitivity, providing a translation-relevant basic sensory phenotype to explore circuit deficits and treatment options in FXS. An extreme manifestation of auditory

hypersensitivity in the *Fmr1* KO mice is audiogenic seizures (AGS), one kind of generalized convulsive seizures induced by a loud sound (Chen & Toth, 2001). The midbrain, especially the inferior colliculus (IC), is involved in the generation of AGS in rodents (Faingold, 2004). The underlying causes of AGS in *Fmr1* KO mice are only beginning to be understood. The IC in *Fmr1* KO mice is hyperresponsive to acoustic stimulus when compared to the WT controls during the developmental time period when the mice are most sensitive to AGS (Nguyen et al., 2020). Conditional deletion of *Fmr1* in vGLUT2-containing glutamatergic neurons in the midbrain/brainstem is necessary and sufficient to induce AGS phenotype; and conditional expression of *Fmr1* in vGLUT2-containing glutamatergic neurons in the IC ameliorates AGS responses (Gonzalez et al., 2019). These data strongly suggest that abnormal responsivity of IC neurons plays a critical role in AGS phenotype in the *Fmr1* KO mouse.

Activation of 5-HT_{1A} receptor in the IC can reduce sound evoked responses (Hurley 2006, 2007) implicating a potentially useful target to reduce auditory hypersensitivity in *Fmr1* KO mice. Consistent with this notion, application of (S)-5-(2'-fluorophenyl)-N,N-dimethyl-1,2,3,4-tetrahydronaphthalen-2-amine (FPT) blocks stereotypic motor behavior and reduces AGS in *Fmr1* KO mice (Armstrong et al., 2020; Canal et al., 2015). Given that FPT is a partial agonist for 5-HT_{1A}, 5-HT_{2C} and 5-HT_7 receptors, the receptor specificity of the effect on AGS is unclear. In addition, non-biased agonists can activate both pre- and post-synaptic serotonin receptors and may limit a mechanistic understanding of actions.

To test the hypothesis that modulation of 5-HT_{1A} receptor is sufficient to reduce auditory hypersensitivity, we tested a specific and biased agonist of 5-HT_{1A} receptor, NLX-101 (also known as F15599). NLX-101 has much higher selectivity for 5-HT_{1A} receptor than the prototypical agonist, 8-OH DPAT, and it preferentially acts on post-synaptic receptors and much less on serotoninergic neurons (Lladó-Pelfort et al., 2010; Newman-Tancredi et al., 2009, 2022) enabling us to narrow down the contribution of serotonin receptors in different brain regions. Both male and female *Fmr1* FVB KO mice (P21-P23) were tested to determine sex differences of 5-HT_{1A} modulation (Armstrong et al., 2020). Data show a strong beneficial effect of NLX-101 on AGS, which is abolished by prior administration of 5-HT_{1A} receptor antagonists. We also observed an increased susceptibility of males, compared to females to AGS, even though all mice were global *Fmr1* KO mice. NLX-101 reduces AGS in females at a lower dose than in males. Protective effects of chronic administration of NLX-101 for 5 days before AGS induction suggests a lack of receptor tolerance build-up for this drug. These data suggest modulation of 5-HT_{1A} receptor as a target for auditory hypersensitivity in children with FXS.

2.2 Methods

2.2.1 Mice

All protocols used in this study were approved by the Institutional Animal Care and Use Committee (IACUC). Breeding pairs of FVB.129P2−Pde6b+Tyrc-ch/AntJ

(Wild-type, WT) and FVB.129P2−Fmr1tm1Cgr/J (*Fmr1* Knock-out, KO) were obtained from Jackson Laboratories and bred in-house at the University of California, Riverside. The mice received *ad libitum* standard lab chow and water. Cages were changed once a week, and the light-dark cycle was on a 12:12 hour cycle. Mice were weaned at P21, and all mice in the AGS experiments were between postnatal day (P) 21 to P23. This study only used *Fmr1* KO mice, as WT mice do not show AGS in our protocol. Both male and female mice were tested, unless stated otherwise.

2.2.2 Drug administration

NLX-101 (also known as F-15599 - (3-Chloro-4-fluorophenyl-(4-fluoro-4-{[(5-methylpyri- midin-2-ylmethyl)-amino]-methyl}-piperidin-1-yl)-methane-one), is a potent and selective 5-HT_{1A} receptor agonist, which primarily acts on post-synaptic 5-HT_{1A} receptor (Newman-Tancredi et al. 2022). NLX-101 was provided as a gift from Neurolixis, Inc. The drug was dissolved in sterile physiological saline and administered (i.p.) at a dose of 2.4 mg/kg, 1.8 mg/kg, 1.2 mg/kg or 0.6 mg/kg in different groups of *Fmr1* KO mice. Control mice received the same volume of physiological saline. In mice, brain concentration of NLX-101 peaks within first 30 minutes and declines thereafter following i.p. administration (Neurolixis Inc., data on file). Therefore, drug or saline was injected in mice 10 minutes before the AGS protocol.

To verify if NLX-101 acts specifically through 5-HT_{1A} receptor, an antagonism assay was done with the selective 5-HT_{1A} receptor antagonists, WAY-100635 and NAD-

299. WAY-100635 was dissolved in physiological saline and administered (i.p.) at a dose of 2.5 mg/kg or 5 mg/kg 20 minutes prior to NLX-101 administration (1.8mg/kg). The control group received the same volume of physiological saline before NLX-101 was injected. WAY-100635 may also act as a dopamine D_4 receptor agonist (Chemel et al., 2006; Martel et al., 2007). To rule out potential involvement of receptors other than 5-HT_{1A} receptor, we tested a second antagonist, NAD-299, which has higher selectivity compared to WAY-100635 (Pehrson et al., 2002). NAD-299 was dissolved in physiological saline and administered (i.p.) at either 2.5 mg/kg or 5 mg/kg, 20 minutes before NLX-101 (1.8mg/kg) was given. Control mice received the same volume of physiological saline before NLX-101 injection. As an additional control, mice were tested for AGS following just the administration of NAD-299.

2.2.3 Sound Stimulus for AGS Induction

The sound to induce AGS was presented to up to 4 mice in a cage that was placed in a sound attenuation booth (Gretch-Ken Inc., OR) for AGS induction. The stimulus was a continuously alternating up and down frequency modulated sweep with frequencies between 2-8 kHz, presented at a sound level between 105-110 dB SPL for 15 minutes. The stimulus was generated using computer software (RPvdsEx, Tucker Davis Technologies, FL) and delivered using the RZ6 hardware system (Tucker Davis Technologies, FL) to an amplifier (Marantz, Integrated Amplifier PM8004) and then to the external speaker (FT17H, Fostex International). The sound level was measured with a

portable sound meter (BK PRECISION 735) just before each AGS experiment was run to maintain stable sound output across days.

To differentiate each mouse in the cage with a unique code in post-hoc video analysis, markers of different colors were applied on the fur (color coding) of each mouse. After drug or saline administration, mice were placed in a clean and empty cage with a lid, the same size as their home cage. 10 minutes later, the cage was moved to the sound attenuation chamber with a speaker placed on the top of the cage lid. The AGS induction procedure lasted 20 minutes, starting with 5 minutes of habituation (without a sound stimulus) followed by 15 minutes of loud sound exposure. The full 20-minute procedure was video recorded (Sony HDR-CX350V) for offline analysis. Mice that survived the AGS protocol were euthanized immediately thereafter, and all tails were collected for genotyping.

2.2.4 AGS Video Analysis

Video analysis was done manually. The typical AGS responses of *Fmr1* KO mice include wild running and jumping (WRJ), tonic-clonic seizures (TCS), and respiratory arrest (RA). AGS score were assigned based on each mouse's motor responses as follows: 0- no seizing at all; 1- only one bout of WRJ; 2- more than one bout of WRJ separated by gaps of normal movement; 3- only one bout of TCS; 4- more than one bout of TCS; 5 - death (respiratory arrest) (AGS scales modified from (Gonzalez et al., 2019)). WRJ behavior was identified as continuous and rapid running accompanied by 'popcorn-

like' jumps. TCS behavior was identified when an animal lay on the cage bottom with hindlimb extension. The time of death was noted when an animal showed respiratory arrest which was indicated by the appearance of a deep respiratory gasp and relaxation of pinna. The latency of each motor response or death from the sound onset was recorded, as well as the duration and bouts of each behavior.

2.2.5 Repeated Administration of NLX-101

To determine if repeated treatment with NLX-101 alters its effects in *Fmr1* KO mice, we performed a multi-day treatment assay. Male and female *Fmr1* KO mice received either saline or NLX-101 (1.8 mg/kg i.p.) each day from P17 to P21 between 2:00 and 3:00 pm each day. The mice continued to be housed in their home cage with mother and siblings until the last day (P21) when AGS were tested. Each mouse was toe-clipped for identification and was weighed every day. On the last day of treatment, mice were subjected to AGS protocol following the last injection of saline or NLX-101 administration. All further analyses and measurements were the same as stated in previous sections.

2.2.6 Data Analysis

Data analysis was done in GraphPad Prism (version 9.3.1). Survival analysis was used to quantify the probability of AGS-induced death, wild-running and jumping (WRJ) and tonic-clonic seizures (TCS). Survival probability was analyzed using the log-rank

test. AGS score under various conditions were analyzed with non-parametric t-test (Mann-Whitney test) or two-way ANOVA with sex (males vs. females) and treatment (saline vs. NLX-101) as two independent variables and AGS score as a dependent variable. Effects of $p<0.05$ were considered statistically significant, and denoted as * $p<0.05$, ** $p<0.01$, *** $p<0.001$, **** $p<0.0001$.

2.3 Results

The main goal of this study was to test the hypothesis that a selective 5-HT_{1A} receptor biased agonist will reduce AGS in the young (P21-23) *Fmr1* KO mice. We tested both male and female mice to determine if there were sex differences in seizure susceptibility and effects of the 5-HT_{1A} agonist.

2.3.1 Fmr1 KO male and female mice are similarly susceptible to AGS when treated with saline

Figure 2.1A shows the probability of wild running and jumping (WRJ) in the form of a survival plot in saline treated *Fmr1* KO male and female mice when exposed to the AGS protocol. Survival plots indicate the percentage of mice that show specific aspects of the AGS (e.g., WRJ or death) at any given time point of the test. AGS are quite robust in *Fmr1* KO mice and almost always start with WRJ. *Fmr1* KO males and females showed similar WRJ probability (male: n=18, female: n= 16, p=0.3887, log-rank test). The survival probability plot in saline treated *Fmr1* KO males and females indicates

that ~75% of mice die within 5 minutes of AGS protocol, and only ~25% survive to the end of the procedure. *Fmr1* KO male and female mice exhibited similar survival probability (Figure 2.1B P=0.1706, log-rank test).

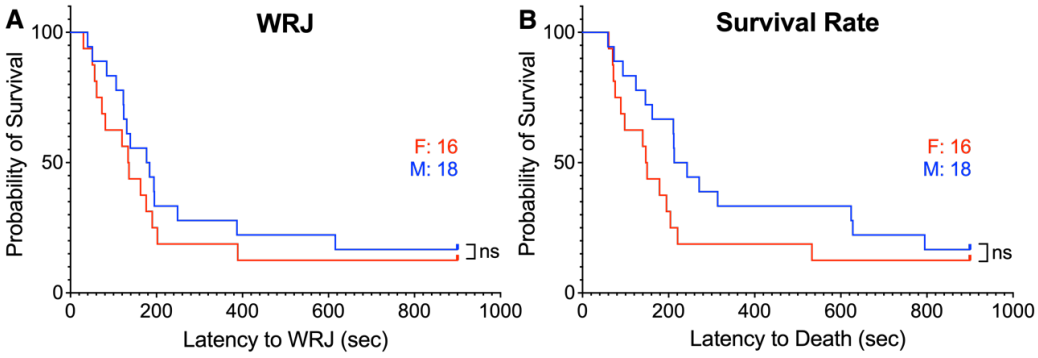

Figure 2.1. Saline treated Fmr1 KO males and females were similarly susceptible to audiogenic seizures (AGS) at ages between P21-P23.

(A) Survival plot of WRJ probability of saline treated *Fmr1* KO males and females when exposed to AGS protocol. KO males and females showed similar WRJ probability. (B) Survival rate plot of saline treated *Fmr1* KO males and females when exposed to the AGS protocol. Latency to death was measured in offline video analysis when a mouse showed respiratory arrest. Most saline-treated mice died within the first 5 minutes (300 seconds).

2.3.2 NLX-101 injection significantly reduces AGS in Fmr1 KO mice in a dose-dependent manner

We tested four doses of NLX-101: 0.6, 1.2, 18 and 2.4 mg/kg and male and female data are combined to show treatment effects. At 0.6 mg/kg, no effects of NLX-101 were observed in AGS-induced survival probability (Figure 2.2A, P=0.166, log-rank test, males and females combined, n=16 saline, n=16 NLX-101) or TCS probability

(Figure 2.2B, males and females combined, P=0.1713, log-rank test, n=16 saline, n=16 NLX-101) or WRJ probability (Figure 2.2C, P=0.0909, log-rank test, n=16 saline, n=16 NLX-101). However, with 1.2, 1.8 and 2.4 mg/kg doses, a strong protective effect of NLX-101 became apparent. At 1.2 mg/kg dose, survival rate was significantly increased in NLX-101 treated group compared to the saline control (Figure 2.2D, P<0.0001, log-rank test, n=21 saline, n=22 NLX-101), but no effects were seen in TCS probability (Figure 2.2E P=0.2332, log-rank test, n=21 saline, n=22 NLX-101) or WRJ probability (Figure 2.2F P=0.3253, log-rank test, n=21 saline, n=22 NLX-101). When NLX-101 dose was increased to 1.8 mg/kg, a significantly higher percentage of mice survived (Figure 2.2G P<0.0001, n=28 saline, n=30 NLX-101). Drug treated mice showed lower TCS probability (Figure 2.2H P=0.0007, n=28 saline, n=30 NLX-101) and lower WRJ probability (Figure 2.2I P=0.0024, n=28 saline, n=30 NLX-101). At the highest dose, 2.4 mg/kg, survival probability in *Fmr1* KO mice was significantly increased (Figure 2.2J P<0.0001, log-rank test) after NLX-101 treatment (n=34) in comparison to saline (n=34). TCS probability was also significantly reduced (Figure 2.2K P=0.0003, log-rank test, n=34 NLX-101, n=34 saline). Surprisingly, 2.4 mg/kg NLX-101 injection had no significant effect on the probability of WRJ in *Fmr1* KO male and female mice (Figure 2.2L P=0.234, log-rank test, n=34 NLX-101, n=34 saline). Taken together, acute treatment with NLX-101 resulted in a dose-dependent and highly significant rescue from AGS in *Fmr1* KO mice.

Dose-dependent effects of NLX-101

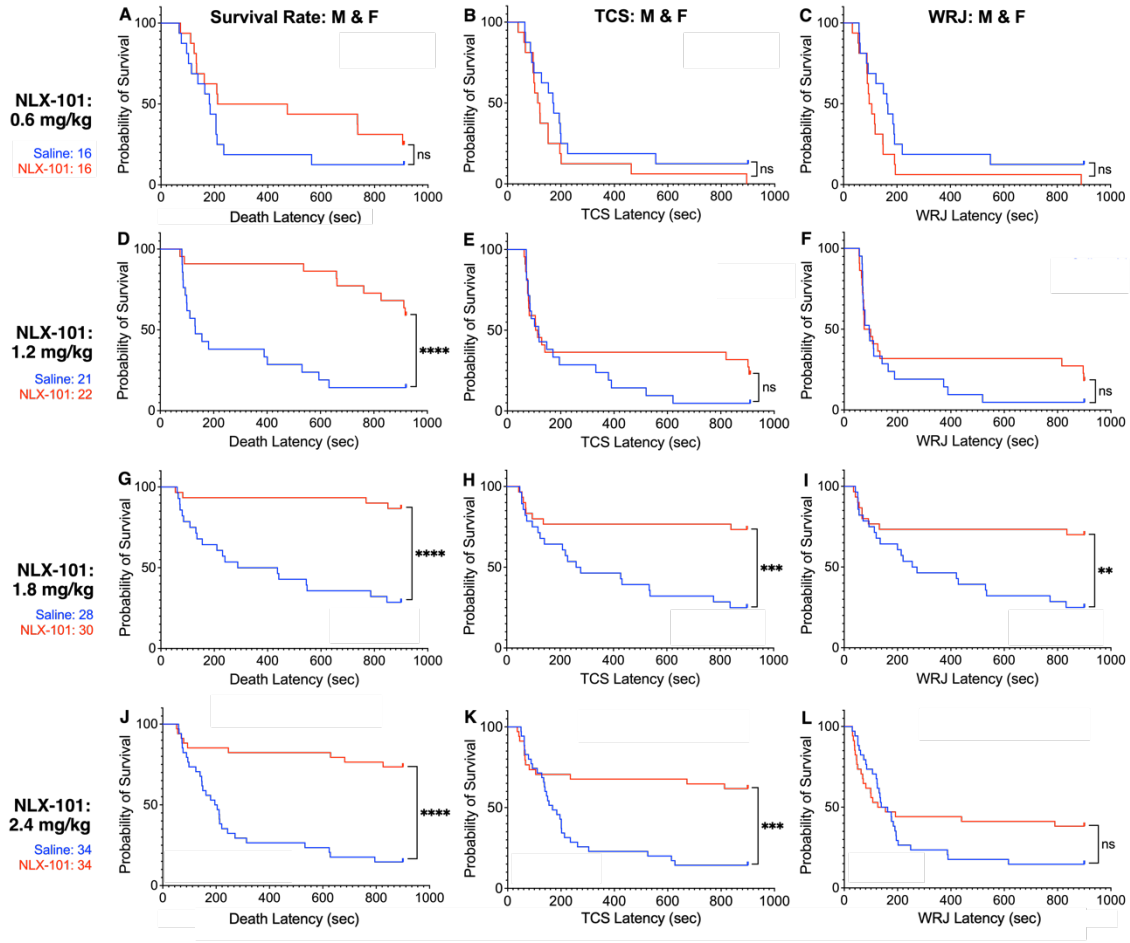

Figure 2.2. Acute NLX-101 i.p. treatment showed dose-dependent effects on probability of AGS-induced death, TCS and WRJ. The analyses shown in the figure combine male and female data.

(A-C) At 0.6 mg/kg, no effects of NLX-101 were observed in AGS-induced death probability, WRJ or TCS probability. (A) Survival plot of AGS-induced death probability, (B) Survival plot of TCS probability, (C) Survival plot of WRJ probability. (D-F) At 1.2 mg/kg, NLX-101 significantly reduced probability of AGS-induced death but not TCS or WRJ probability. (D) Survival plot of AGS-induced death probability, (E) Survival plot of TCS probability, (F) Survival plot of WRJ probability. (G-I) At 1.8 mg/kg, NLX-101 significantly reduced probability of AGS-induced death, TCS and WRJ. (G) Survival plot of AGS-induced death probability, (H) Survival plot of TCS probability and (I) Survival plot of WRJ probability. (J-L) At 2.4 mg/kg, NLX-101 significantly reduced probability of AGS-induced death, TCS but not WRJ. (J) Survival plot of AGS-induced death probability, (K) Survival plot of TCS probability and (L) Survival plot of WRJ probability.

2.3.3 Both Fmr1 KO males and females benefit from NLX-101 treatment similarly

To explore if male and female *Fmr1* KO mice benefit differently from NLX-101 treatment in survival rate and TCS as well as WRJ probability, the same data from Figure 2.2 were split into male and female groups. Probability of death (survival rate), TCS and WRJ were compared within each group (figures not shown).

As mentioned above, at 0.6 mg/kg, there was no effect of the drug on AGS and there were no significant sex differences in survival (Male: p=0.1808. Female: p=0.7120. Log-rank test), TCS (Male: p=0.5035. Female: p=0.2058. Log-rank test) or WRJ probability (Male: p=0.4802. Female: p=0.1053. Log-rank test) in male (Saline: n=9, NLX-101: n=8) or female (Saline: n=7, NLX-101: n=8) group.

At 1.2 mg/kg, significant treatment effect was found in survival rate in both male (P=0.0204, log-rank test. Saline: n=10, NLX-101: n=10) and female (P=0.0012, log-rank

test. Saline: n=11, NLX-101: n=12). But no difference was observed in TCS (Male: p=0.6314. Female: p=0.2478. Log-rank test) or WRJ probability (Male: p=0.9133. Female: p=0.2393. Log-rank test) in either male or female.

At 1.8 mg/kg, NLX-101 treatment significantly increased survival rate (Male: p=0.0003. Female: p=0.0012. Log-rank test), decreased TCS (Male: p=0.0082. Female: p=0.0261. Log-rank test) and WRJ probability (Male: p=0.0417. Female: p=0.0269. Log-rank test) in both male (Saline: n=10, NLX-101: n=11) and female (Saline: n=18, NLX-101: n=19) groups.

At 2.4 mg/kg, beneficial effects of the 2.4 mg/kg NLX-101 were similar in males (Saline: n=18, NLX-101: n=16) and females (Saline: n=16, NLX-101: n=18) on survival rate (Male: p=0.0019. Female: p<0.0001. Log-rank test) and TCS probability (Male: p=0.0057. Female: p=0.0148. Log-rank test). NLX-101 at this dose failed to change WRJ probability (Male: p=0.6568. Female: p=0.0579. Log-rank test) in either male or female.

Taken together, these data show the strong protective effects of acute NLX-101 in survival, WRJ and TCS probability in both male and female mice, with no sex differences.

2.3.4 Dose and sex-dependent effects of NLX-101 on overall AGS score

To evaluate severity of overall AGS, we generated a scale in which WRJ, TCS and death are considered simultaneously (see Methods). The data below are from the same group of animals mentioned above. The NLX-101 dose-dependent improvement of AGS scores can be seen in Figure 2.3. At 0.6 mg/kg (Figure 2.3A), NLX-101 had no

effect on the AGS score in both male and female mice (male: n=9 saline: n=8 NLX-101; female: n=7 saline, n=8 NLX-101, treatment effect: p=0.3581, sex effect: p=0.0816, interaction effect: p=0.1408, two-way ANOVA). At 1.2 mg/kg (Figure 2.3B), NLX-101 significantly reduced overall AGS score in *Fmr1* KO mice. Two-way ANOVA showed a significant treatment effect (p=0.0213), but no main effect of sex (p=0.0911) or interaction (p=0.3596) were revealed (male: n=10 saline, n=10 NLX-101; female: n=12 saline: n=12 NLX-101). When examined separately by sex (Figure S2.1), males showed no significant effect of NLX-101 on AGS score (p=0.2492, Mann-Whitney test); however, females showed a significant reduction in AGS score after treatment with 1.2 mg/kg NLX-101 (p=0.0382, Mann-Whitney test). This suggests a benefit in females at a lower dose of NLX-101 compared to males.

At 1.8 mg/kg (Figure 2.3C), NLX-101 reduced AGS scores in both male and female *Fmr1* KO mice compared to saline controls (male: n=10 saline, n=11 NLX-101; female: n=18 saline, n=19 NLX-101). The AGS score were significantly reduced in NLX-101 treatment group compared to the saline group regardless of sex (p<0.0001, two-way ANOVA). No main effect of sex (p=0.1791) or interactions (p=0.3704) was observed. Finally, with a dose of 2.4 mg/kg (Figure 2.3D), NLX-101 reduced overall AGS score in *Fmr1* KO male and female mice compared to saline controls (male: n=18 saline, n=16 NLX-101; female: n=16 saline, n=18 NLX-101). Two-way ANOVA revealed a significant main effect of treatment (P<0.0001), but no significant sex effect (P=0.9651) or interactions (P=0.6306). Taken together, these data point to no effect of

NLX-101 at 0.6 mg/kg, a stronger effect in females than males at 1.2 mg/kg and similar beneficial effects across sex at 1.8 and 2.4 mg/kg.

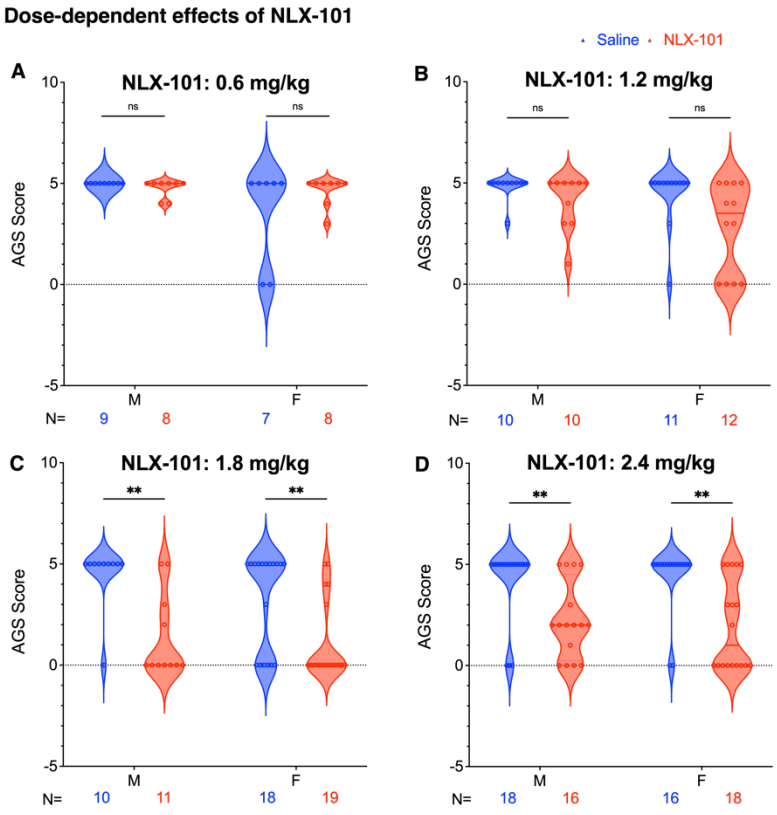

Figure 2.3. Acute NLX-101 i.p. treatment showed dose- and sex-dependent effects in overall AGS score.

AGS scores were used to evaluate the severity of AGS responses. Score were assigned based on AGS responses: 0-no seizing; 1-only one bout of WRJ; 2-more than one bout of WRJ; 3-only one bout of TCS; 4-more than one bout of TCS; 5-death. (A) At 0.6mg/kg, NLX-101 failed to reduce overall AGS score in both male and female groups. The error bars present the mean with standard deviation (SD). (B) At 1.2mg/kg, NLX-101 significantly reduced overall AGS score when both sexes combined. The error bars present the mean with SD. (C) At 1.8mg/kg, NLX-101 reduced overall AGS score in both male and female *Fmr1* KO mice compared to saline. (D) At 2.4mg/kg, NLX-101 reduced overall AGS score in *Fmr1* KO male and female mice compared to saline controls.

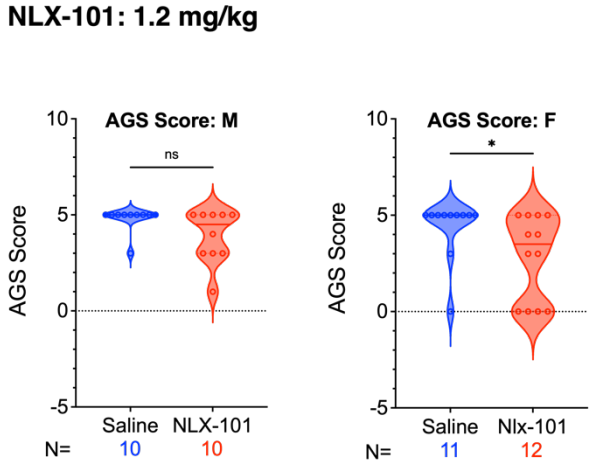

Figure S2.1. Fmr1 KO female mice benefit more from NLX-101 at a lower dose.

(A) No difference regarding AGS score was found in KO males when treated with NLX-101 at 1.2mg/kg (Saline: n=10, NLX-101: n=10. P=0.2492, Mann-Whitney test). (B) AGS score in KO females was significantly decreased with NLX-101 treatment at the same dose (Saline: n=11, NLX-101: n=12. P=0.0382, Mann-Whitney test).

2.3.5 Antagonists of 5-HT$_{1A}$ receptor prevent the beneficial effects of NLX-101

To determine the specificity of the effects of NLX-101 via 5-HT$_{1A}$ receptor, we tested a combination of 5-HT$_{1A}$ receptor antagonists and NLX-101 prior to AGS induction (Figure 2.4). Two different antagonists were tested (WAY-100635 and NAD-299) at two different doses of each (2.5 mg/kg and 5 mg/kg). NLX-101 was injected at 1.8 mg/kg in these experiments. Separate groups of mice were tested for each combination and concentration of drugs. The control condition for this experiment was saline injection combined with NLX-101. The prediction was that the beneficial effects of NLX-101 on AGS will be seen in saline/NLX-101 condition, but not the antagonist/NLX-101 condition.

Figure 2.4A shows that the combined 2.5mg/kg WAY-100635 and 1.8 mg/kg NLX-101 significantly reduced AGS survival probability of *Fmr1* KO mice (male and females combined) compared to saline controls (Saline + NLX-101: n=24, 2.5mg/kg WAY-100635 + NLX-101: n=23, P=0.0030, log-rank test). Figure 2.4B shows that 2.5mg/kg WAY-100635 significantly increased AGS score in treatment group in comparison to saline group (Saline + NLX-101: n=24, 2.5mg/kg WAY-100635 + 1.8mg/kg NLX-101: n=23, P=0.0057, Mann-Whitney test). Figure 2.4C-D shows a similar effect of a higher dose of WAY-100635 (5mg/kg) in combination with NLX-101 on probability of survival (Figure 2.4C, Saline + NLX-101: n=24, 5mg/kg WAY-100635 + NLX-101: n=21, P=0.0015, log-rank test), and AGS score (Figure 2.4D, Saline + NLX-101: n=24, 5mg/kg WAY-100635 + NLX-101: n=21, P=0.0125, Mann-Whitney test).

Due to the potential for WAY-100635 to act on dopamine receptors (Chemel et al., 2006), we tested a second and more specific 5-HT_{1A} receptor antagonist, NAD-299 (Pehrson et al., 2002) at 2.5 and 5 mg/kg or saline in combination with 1.8 mg/kg NLX-101 in separate groups of *Fmr1* KO mice (Figure 2.4E-H). Treatment with 2.5mg/kg NAD-299 prior to NLX-101 significantly decreased survival probability in the treatment group compared to the saline group (Figure 2.4E, Saline + NLX-101: n= 24, 2.5mg/kg NAD-299 + NLX-101: n=21, P=0.0005, log-rank test). Likewise, combined treatment of NAD-299 and NLX-101 increased the AGS score in the treatment group compared to saline group Figure 2.4F, Saline + NLX-101: n= 24, 2.5mg/kg NAD-299 + NLX-101: n=21, P=0.0015, Mann-Whitney test). Similar results were obtained when the concentration of NAD-299 was increased to 5 mg/kg for survival probability (Figure

2.4G, saline + NLX-101: n= 24, 5mg/kg NAD-299 + NLX-101: n=24, P=0.0008, log-rank test), and AGS score (Figure 2.4H, saline + NLX-101: n= 24, 5mg/kg NAD-299 + 1.8mg/kg NLX-101: n=24. P=0.0056, Mann-Whitney test). Taken together, these antagonist experiments indicate that the protective effects of NLX-101 on AGS in *Fmr1* KO mice are mediated by its actions on 5-HT_{1A} receptor.

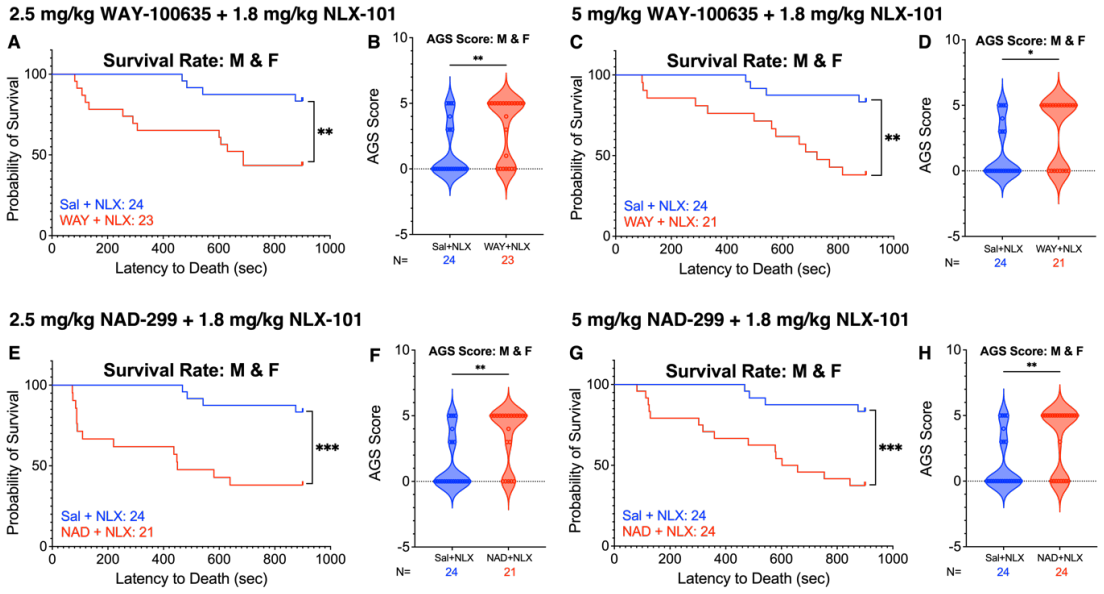

Figure 2.4. Administration of 5-HT$_{1A}$R eceptor antagonist (WAY-100635 or NAD-299) before NLX-101, abolished beneficial effects of NLX-101 in reducing AGS in Fmr1 KO mice.

(A) 2.5 mg/kg WAY-100635 + NLX-101 significantly reduced survival probability after the exposure of AGS protocol in *Fmr1* KO mice (male and females combined) compared to saline + NLX-101 treated mice. (B) 2.5 mg/kg WAY-100635 + NLX-101 significantly increased AGS score in treatment group in comparison to saline + NLX-101 group. (C) 5 mg/kg WAY-100635 + NLX-101 treatment significantly reduced survival probability after being exposed to AGS protocol in *Fmr1* KO mice (male and females combined) compared to saline + NLX-101 treated mice (D) 5 mg/kg WAY-100635 pre-treatment significantly increased AGS score in treatment group in comparison to saline group. (E) Prior treatment of 2.5 mg/kg NAD-299 before NLX-101 significantly lowered survival probability (E) and AGS score (F) in the treatment group in contrast with saline + NLX-101 group. (G) Survival probability significantly dropped due to preceding 5 mg/kg administration of NAD-299 before NLX-101 in comparison to the saline + NLX-101 group. (H) AGS score was significantly elevated due to the combined treatment of agonist and antagonist when compared to saline + agonist group. The error bars in the relevant panels show the standard deviation (SD).

2.3.6 NAD-299 alone does not affect AGS responses in Fmr1 KO mice

As an additional control, we tested the effects of NAD-299 alone on AGS responses (Figure 2.5). Male and female *Fmr1* KO were exposed to the AGS protocol after being injected with either saline or 5mg/kg NAD-299. No difference was observed between the two groups in either survival probability (Figure 2.5A Saline: n=8, NAD-299: n=9. P=0.7347, log-rank test) or AGS score (Figure 2.5B Saline: n=8, NAD-299: n=9. P=0.4706, Mann-Whitney test), indicating NAD-299 alone does not impact AGS.

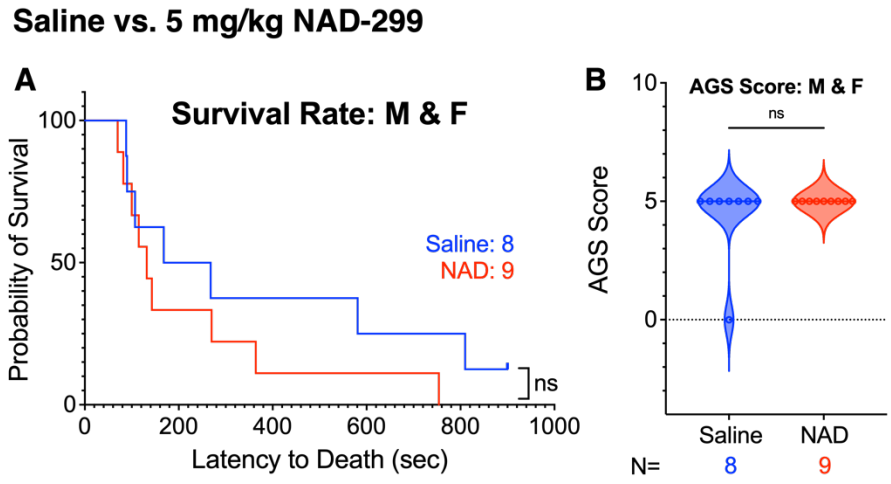

Figure 2.5. 5 mg/kg NAD-299 alone does not affect AGS responses in Fmr1 KO mice.

Mice were subjected to AGS protocol after either saline or 5 mg/kg NAD-299 i.p. administration. No difference was seen in terms of survival rate (A) or AGS scores (B) between the two groups. The error bars show SD.

2.3.7 Repeated exposure to NLX-101 does not elicit tachyphylaxis for reducing AGS in Fmr1 KO mice

Repeated treatment with NLX-101 (1.8 mg/kg i.p./day for 5 days) dramatically increased survival rate in the treatment group compared to saline group (Figure 2.6A. P=0.0001, log rank test. Saline: n=12, NLX-101: n=11). The overall AGS score in NLX-101 group was also considerably reduced (Figure 2.6B. P=0.0011, Mann-Whitney test. Saline: n=12, NLX-101: n=11). The similar beneficial effects of NLX-101 under acute and chronic conditions strongly argue that repeated exposure of the mice to NLX-101 does not cause tachyphylaxis to the compound's ability to alleviate AGS in *Fmr1* KO mice, at least within the tested time range of this study.

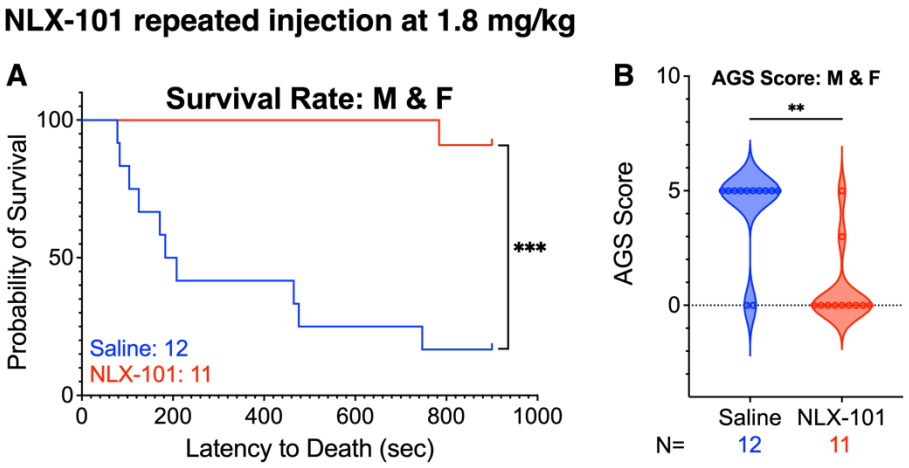

Figure 2.6. Repeated treatment of NLX-101 remains effective in reducing AGS in Fmr1 KO mice.

Fmr1 KO mice, both males and females, were given either saline or NLX-101 at 1.8 mg/kg i.p. daily from P17 to P21 and then tested for AGS on P21. The drug treated group showed high survival rate (A) and low AGS score (B). The majority of NLX-101 treated showed no seizures at all.

2.3.8 Sex differences in AGS susceptibility was seen in mice that were not treated with saline or drug

One curious aspect of our study that may be relevant to treatment development was that when mice not treated with either drug or saline were exposed to AGS protocol, a significant sex difference emerged (Figure 2.7). Untreated female *Fmr1* KO mice have lower susceptibility to AGS protocol compared to male *Fmr1* KO mice, indicated by reduced probability of AGS-induced death, TCS, and WRJ, as well as lower AGS score. Females have higher survival probability (Figure 2.7A, male: n=19, female: n=27. $P<0.0001$, log-rank test), lower probability of TCS (Figure 2.7B, $P=0.0009$, log-rank test), lower probability of WRJ (Figure 2.7C, $P<0.0001$) and lower AGS score (Figure 2.7D, $P=0.0001$, Mann-Whitney test). This contrasts with data shown in Figure 1 in which *Fmr1* KO mice treated with saline showed similar AGS susceptibility. This suggests that susceptibility in females may be increased (primed) with handling and injection procedures.

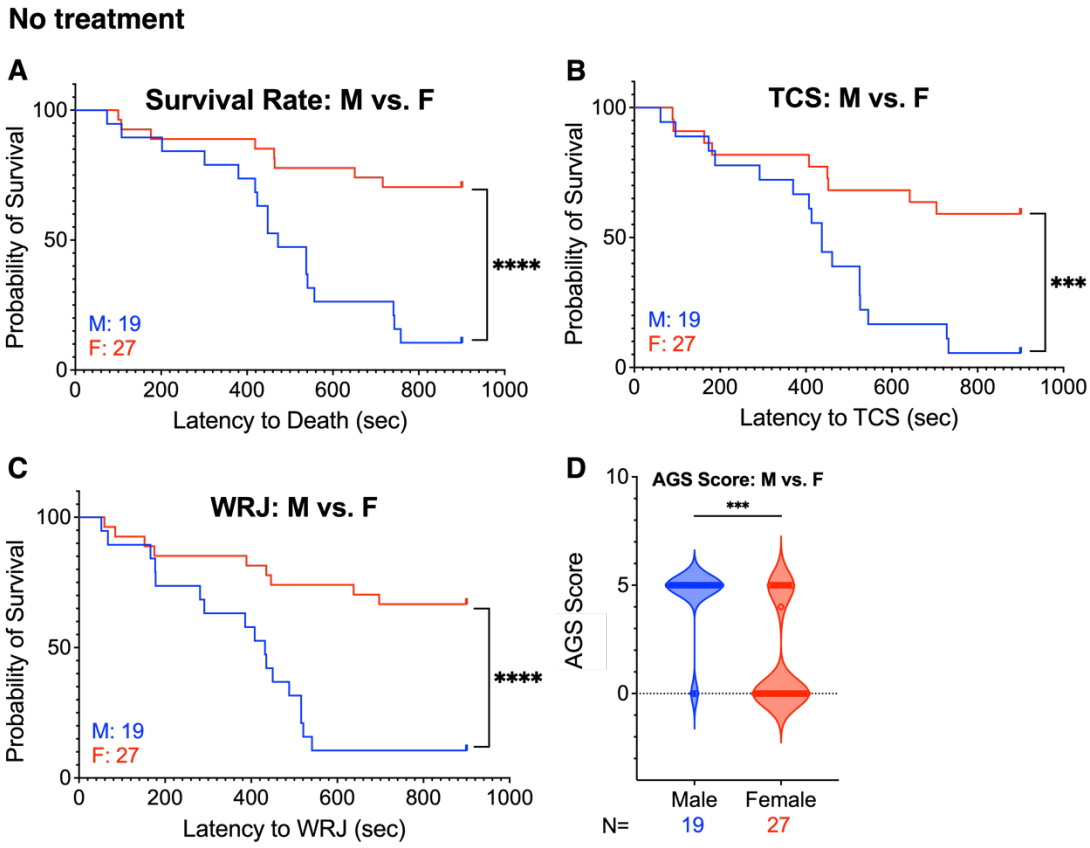

Figure 2.7. Non-treated female Fmr1 KO mice had lower susceptibility to AGS compared to the male counterparts, indicated by reduced probability of AGS-induced death (A), TCS (B), and WRJ (C), and lower AGS score (D). The error bars show SD.

2.4 Discussion

Acute and systemic treatment with NLX-101, a selective 5-HT_{1A} receptor biased agonist, is sufficient to reduce AGS responses and death in young *Fmr1* KO male and female mice. The beneficial effects of NLX-101 on AGS were dose-dependent with no effect at the lowest dose (0.6 mg/kg i.p.), but significant and striking beneficial effects at higher doses (1.2, 1.8 and 2.4 mg/kg i.p.). Prior administration of 5-HT_{1A} receptor antagonists (either WAY-100635 or NAD-299) abolished the effects of NLX-101, indicating that NLX-101 acts specifically through 5-HT_{1A} receptor. We also show that tachyphylaxis to the effects of NLX-101 does not develop over a 5-day treatment before AGS, a finding which is important when considering future clinical trials. Three lines of evidence suggest a sex difference in AGS susceptibility in the *Fmr1* KO mice. First, in mice that were not injected with saline or drug, females were less susceptible to AGS compared to males (Figure 2.7). Curiously females injected with saline do not show reduced seizure susceptibility suggesting that the process of injection and handling them may prime AGS in female *Fmr1* KO mice. Second, females benefited more at a lower dose of NLX-101 (Figure S2.1), indicated by a significantly reduced AGS score at 1.2mg/kg for females but not for males. Third, a higher dose of antagonist, either WAY-100635 (Figure S2.2) or NAD-299 (Figure S2.3), is needed to reduce beneficial effects of NLX-101 in females compared to males. Taken together, these data point to strong effects of a selective 5-HT_{1A} biased agonist in reducing an extreme form of sensory hypersensitivity in FXS, suggesting that this receptor could constitute a promising therapeutic target for clinical development.

2.5 mg/kg WAY-100635 + 1.8 mg/kg NLX-101

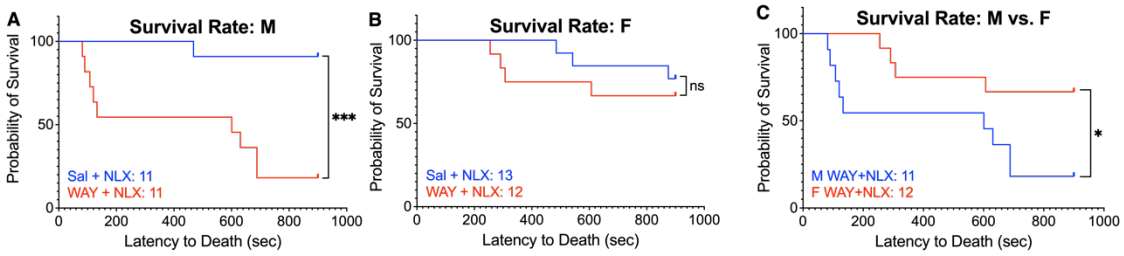

5 mg/kg WAY-100635 + 1.8 mg/kg NLX-101

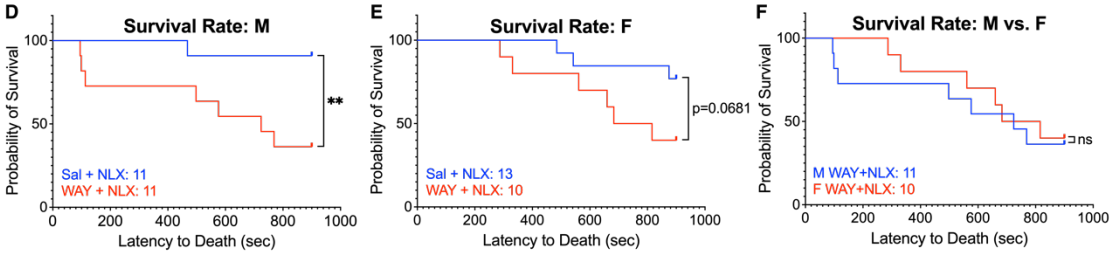

Figure S2.2. Higher dose of WAY-100635 is needed to abolish beneficial effects of NLX-101 in female than in male Fmr1 KO mice.

(A-C) Prior treatment of WAY-100635 at 2.5 mg/kg significantly abolished beneficial effects of NLX-101 in *Fmr1* KO males but not in females. (A) Survival rate was significantly dropped in *Fmr1* KO males when they were treated with 2.5 mg/kg WAY-100635 followed by NLX-101 (1.8 mg/kg) (Saline + 1.8 mg/kg NLX-101: n=11, 2.5 mg/kg WAY-100635 + 1.8 mg/kg NLX-101: n=11. P=0.0007, log-rank test). (B) When the same treatment as (A) was applied, survival rate was not significantly changed in female KO mice compared to saline controls (Saline + 1.8 mg/kg NLX-101: n=13, 2.5 mg/kg WAY-100635 + 1.8 mg/kg NLX-101: n=12. P=0.4841, log-rank test). (C) When only WAY-100635 treated groups from the male (A) and female (B) were compared, *Fmr1* KO females exhibited higher survival rate than male counterparts (Male 2.5 mg/kg WAY-100635 + 1.8 mg/kg NLX-101: n=11, female 2.5 mg/kg WAY-100635 + 1.8 mg/kg NLX-101: n=12. P=0.0211, log-rank test). (D-F) Preceding treatment of WAY-100635 at 5mg/kg significantly abolished beneficial effects of NLX-101 in both *Fmr1* KO males and females. (D) Survival rate in *Fmr1* KO males significantly declined after combination treatment of 5 mg/kg WAY-100635 and NLX-101 (1.8 mg/kg) (Saline + 1.8mg/kg NLX-101: n=11, 5mg/kg WAY-100635 + 1.8mg/kg NLX-101: n=11. P=0.0099 log-rank test). (E) Survival probability in *Fmr1* KO females with the same treatment as A) was also reduced but not yet significant (Saline + 1.8 mg/kg NLX-101: n=13, 5 mg/kg WAY-100635 + 1.8 mg/kg NLX-101: n=10. P=0.0729, log-rank test). (F) When only WAY-100635 treated groups from the male (D) and female (E) were considered, *Fmr1* KO males and females demonstrated similar survival (Male 5 mg/kg WAY-100635 + 1.8 mg/kg NLX-101: n=11, female 5 mg/kg WAY-100635 + 1.8 mg/kg NLX-101: n=10. P=0.7099, log-rank test).

2.5 mg/kg NAD-299 + 1.8 mg/kg NLX-101

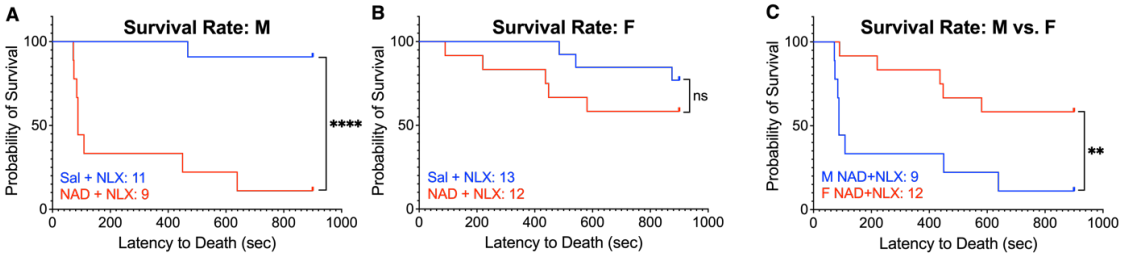

5 mg/kg NAD-299 + 1.8 mg/kg NLX-101

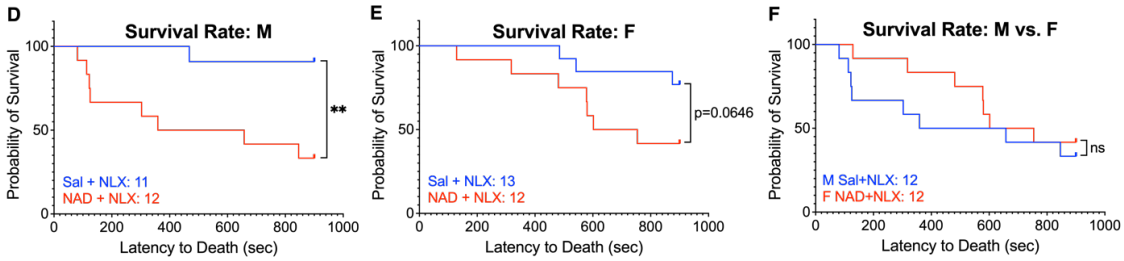

Figure S2.3. A higher dose of NAD-299 is required to take away beneficial effects of NLX-101 in Fmr1 KO female mice.

(A-C) Preceding treatment of NAD-299 at 2.5mg/kg significantly abolished beneficial effects of NLX-101 in KO males but not in females. (A) Survival probability was significantly decreased in KO males when they were treated with 2.5 mg/kg NAD-299 and NLX-101 (1.8mg/kg) (Saline + 1.8 mg/kg NLX-101: n=11, 2.5 mg/kg NAD-299 + 1.8 mg/kg NLX-101: n=9. P<0.0001, log-rank test). (B) With the same treatment as A), survival probability in females was not significantly changed (Saline + 1.8mg/kg NLX-101: n=13, 2.5 mg/kg NAD-299 + 1.8 mg/kg NLX-101: n=12. P=0.2431, log-rank test). (C) When only NAD-299 groups from male (A) and female (B) were plotted together, *Fmr1* KO females showed higher survival rate than male counterparts (Male 2.5 mg/kg NAD-299 + 1.8 mg/kg NLX-101: n=9, female 2.5 mg/kg NAD-299 + 1.8 mg/kg NLX-101: n=12. P=0.0211, log-rank test). (D-F) Combined treatment of NAD-299 (5 mg/kg) and NLX-101 (1.8 mg/kg) significantly abolished beneficial effects of NLX-101 in both *Fmr1* KO males and females. (D) *Fmr1* KO males exhibited significantly lower survival probability with pretreatment of 5mg/kg NAD-299 followed by NLX-101 (Saline + 1.8 mg/kg NLX-101: n=11, 5 mg/kg NAD-299 + 1.8 mg/kg NLX-101: n=12. P=0.0045 log-rank test). (E) Survival probability in *Fmr1* KO females with the same treatment as (D) was also reduced but not significant (Saline + 1.8 mg/kg NLX-101: n=13, 5 mg/kg NAD-299 + 1.8 mg/kg NLX-101: n=12. P=0.0627, log-rank test). (F) *Fmr1* KO males and females showed similar survival probability when treated with 5mg/kg NAD-299 precedingly (Male 5 mg/kg NAD-299 + 1.8 mg/kg NLX-101: n=12, female 5 mg/kg NAD-299 + 1.8 mg/kg NLX-101: n=12. P=0.4659, log-rank test).

The present data showing a reduction of AGS in *Fmr1* KO mice by a selective 5-HT_{1A} agonist constitute a step forward in understanding abnormal serotoninergic function in various models of generalized seizures, including reduced seizure threshold and increases seizure-induced mortality when 5-HT neurons are impaired (Buchanan et al. 2014; Griffin et al. 2017; Zhang et al. 2016, 2018). One of the most widely used 5-HT_{1A} receptor agonists, 8-OH-DPAT (which also possesses marked 5-HT_7 receptor agonist properties), has previously been shown to reduce seizures (Gariboldi et al., 1996; Heydari & Davoudi, 2017) induced by kainic acid or pentylenetetrazol infusion. Tupal and Faingold (Tupal and Faingold 2006) found that fluoxetine, a selective serotonin reuptake inhibitor (SSRI) significantly reduced AGS-induced death in DBA/2 mice. Heydari and Davoudi (2017) showed that sertraline, another SSRI, significantly increased seizure threshold induced by pentylenetetrazol. One of the difficulties in understanding underlying serotoninergic mechanisms with SSRIs is that the action of serotonin through multiple subtypes of receptors may cause mixed effects, making it hard to pinpoint the contribution of specific subtype receptors. Indeed, while fluoxetine has been prescribed for children with autism, a meta-analysis of the studies shows mixed results (Williams et al., 2013). Therefore, more specific drugs such as the 5-HT_{1A} receptor biased agonist used here may prove to be a fruitful approach for improved serotoninergic modulation in epilepsy and autism.

In the case of AGS in *Fmr1* KO mice, we speculate that the midbrain inferior colliculus (IC) might be involved in suppressing AGS responses through activation of post-synaptic 5-HT_{1A} heteroreceptors by NLX-101. The main rationale for the hypothesis

arises from four previous findings. First, the IC is a major hub involved in AGS in different types of seizure models (Faingold, 2005) as AGS susceptibility can be induced in normal rats by focal microinjection of the agents that either enhance excitation or reduce inhibition in the IC and it is not the case when the same agents are injected in other brain regions. Second, Gonzalez et al. (2020) showed that loss of FMRP in VGlut2 expressing glutamatergic neurons of the midbrain/brainstem is sufficient to cause AGS. Expression of FMRP in the IC eliminates AGS. Third, Nguyen et al. (2020) showed that the IC is hyper-responsive to sounds both at the single neuron and population levels. This is particularly true at ages associated with AGS. These studies implicate hyperactivity in the midbrain as a major source of auditory hypersensitivity in the *Fmr1* KO mice. Fourth, serotonin increases within minutes in the IC in response to loud sound (Hall, et al., 2010), and in most IC neurons, serotonin suppresses responses and reduces gain (Hurley & Pollak, 1999). Hurley (2006) showed that the 5-HT_{1A} / 5-HT_7 receptor agonist, 8-OH-DPAT, produced similar suppressive effects as applying serotonin, implicating these receptors in such response suppression in the IC. Activation of 5-HT_{1A} receptor hyperpolarize neurons (Hurley 2006; Hurley and Sullivan 2012) and are expressed on both inhibitory and excitatory neurons (Hurley 2006; Peruzzi and Dut 2004). However, low concentrations of serotonin may primarily bind 5-HT_{1A} receptor on GABAergic neurons whereas higher concentrations activate 5-HT_{1A} receptor expressed on both inhibitory and excitatory neurons (Llado-Pelfort et al., 2012). Taken together, the above studies suggest either abnormal activation of sound-driven serotonin release and/or deficient 5-HT_{1A} activation in the IC of developing *Fmr1* KO mice. Therefore, the

large beneficial effects of NLX-101 we observed here may provide an important avenue to treat auditory hypersensitivity in FXS by acting on IC hyperactivity. Future studies should evaluate serotonin release and 5-HT_{1A} expression in developing *Fmr1* KO mouse IC to test underlying mechanisms of serotonin dysfunction in the midbrain.

Hypersensitivity elicited by various sensory stimuli is one of the most debilitating symptoms seen in humans with FXS (Hagerman and Hagerman 2002; Hagerman et al. 1999; Merenstein et al. 1996; Miller et al. 1999). Auditory hypersensitivity and abnormal processing is consistently seen clinically and may cause language delays, high anxiety and social impairments in FXS (Ethridge et al., 2016; Wang et al., 2017). Auditory hypersensitivity in FXS has been replicated in the *Fmr1* KO mice, amongst other auditory processing abnormalities, including expanded tuning curve, abnormal temporal processing, abnormal neural oscillations in the auditory cortex and increased tone-induced responses in the IC and AC (Lovelace et al., 2018; Nguyen et al., 2020; Razak et al., 2021; Rotschafer & Razak, 2013; Wen et al., 2018). AGS are the most robust, consistent, and extreme expression of hyperacusis in *Fmr1* KO mice. Thus, in this study we employed AGS responses as main outcome measure to test the effects of NLX-101 in reducing auditory hypersensitivity. Children with FXS and co-morbid seizures show increased aggression and are more likely to receive a co-diagnosis of autism. Early life seizures lead to long-term behavioral changes in rodents (Bernard et al., 2015; Bernard & Benke, 2015). Whether NLX-101 treatment in early life, and consequent reduction of hypersensitivity, leads to additional benefits with transition to adolescence and adulthood remains to be tested and will be the goal of future work.

Table S2.1. Full Statistics Results of Survival Analysis

Figure No.	Stats	Chi square	df	P-value	significance	95% CI of ratio (A:control B:treatment) A/B	B/A
Fig.1A	Log-rank (Mantel-Cox) test	0.7431	1	0.3887	ns	0.3468 to 1.528	0.6543 to 2.883
Fig.1B	Log-rank (Mantel-Cox) test	1.878	1	0.1706	ns	0.2849 to 1.296	0.7716 to 3.509
Fig.2A	Log-rank (Mantel-Cox) test	1.919	1	0.166	ns	0.7760 to 3.710	0.2696 to 1.289
Fig.2B	Log-rank (Mantel-Cox) test	1.872	1	0.1713	ns	0.2971 to 1.271	0.7866 to 3.366
Fig.2C	Log-rank (Mantel-Cox) test	2.859	1	0.0909	ns	0.2650 to 1.152	0.8683 to 3.774
Fig.2D	Log-rank (Mantel-Cox) test	16.13	1	<0.0001	****	1.895 to 9.553	0.1047 to 0.5277
Fig.2E	Log-rank (Mantel-Cox) test	1.422	1	0.2332	ns	0.7633 to 2.791	0.3584 to 1.310
Fig.2F	Log-rank (Mantel-Cox) test	0.9674	1	0.3253	ns	0.7184 to 2.580	0.3877 to 1.392
Fig.2G	Log-rank (Mantel-Cox) test	21.38	1	<0.0001	****	3.559 to 18.48	0.05411 to 0.2810
Fig.2H	Log-rank (Mantel-Cox) test	11.47	1	0.0007	***	1.747 to 7.640	0.1309 to 0.5726
Fig.2I	Log-rank (Mantel-Cox) test	9.205	1	0.0024	**	1.503 to 6.379	0.1568 to 0.6655
Fig.2J	Log-rank (Mantel-Cox) test	24.89	1	<0.0001	****	2.719 to 10.07	0.09930 to 0.3678
Fig.2K	Log-rank (Mantel-Cox) test	12.89	1	0.0003	***	1.647 to 5.503	0.1817 to 0.6071
Fig.2L	Log-rank (Mantel-Cox) test	1.416	1	0.234	ns	0.8029 to 2.433	0.4110 to 1.246
Fig4A	Log-rank (Mantel-Cox) test	8.816	1	0.003	**	0.08215 to 0.5668	1.764 to 12.17
Fig4C	Log-rank (Mantel-Cox) test	10.08	1	0.0015	**	0.07459 to 0.5234	1.911 to 13.41
Fig4E	Log-rank (Mantel-Cox) test	12.05	1	0.0005	***	0.06542 to 0.4722	2.118 to 15.29
Fig4G	Log-rank (Mantel-Cox) test	11.36	1	0.0008	***	0.07468 to 0.4645	2.153 to 13.39
Fig.5A	Log-rank (Mantel-Cox) test	1.323	1	0.25	ns	0.2140 to 1.553	0.6438 to 4.673
Fig.6A	Log-rank (Mantel-Cox) test	14.62	1	0.0001	***	5.026 to 58.22	0.01718 to 0.1990
Fig.7A	Log-rank (Mantel-Cox) test	15.75	1	<0.0001	****	1.964 to 10.58	0.09456 to 0.5091
Fig.7B	Log-rank (Mantel-Cox) test	11.02	1	0.0009	***	1.557 to 7.790	0.1284 to 0.6422
Fig.7C	Log-rank (Mantel-Cox) test	15.23	1	<0.0001	****	1.837 to 9.693	0.1032 to 0.5444
Fig.S2A	Log-rank (Mantel-Cox) test	11.5	1	0.0007	***	0.01964 to 0.2503	3.995 to 50.92
Fig.S2B	Log-rank (Mantel-Cox) test	0.4897	1	0.4841	ns	0.1326 to 2.624	0.3812 to 7.539
Fig.S2C	Log-rank (Mantel-Cox) test	5.316	1	0.0211	*	1.178 to 11.01	0.09086 to 0.8490
Fig.S2D	Log-rank (Mantel-Cox) test	6.649	1	0.0099	**	0.02617 to 0.4313	2.319 to 38.22
Fig.S2E	Log-rank (Mantel-Cox) test	3.328	1	0.0681	ns	0.07746 to 1.153	0.8673 to 12.91
Fig.S2F	Log-rank (Mantel-Cox) test	0.1384	1	0.7099	ns	0.4142 to 3.647	0.2742 to 2.414
Fig.S3A	Log-rank (Mantel-Cox) test	15.3	1	<0.0001	****	0.01347 to 0.2287	4.373 to 74.23
Fig.S3B	Log-rank (Mantel-Cox) test	1.363	1	0.2431	ns	0.1075 to 1.780	0.5619 to 9.301
Fig.S3C	Log-rank (Mantel-Cox) test	6.925	1	0.0085	**	1.182 to 12.98	0.07706 to 0.8459
Fig.S3D	Log-rank (Mantel-Cox) test	8.082	1	0.0045	**	0.02457 to 0.3456	2.894 to 40.70
Fig.S3E	Log-rank (Mantel-Cox) test	3.414	1	0.0646	ns	0.08587 to 1.064	0.9397 to 11.64
Fig.S3F	Log-rank (Mantel-Cox) test	0.5317	1	0.4659	ns	0.5244 to 4.029	0.2482 to 1.907

Table S2.2. Full Statistics Results of AGS Scores Analysis with Two Independent Variables

Figure No.	Sex	Below threshold?	P value	Mean rank of Saline	Mean rank of Nlx-101	Mean rank diff.	Mann-Whitney U	Adjusted P Value
Fig 3A	M	No	0.205882	10	7.875	2.125	27	0.369377
	F	No	0.641026	7.571	8.375	-0.8036	25	0.641026
Fig 3B	M	No	0.249226	12	9	3	35	0.249226
	F	No	0.028671	15.42	9.583	5.833	37	0.056521
Fig 3C	M	Yes	0.002061	14.85	7.5	7.35	16.5	0.004118
	F	Yes	0.004204	23.64	14.61	9.034	87.5	0.004204
Fig 3D	M	Yes	0.005897	21.5	13	8.5	72	0.005897
	F	Yes	0.001251	22.63	12.94	9.681	62	0.0025

Table S2.3. Full Statistics Results of AGS Scores Analysis with One Independent Variable

Figure No.	Significantly different?	P-value	Mann Whitney U
Fig 4B	Yes	0.0057	157
Fig 4D	Yes	0.0125	154
Fig 4F	Yes	0.0015	123.5
Fig 4H	Yes	0.0056	164.5
Fig 5B	No	0.4706	31.5
Fig 6B	Yes	0.0011	18
Fig 7D	Yes	0.0001	104
Fig S1A	No	0.1192	30
Fig S1B	Yes	0.0382	35

References

Adhikari, Yadav, and Xiaoming Jin. 2020. “Intraperitoneal Injection of Lipopolysaccharide Prevents Seizure-induced Respiratory Arrest in a DBA/1 Mouse Model of SUDEP.” *Epilepsia Open* 5(3): 386–96.

Armstrong, Jessica L et al. 2020. “(S)-5-(2′-Fluorophenyl)- N , N -Dimethyl-1,2,3,4-Tetrahydronaphthalen-2-Amine, a Serotonin Receptor Modulator, Possesses Anticonvulsant, Prosocial, and Anxiolytic-like Properties in an Fmr1 Knockout Mouse Model of Fragile X Syndrome and Autism Spectrum.” *ACS Pharmacology & Translational Science*.

Bernard, Paul B. et al. 2015. “Behavioral Changes Following a Single Episode of Early-Life Seizures Support the Latent Development of an Autistic Phenotype.” *Epilepsy & Behavior* 44: 78–85.

Bernard, Paul B., and Tim A. Benke. 2015. “Early Life Seizures: Evidence for Chronic Deficits Linked to Autism and Intellectual Disability across Species and Models.” *Experimental Neurology* 263: 72–78.

Buchanan, Gordon F., Nicholas M. Murray, Michael A. Hajek, and George B. Richerson. 2014. “Serotonin Neurones Have Anti-Convulsant Effects and Reduce Seizure-Induced Mortality.” *The Journal of Physiology* 592(19): 4395–4410.

Canal, Clinton E. et al. 2015. “An Orally Active Phenylaminotetralin-Chemotype Serotonin 5-HT7 and 5-HT1AR eceptor Partial Agonist That Corrects Motor Stereotypy in Mouse Models.” *ACS Chemical Neuroscience* 6(7): 1259–70.

Chemel, Benjamin R. et al. 2006. “WAY-100635 Is a Potent Dopamine D4 Receptor Agonist.” *Psychopharmacology* 188(2): 244–51.

Chen, L., and M. Toth. 2001. “Fragile X Mice Develop Sensory Hyperreactivity to Auditory Stimuli.” *Neuroscience* 103(4): 1043–50.

Dombrowski, C et al. 2002. “Premutation and Intermediate-Size FMR1 Alleles in 10 572 Males from the General Population: Loss of an AGG Interruption Is a Late Event in the Generation of Fragile X.” *Human Molecular Genetics* 11(4): 371–78.

Ethridge, L E et al. 2016. “Reduced Habituation of Auditory Evoked Potentials Indicate Cortical Hyper-Excitability in Fragile X Syndrome.” *Translational Psychiatry* 6(4): e787–e787.

Faingold, Carl L. 2004. “Chapter 21 The Midbrain and Audiogenic Seizures.” In *The Inferior Colliculus*, , 603–24.

Gariboldi, Marco, Piotr Tutka, Rosario Samanin, and Annamaria Vezzani. 1996. “Stimulation of 5-HT1AR eceptors in the Dorsal Hippocampus and Inhibition of Limbic Seizures Induced by Kainic Acid in Rats.” *British Journal of Pharmacology* 119(5): 813–18.

Gonzalez, Darya et al. 2019. “Audiogenic Seizures in the Fmr1 Knock-Out Mouse Are Induced by Fmr1 Deletion in Subcortical, VGlut2-Expressing Excitatory Neurons and Require Deletion in the Inferior Colliculus.” *The Journal of neuroscience : the official journal of the Society for Neuroscience* 39(49): 9852–63.

Goodlin-Jones, Beth L., Flora Tassone, Louise W. Gane, and Randi J. Hagerman. 2004. "Autistic Spectrum Disorder and the Fragile X Premutation." *Journal of Developmental and Behavioral Pediatrics* 25(6): 392–98.

Greiss Hess, Laura et al. 2016. "A Randomized, Double-Blind, Placebo-Controlled Trial of Low-Dose Sertraline in Young Children with Fragile X Syndrome." *Journal of Developmental and Behavioral Pediatrics* 37(8): 619–28.

Griffin, Aliesha et al. 2017. "Clemizole and Modulators of Serotonin Signalling Suppress Seizures in Dravet Syndrome." *Brain* 140(3): 669–83.

Hagerman, Randi Jenssen, and Paul J. Hagerman. 2002. *Fragile X Syndrome: Diagnosis, Treatment, and Research*. Taylor & Francis US.

Hagerman, R.J., J. Hills, S. Scharfenaker, and H. Lewis. 1999. "Fragile X Syndrome and Selective Mutism." *American Journal of Medical Genetics* 83(4): 313–17.

Hall, Ian C., George V. Rebec, and Laura M. Hurley. 2010. "Serotonin in the Inferior Colliculus Fluctuates with Behavioral State and Environmental Stimuli." *Journal of Experimental Biology* 213(7): 1009–17.

Heydari, Azhdar, and Shima Davoudi. 2017. "The Effect of Sertraline and 8-OH-DPAT on the PTZ_induced Seizure Threshold: Role of the Nitrergic System." *Seizure* 45: 119–24.

Hurley, Laura M. 2006. "Different Serotonin Receptor Agonists Have Distinct Effects on Sound-Evoked Responses in Inferior Colliculus." *Journal of Neurophysiology* 96(5): 2177–88.

Hurley, Laura M. 2007. “Activation of the Serotonin 1A Receptor Alters the Temporal Characteristics of Auditory Responses in the Inferior Colliculus.” *Brain Research* 1181(1): 21–29.

Hurley, Laura M., and George D. Pollak. 1999. “Serotonin Differentially Modulates Responses to Tones and Frequency-Modulated Sweeps in the Inferior Colliculus.” *The Journal of Neuroscience* 19(18): 8071–82.

Hurley, Laura M., and Megan R. Sullivan. 2012. “From Behavioral Context to Receptors: Serotonergic Modulatory Pathways in the IC.” *Frontiers in Neural Circuits* 6. http://journal.frontiersin.org/article/10.3389/fncir.2012.00058/abstract (April 25, 2022).

Lladó-Pelfort, L et al. 2010. “Preferential in Vivo Action of F15599, a Novel 5-HT1AR eceptor Agonist, at Postsynaptic 5-HT1AR eceptors: Actions of F15599 at 5-HT1AR eceptors.” *British Journal of Pharmacology* 160(8): 1929–40.

Llado-Pelfort, L. et al. 2012. “5-HT1AR eceptor Agonists Enhance Pyramidal Cell Firing in Prefrontal Cortex Through a Preferential Action on GABA Interneurons.” *Cerebral Cortex* 22(7): 1487–97.

Lovelace, Jonathan W., Iryna M. Ethell, Devin K. Binder, and Khaleel A. Razak. 2018. “Translation-Relevant EEG Phenotypes in a Mouse Model of Fragile X Syndrome.” *Neurobiology of Disease* 115: 39–48.

Martel, Jean Claude et al. 2007. “WAY-100635 Has High Selectivity for Serotonin 5-HT1A versus Dopamine D4 Receptors.” *European Journal of Pharmacology* 574(1): 15–19.

Merenstein, Scott A. et al. 1996. “Molecular-Clinical Correlations in Males with an Expanded FMR1 Mutation.” *American Journal of Medical Genetics* 64(2): 388–94.

Miller, L.J. et al. 1999. “Electrodermal Responses to Sensory Stimuli in Individuals with Fragile X Syndrome: A Preliminary Report.” *American Journal of Medical Genetics* 83(4): 268–79.

Newman-Tancredi, A et al. 2009. “Signal Transduction and Functional Selectivity of F15599, a Preferential Post-Synaptic 5-HT $_{1A}$ Receptor Agonist.” *British Journal of Pharmacology* 156(2): 338–53.

Newman-Tancredi, Adrian. 2011. “Biased Agonism at Serotonin 5-HT1AR eceptors: Preferential Postsynaptic Activity for Improved Therapy of CNS Disorders.” *Neuropsychiatry* 1(2): 149–64.

Newman-Tancredi, Adrian et al. 2022. “Translating Biased Agonists from Molecules to Medications: Serotonin 5-HT1AR eceptor Functional Selectivity for CNS Disorders.” *Pharmacology and Therapeutics* 229.

Nguyen, Anna O., Devin K. Binder, Iryna M. Ethell, and Khaleel A. Razak. 2020. “Abnormal Development of Auditory Responses in the Inferior Colliculus of a Mouse Model of Fragile X Syndrome.” *Journal of Neurophysiology* 123(6): 2101–21.

Pehrson, Rikard, Göran Öjteg, Osamu Ishizuka, and Karl Erik Andersson. 2002. “Effects of NAD-299, a New, Highly Selective 5-HT1AR eceptor Antagonist, on Bladder

Function in Rats." *Naunyn-Schmiedeberg's Archives of Pharmacology* 366(6): 528–36.

Peruzzi, Daniel, and Avijeet Dut. 2004. "GABA, Serotonin and Serotonin Receptors in the Rat Inferior Colliculus." *Brain Research* 998(2): 247–50.

Razak, Khaleel A., Devin K. Binder, and Iryna M. Ethell. 2021. "Neural Correlates of Auditory Hypersensitivity in Fragile X Syndrome." *Frontiers in Psychiatry* 12. https://www.frontiersin.org/article/10.3389/fpsyt.2021.720752 (May 8, 2022).

Rotschafer, Sarah, and Khaleel Razak. 2013. "Altered Auditory Processing in a Mouse Model of Fragile X Syndrome." *Brain Research* 1506: 12–24.

Rousseau, Fransois et al. 1995. "Prevalence of Carriers of Premutation-Size Alleles of the FMRI Gene-and Implications for the Population Genetics of the Fragile X Syndrome." *Am. J. Hum. Genet* 57: 1006–18.

Tupal, Srinivasan, and Carl L. Faingold. 2006. "Evidence Supporting a Role of Serotonin in Modulation of Sudden Death Induced by Seizures in DBA/2 Mice." *Epilepsia* 47(1): 21–26.

Wang, Jun et al. 2017. "A Resting EEG Study of Neocortical Hyperexcitability and Altered Functional Connectivity in Fragile X Syndrome." *Journal of Neurodevelopmental Disorders* 9(1): 11.

Wen, Teresa H et al. 2018. "Genetic Reduction of Matrix Metalloproteinase-9 Promotes Formation of Perineuronal Nets Around Parvalbumin-Expressing Interneurons and Normalizes Auditory Cortex Responses in Developing Fmr1 Knock-Out Mice." *Cerebral Cortex* 28(11): 3951–64.

Williams, Katrina et al. 2013. “Selective Serotonin Reuptake Inhibitors (SSRIs) for Autism Spectrum Disorders (ASD).” *Cochrane Database of Systematic Reviews* (8). https://www.cochranelibrary.com/cdsr/doi/10.1002/14651858.CD004677.pub3/full (May 8, 2022).

Zhang, Honghai et al. 2016. “5-Hydroxytryptophan, a Precursor for Serotonin Synthesis, Reduces Seizure-Induced Respiratory Arrest.” *Epilepsia* 57(8): 1228–35.

Zhang, Honghai et al. 2018. “Optogenetic Activation of 5-HT Neurons in the Dorsal Raphe Suppresses Seizure-Induced Respiratory Arrest and Produces Anticonvulsant Effect in the DBA/1 Mouse SUDEP Model.” *Neurobiology of Disease* 110: 47–58.

Chapter 3: Acute Administration of Serotonin-1A Receptor Agonist NLX-101 Improves Auditory Temporal Processing in Developing *Fmr1* KO Mice

Abstract

Fragile X syndrome (FXS) is a leading known genetic cause of intellectual disability and autism spectrum disorders (ASD)-associated behaviors. A consistent and debilitating phenotype of FXS is auditory hypersensitivity that may lead to delayed language and high anxiety. Consistent with findings in FXS human studies, the mouse model of FXS, the *Fmr1* KO mouse, shows auditory hypersensitivity and temporal processing deficits. In electroencephalograph (EEG) recordings from both humans and mice, these deficits manifest as increased N1 amplitudes in event-related potentials (ERP), increased single trial power (STP) and reduced phase locking to rapid temporal modulations of sound. In our previous study, we found that administration of the selective serotonin-1A receptor biased agonist, NLX-101, significantly protected *Fmr1* KO mice from auditory hypersensitivity-associated seizures. Here we tested the hypothesis that NLX-101 will normalize EEG phenotypes in developing *Fmr1* KO mice. We recorded sound-evoked EEGs at two ages, postnatal (P) 21 and 30 days, following NLX-101 (at 1.8mg/kg i.p.) or saline administration. Saline-injected *Fmr1* KO mice showed increased N1 amplitudes, increased STP and reduced phase locking to auditory gap-in-noise stimuli versus wild-type mice, reproducing previously published EEG phenotypes. An acute injection of NLX-101 did not alter ERP amplitudes at either P21 or P30, but it did significantly reduce STP at P30. Inter-trial phase clustering was significantly increased in both age groups with NLX-101, indicating improved temporal processing. The differential effects of serotonin modulation on ERP, background power and temporal processing suggest different developmental mechanisms leading to these phenotypes.

Together, these results suggest that NLX-101 could constitute a promising treatment option for targeting post-synaptic 5-HT_{1A} receptors to improve auditory temporal processing, which in turn may improve language function in FXS.

3.1 Introduction

Fragile X Syndrome (FXS) is caused by the lack of fragile X messenger ribonucleoprotein (FMRP) and affects approximately 1 in 4000 males and 1 in 8000 females (Hunter et al., 2014). FXS is the leading known genetic cause of intellectual disability and autism spectrum disorder (ASD)-like behaviors. Fragile X Syndrome (FXS) occurs when the number of CGG repeats in the promoter region of the Fragile X messenger ribonucleoprotein (*Fmr1*) gene exceeds approximately 200. This leads to the gene being transcriptionally silenced, resulting in the loss of the fragile X messenger ribonucleoprotein (FMRP) (Pieretti et al., 1991). Children with FXS show cognitive deficits, repetitive behaviors, anxiety, hyperactivity, seizure susceptibility and sensory hypersensitivity (Cordeiro et al., 2010; Hagerman & Hagerman, 2002; Kaufmann et al., 2004). Strong and consistent auditory hypersensitivity impairs daily functioning and may lead to delayed language, high anxiety, and social impairments in FXS. Currently, there are no effective treatments to reduce sensory hypersensitivity in FXS, or other forms of ASD.

Humans with FXS consistently exhibit various sensory processing differences including tactile, visual and auditory hypersensitivity [Tactile: (Miller et al., 1999).

Visual: (Miller et al., 1999; Rigoulot et al., 2017; Van der Molen et al., 2012a). Auditory: (L. E. Ethridge et al., 2016, 2019; D. C. Rojas et al., 2001; Van der Molen et al., 2012b, 2012a)]. The *Fmr1* knockout (KO) mouse shows many of the sensory phenotypes seen in humans [Tactile: (Juczewski et al., 2016). Visual: (Rigoulot et al., 2017). Auditory: (Rotschafer & Razak, 2013); reviewed in (Sinclair et al., 2017).], making it a useful animal model for FXS research, particularly for sensory processing abnormalities. An extreme manifestation of auditory hypersensitivity in the *Fmr1* KO mice is audiogenic seizures (AGS), one kind of generalized convulsive seizures induced by a loud sounds (Chen & Toth, 2001).

Previous studies have shown that activation of serotonin receptors is beneficial in reducing seizures in various epileptic models, including FXS (Armstrong et al., 2020; Heydari & Davoudi, 2017; Tupal & Faingold, 2019; Zhang et al., 2018). Specifically, FPT ((S)-5-(2'-fluorophenyl)-N,N-dimethyl-1,2,3,4-tetrahydronaphthalen-2-amine), a partial agonist of serotonin-1A (5-HT_{1A}) receptor reduced AGS incidence in *Fmr1* KO mice (Armstrong et al., 2020; Canal et al., 2015). Given that FPT is a partial agonist for 5-HT_{1A}, 5-HT_{2C} and 5-HT_{7} receptors, the receptor mechanisms underlying its effect on AGS are unclear. A highly selective agonist of the 5-HT_{1A} receptor, NLX-101, attenuated AGS-induced tonic-clonic seizures and death (Tao et al., 2023). NLX-101 (also known as F15599) has a higher selectivity for 5-HT_{1A} receptors than the commonly used agonist, 8-OH-DPAT, it preferentially acts on post-synaptic receptors and has minimal effect on somatodendritic auto-receptors in raphe nuclei (Lladó-Pelfort et al., 2010; Newman-

Tancredi et al., 2009, 2022), allowing us to narrow down the brain regions and 5-HT_{1A} receptor subpopulations involved.

Electroencephalograph (EEG) recordings have identified remarkably similar auditory processing phenotypes in humans with FXS and the *Fmr1* KO mouse. Physiological measures of auditory hypersensitivity have been observed in humans with FXS, including augmented N1 (first negative peak in sound evoked event related potentials, ERP) amplitudes (Van der Molen et al., 2012a), decreased N1 suppression for repeated sound presentation (Ethridge et al., 2016; Van der Molen et al., 2012b), reduced phase-locking to temporally modulated sound (Ethridge et al., 2017) and increased single trial power (STP) (Ethridge et al., 2017). STP is a measure of background power during stimulus processing, and elevated noise may impact temporal processing. Together, these data indicate elevated background and sound induced power, reduced habituation to repeated stimuli and abnormal temporal processing. Such an abnormal cortical milieu is likely to affect normal auditory processing which is required for speech recognition and language function during development. The *Fmr1* KO mice also show robust N1 amplitude elevation (Croom et al., 2023, 2024; Wen et al., 2019), reduced habituation to repeated stimuli, reduced phase-locking to temporally modulated sound (Croom et al., 2023, 2024; Lovelace et al., 2018) and increased STP (Lovelace et al., 2020). The similarities in EEG phenotypes between humans with FXS and animal models make EEG recordings a promising translational method for evaluation of potential treatments (Razak et al., 2021). These recordings provide data supporting target engagement and offer an early indication of efficacy in clinical studies.

A recent study showed juvenile *Fmr1* KO mice had lower whole-brain 5-HT_{1A} receptor expression than WT mice (Saraf et al., 2024). Considering the promising effects of NLX-101 in reducing severity of behavioral auditory hypersensitivity during development (Tao et al., 2023), we tested the hypothesis that NLX-101 would also reduce EEG measures of auditory hypersensitivity and improve temporal processing. EEG recordings were obtained from *Fmr1* FVB WT and KO mice at two different ages (P21 and P30) with measurements of sound evoked (ERPs) and background responses (non-phase locked STP). The 40 Hz auditory steady state response (ASSR) has been used to study auditory temporal processing and is suggested as a biomarker in neurodevelopmental disorders such as schizophrenia (Thuné et al., 2016) and autism spectrum disorders (Seymour et al., 2020). Therefore, we used this paradigm to quantify temporal processing.

3.2 Methods

3.2.1 Mice

All procedures were approved by the Institutional Animal Care and Use Committee at the University of California, Riverside. Mice were obtained from an in-house breeding colony that originated from Jackson Laboratory (Bar Harbor, ME). The mice used for the study are sighted FVB wild-type (Jax, stock# 004828; WT) and sighted FVB *Fmr1* knock-out (Jax, stock# 004624; *Fmr1* KO). The choice of FVB background strain (as opposed to the C57bl6/J strain) for the WT and *Fmr1* KO mice was guided by

developmental deficits seen in single unit electrophysiology from auditory cortex (Wen et al., 2018) and inferior colliculus (Nguyen et al., 2020) in FVB mice, as well as temporal processing abnormalities (Croom et al., 2023, 2024). In addition, NLX-101 reduces audiogenic seizures in this strain (Tao et al., 2023). One to five mice were housed in each cage under a 12:12-h light-dark cycle and fed ad libitum. The age ranges and sample sizes used in this study (both males and females) are listed in Table 3.1.

Table 3.1. Sample size of the study.

Both *Fmr1* WT and KO (males and females) at two age points (P21 and P30) were used.

	P21				**P30**			
	Saline		NLX-101		Saline		NLX-101	
	WT	KO	WT	KO	WT	KO	WT	KO
M	11	12	11	12	11	11	11	11
F	8	9	9	9	9	10	9	10

3.2.2 Surgery

Different groups of mice underwent epidural electrode implant surgery at two ages: postnatal (P)18-20 and P27-P29. Mice were anesthetized using intraperitoneal (i.p.) injections of 80/20 mg/kg of ketamine/xylazine. Ketamine supplements were given if necessary. ETHIQA-XR (1-shot buprenorphine, 3.25 mg/kg body weight) was administered via subcutaneous injection prior to surgery as an analgesic. Following the removal of fur (Nair), and sterilization (alcohol and iodine wipes) of the scalp, an incision was made to expose the scalp. A Foredom dental drill was used to drill ~1mm diameter

holes in the skull over the right AC, right FC, and left occipital cortex. The screw positions were determined using skull landmarks and coordinates previously reported (Lovelace et al., 2020; Rumschlag et al., 2021; Rumschlag & Razak, 2021; Wen et al., 2019) and were based on single unit recordings (Rotschafer & Razak, 2014; Wen et al., 2019). The wires extending from three-channel posts were wrapped around 1 mm screws and driven into the pre-drilled holes. Dental cement was applied around the screws, on the base of the post, and exposed skull, to secure the implant. Mice were placed on a heating pad until fully awake and were allowed 48-72 hours for recovery before EEG recordings were made.

3.2.3 Drug administration

NLX-101 (also known as F-15599 - (3-Chloro-4-fluorophenyl-(4-fluoro-4- {[(5-methylpyri- midin-2-ylmethyl)-amino]-methyl}-piperidin-1-yl)-methane-one) was provided as a gift from Neurolixis, Inc. The drug was dissolved in sterile physiological saline and diluted to a dose of 1.8 mg/kg, a dose that attenuated AGS in our previous study (Tao et al., 2023). In mice, brain concentration of NLX-101 peaks within first 30 minutes and declines to half concentration after 1h following intraperitoneal (i.p.) administration (Neurolixis Inc., data on file). Saline or 1.8 mg/kg NLX-101 was given to mice through i.p. injection immediately before EEG recordings. The total duration of the EEG recording was 58 minutes, including 8 minutes of resting recording (no stimuli), followed by 30 minutes of gap-in-noise ASSR and 20 minutes of broadband noise. The latter two stimuli were counterbalanced in presentation sequence across mice.

3.2.4 EEG recordings

All EEG recordings were obtained from awake and freely moving mice. EEG recordings were performed at two developmental time points: P20-23 and P29-31, which we refer to as P21 and P30, respectively. Recordings were obtained from the auditory and frontal cortex (AC, FC) electrodes, using the occipital screw as reference. Mice were placed in an arena where they could move freely during the recording. The arena was inside a Faraday cage placed on a vibration isolation table in a sound-insulated and anechoic booth (Gretch-Ken, OR). Mice were attached to an EEG cable via the implanted post under brief anesthesia with isoflurane. The EEG recording set-up has been previously reported (Rumschlag et al., 2021; Rumschlag & Razak, 2021). Briefly, the attached cable was connected via a commutator to a TDT (Tucker Davis Technologies, FL) RA4LI/RA4PA headstage/pre-amp, which was connected to a TDT RZ6 multi-I/O processor. OpenEx (TDT) was used to simultaneously record EEG signals and operate the LED light used to synchronize the video and waveform data. TTL pulses were utilized to mark stimulus onsets on a separate channel in the collected EEG data. The EEG signals were recorded at a sampling rate of 24.414 kHz and down-sampled to 1024 Hz for analysis. All raw EEG recordings were visually examined prior to analysis for artifacts, including loss of signal or signs of clipping, but none were seen. Therefore, no EEG data was rejected. Sound evoked EEGs were recorded as follows:

Auditory ERP: Broadband noise stimuli (1-12 kHz) were presented at 75 dB SPL (120 repetitions, 100 ms duration, 5ms rise/fall time, 0.25 Hz repetition rate) using a speaker (MF1, Tucker Davis Technologies, FL) situated 20 cm above the floor of the

arena. ERP analysis and statistics have been previously described (Rumschlag et al., 2021; Rumschlag & Razak, 2021). Briefly, the EEG trace was split into trials, using the TTL pulses to mark sound onset. Each trial was baseline corrected, such that the mean of the 250 ms baseline period prior to sound onset was subtracted from the trial trace for each trial. Each trial was then detrended (MATLAB detrend function) and all trials were averaged together. Time-frequency analysis was performed with a dynamic complex Morlet wavelet transform with Gabor normalization. The wavelet parameter was set for each frequency to optimize time-frequency resolution.

The single trial power (STP) does not correct for baseline power, allowing for the identification of ongoing 'background activity' during stimulus presentation. To compare the responses across genotype at each developmental time point, a non-parametric permutation test was used, to find clusters of significant values (Maris & Oostenveld, 2007). First, a t-test was run on each time-frequency point for the two groups being compared, yielding the T-values for all points. T-values corresponding to $p<0.025$ were considered significant. Clusters of significant T-values were found, and their area was measured. Next, the group assignments were shuffled randomly, and the t-tests and cluster-measurements were run again on the surrogate groups. This surrogate analysis was performed 2000 times to generate a distribution of cluster sizes that we would expect to find by chance. Originally identified clusters that were larger than 95% of the surrogate clusters were considered significant. This method allows for the identification of significant differences between groups without performing excessive comparisons.

Gap-ASSR: The stimulus used to assess auditory temporal processing is termed the '40 Hz gap-in-noise ASSR' (auditory steady state response, henceforth, 'gap-ASSR') (Rumschlag and Razak, 2021). The stimulus contains alternating 250 ms segments of noise and gap interrupted noise presented at 75 dB SPL. The gaps are strategically placed 25 ms apart, resulting in a presentation rate of 40 Hz, a rate that produces the strongest ASSR signal when measured from the AC and frontal regions and may reflect the resonance frequency of the underlying neural circuits (Galambos et al., 1981; Hwang et al., 2019; Kim et al., 2015; Llinás, 1988; Pastor et al., 2002; Rosanova et al., 2009). For each gap-in-noise segment, the gap widths are chosen at random. Gaps of 3-9 ms widths (with 1 ms as a step) and modulation depths of 75% were used. To measure the ability of the cortex to consistently respond to the gaps in noise, inter-trial phase clustering (ITPC) at 40 Hz was measured (Cohen, 2014). The ITPC is based on the distribution of phase angles in the EEG response at 40 Hz (because the stimulus is a 40 Hz train) across all trials and reflects the precise timing of 40 Hz activity in the underlying neural generators. ITPC can be interpreted independently of power. ITPC ranges between 0 and 1, with 0 indicating high variability (uniform distribution) of phase angles across trials, and 1 indicating the same phase angle for every trial. Because ITPC is sensitive to temporal jitter of responses from one trial to the next, this is a useful and commonly used measure of temporal reliability of responses. (An et al., 2022; Euler et al., 2015; Koerner et al., 2017; Koerner & Zhang, 2015; Rumschlag & Razak, 2021; Yu et al., 2018). The EEG trace was transformed using a dynamic complex Morlet wavelet transform. The ITPC was calculated for each time-frequency point as the average vector for each of the phase

unit vectors recorded across trials (trial count >100 trials per parametric pair). The ITPC values at 40 Hz were averaged to extract the mean ITPC for the parametric pairs in the AC and FC.

3.2.5 Sound Stimulus for C-Fos Expression Analysis

Our previous study showed increased sound evoked cFos activation in the IC of *Fmr1* KO mice compared to WT (Nguyen et al., 2020). To determine if NLX-101 reduced STP by altering neural activity in the IC and/or AC, we examined neural activation by quantifying density of c-Fos expressing cells in these regions in saline vs. NLX-101 treated *Fmr1* KO mice. We used a reduced sound level stimulus for this experiment as our goal was to determine sound evoked responses without confounding motor responses involved in AGS as was done in Nguyen et al. (2020). P21-23 mice were placed in a sound attenuation booth (Gretch-Ken Inc., OR) for sound exposure. The stimulus was a mixture of noise, frequency sweeps and tones (5kHz-30kHz), presented at a sound level of 85 dB SPL for 15 minutes. Pilotstudies show robust c-Fos activation in the IC and AC with this stimulus, without AGS. The stimulus was generated using computer software Audacity and delivered using an amplifier (Marantz, Integrated Amplifier PM8004) and then to the external speaker (FT17H, Fostex International). The sound level was measured with a portable sound meter (BK PRECISION 735) just before each experiment to maintain stable sound output across days.

The sound stimuli were presented to up to 3 mice in a cage, color marked the same way as in AGS experiments. After color coding, i.p. injection of NLX-101 (1.8 mg/kg) or saline was given to each mouse according to its bodyweight. Injected mice were placed in a clean and empty cage with a lid. 10 minutes later, the cage was moved to the sound attenuation chamber with a speaker placed on the top of the cage lid. The full procedure lasted 65 minutes with 5 minutes of habituation (without a sound stimulus) followed by 15 minutes of sound exposure and 45 minutes wait time for c-Fos activation. The sound exposure portion was video recorded (Sony HDR-CX350V) for offline analysis to ensure no AGS were present. Mice were then euthanized with sodium pentobarbital and transcardially perfused with PBS and 4% PFA. All tails were collected for genotyping. The harvested brains were left in 4% PFA overnight and were sunk in 30% sucrose before cryostat sectioning. Brains were sliced in the coronal plane at 40 μm thickness.

3.2.6 Immunohistochemistry

On the first day, brain slices of were washed with PBS 3 times for 3 minutes and quenched with 50mM NH_4Cl in PBS for 15 minutes followed by PBS wash 3 times x 3 minutes. Slices were then blocked with 3% bovine serum albumin (BSA) in PBS for 1 hour at room temperature. Next, brain slices were incubated overnight at 4°C in primary rabbit anti-c-Fos antibody and wisteria floribunda agglutinin (WFA) [c-Fos: 1:2000, Synaptic Systems, #226 003; WFA Lectin conjugated with Fluorescein: 1:500 dilution,

Vector Laboratories, #FL-1351-2] in 1% BSA and 0.1% Triton X-100 in 0.1 M PBS. On the next day, slices were washed (3 x 3 minutes) with PBS and incubated in the secondary antibody (1:500; donkey anti-rabbit AlexaFluor594 #A21207) with 1% BSA in PBS for 1 hour at room temperature. Then slices were washed in PBS (3 x 3 minutes) and mounted on glass slides with a mounting media (DABCO, #17985-200), cover-slipped and sealed with nail polish. The sections were stored in the dark at 4°C until imaging was done. Stained slides were imaged using an inverted confocal microscope (zeiss LSM880) with 10x objective and a stack of images was collected with 2048 x 2048 resolution at 6 µm- z-steps. Image analysis was done with ImageJ Software (Schneider et al., 2012) and QuPath (Bankhead et al., 2017) . The counting area of the IC and AC were windowed with ImageJ based on Allen Brain Atlas. The window size was determined by sufficient coverage of the region of interest. A 400µm wide window was placed on the IC and the AC as shown in Figure 8A-D. The number of c-Fos positive cells was quantified in QuPath with the built-in background subtraction program (background radius = 8 µm). The same setting was applied across images for counting.

3.2.7 Statistics

Statistics were performed on GraphPad Prism 9. To evaluate the effects of genotype (2 levels) and treatment (2 levels), multiple Mann-Whitney tests were used for ERP analysis. P-values were adjusted for multiple comparisons with Holm-Sidak method. A two-way ANOVA with repeated measures was used for gap-ASSR analysis, with the

two factors being genotype (2 levels) and treatment (2 levels). A repeated measures ANOVA was chosen as multiple gap duration data points were collected from a single mouse in a recording session. Greenhouse-Geisser corrections were applied if necessary. Post hoc contrasts with Sidak corrections for multiple comparisons were used. Cortical regions (AC, FC) and ages (P21 and P30) were analyzed separately. Male and female data were combined for the main analysis. The supplemental analysis shows effect of sex on measurements. Effects of $p < 0.05$ were considered statistically significant, and denoted as *$p < 0.05$, **$p < 0.01$, ***$p < 0.001$, ****$p < 0.0001$. C-Fos positive cell density (saline vs. NLX-101) was analyzed with a non-parametric t-test (Mann-Whitney test). Effects of $p<0.05$ were considered statistically significant, and denoted as * $p<0.05$, ** $p<0.01$, *** $p<0.001$, **** $p<0.0001$.

3.3 Results

3.3.1 Larger ERP amplitudes seen in Fmr1 KO mice were not affected by NLX101 at P21 or P30

As seen in humans with FXS (Ethridge et al., 2016, 2019; Rigoulot et al., 2017; D. C. Rojas et al., 2001; Van der Molen et al., 2012a, 2012b), *Fmr1* KO mice show increased amplitude of ERP peaks relative to WT mice (Croom et al., 2023, 2024; Wen et al., 2019). Here we tested whether acute administration of NLX-101 altered auditory hypersensitivity as measured using ERP amplitudes (Figure 3.1). At P21, Figure 3.1 A1-A2 shows average ERP waveforms in the AC in WT and *Fmr1* KO mice, comparing

saline and NLX-101. Qualitative examinations of ERPs from saline treated WT and saline treated KO reveal a significant genotype difference (Figure 3.1 A3-A5). This is also seen in the FC (Figure 3.1 B3-B5). At P21, no significant differences were seen in P1 or P2 amplitudes in both AC (Figure 3.1 A3, A5) and FC (Figure 3.1 B3, B5). Significantly increased N1 amplitudes were seen in both AC (Figure 3.1 A4) and FC (Figure 3.1 B4) in *Fmr1* KO mice compared to WT mice regardless of treatment (AC: Saline – Multiple Mann-Whitney test. Adjusted p=0.002479 and NLX-101 – Multiple Mann-Whitney test. Adjusted p=0.000041; FC: Saline - Multiple Mann-Whitney test. Adjusted p=0.003659 and NLX-101 - Multiple Mann-Whitney test. Adjusted p=0.003659).

Similar results were observed at P30 (Figure 3.2). Larger N1, but not P1 or P2, amplitudes were seen in both AC (Figure 3.2 A3-A5) and FC (Figure 3.2 B3-B5) in *Fmr1* KO mice compared to WT mice. NLX-101 treatment failed to change N1 amplitude in AC (N1 amplitude: Saline - Multiple Mann-Whitney test. Adjusted p=0.002681 and NLX-101 - Multiple Mann-Whitney test. Adjusted p=0.018409) and FC (N1 amplitude: Saline - Multiple Mann-Whitney test. Adjusted p=0.003279 and NLX-101 -Multiple Mann-Whitney test. Adjusted p=0.004622). Taken together, these data indicate that at P21 and P30, N1 amplitude that reflects auditory cortical processing and synchrony is elevated toward sound stimulus in the KO mice, but acute NLX-101 treatment does not correct this phenotype.

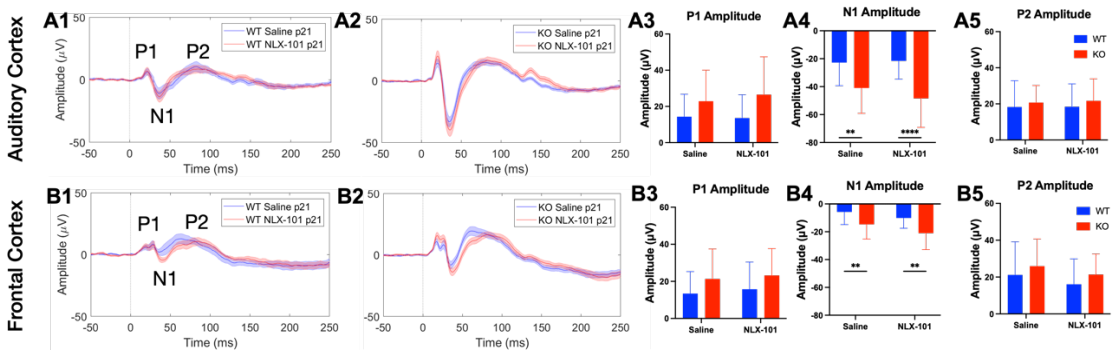

Figure 3.1. Larger ERP N1 amplitudes in Fmr1 KO mice at P21 are not corrected by NLX-101.

(A1-A5) ERP in response to noise stimulus recorded from the auditory cortex at P21. (A1-A2) Grand averaged ERP traces from WT (A1) and KO (A2) mice, showing treatment comparison. (A3-A5) Genotype and treatment comparison in P1, N1 and P2 amplitudes. (B1-B5) ERP responses from the frontal cortex at P21. (B1-B2) Grand averaged ERP traces from WT (B1) and KO (B2), showing treatment comparison. (B3-B5) Genotype and treatment comparison in P1, N1 and P2 amplitudes. In both cortical regions, N1 amplitudes were larger in *Fmr1* KO mice, compared to WT mice regardless of treatment. There were no significant differences in P1 or P2 amplitudes. Full statistics report is in Table 3.2. *p < 0.05, **p < 0.01, ***p < 0.001, ****p < 0.0001. Error bars show standard deviation.

Table 3.2. Event related potentials P1, N1, P2 amplitude statistics at P21

Cortical Region	ERP component	Factor	Genotype/Treatment	Mann-Whitney U	Adjusted P Value
Auditory Cortex	P1 Amplitude	Treatment	WT	185	0.9005
			KO	200	0.8544
		Genotype	Saline	131	0.0651
			NLX-101	126	0.0558
	N1 Amplitude	Treatment	WT	184	0.8786
			KO	182	0.5681
		Genotype	**Saline**	**90**	**0.0025**
			NLX-101	**56**	**0.00004**
	P2 Amplitude	Treatment	WT	183	0.8567
			KO	187	0.6524
		Genotype	Saline	157	0.2585
			NLX-101	148	0.2066
Frontal Cortex	P1 Amplitude	Treatment	WT	180	0.8122
			KO	197	0.8122
		Genotype	Saline	138	0.0989
			NLX-101	133	0.0883
	N1 Amplitude	Treatment	WT	128	0.1610
			KO	162	0.1610
		Genotype	**Saline**	**87**	**0.0037**
			NLX-101	**98**	**0.0037**
	P2 Amplitude	Treatment	WT	153	0.5223
			KO	187	0.5223
		Genotype	Saline	155	0.2363
			NLX-101	137	0.1128

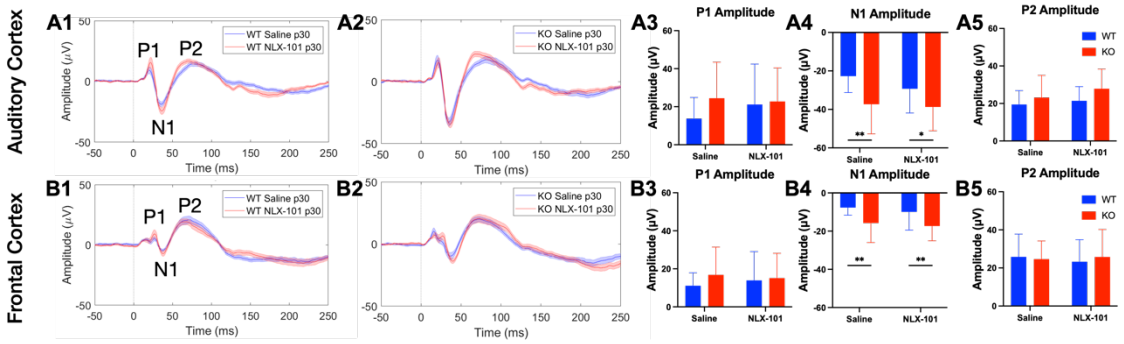

Figure 3.2. Larger ERP N1 amplitudes in Fmr1 KO mice at P30 are not corrected by NLX-101.

(A1-A5) ERP in response to noise stimulus recorded from the auditory cortex at P30. (A1-A2) Grand averaged ERP traces from WT (A1) and KO (A2) mice, showing treatment comparison. (A3-A5) Genotype and treatment comparison in P1, N1 and P2 amplitudes. (B1-B5) ERP responses from the frontal cortex at P30. B1-B2) Grand averaged ERP traces from WT (B1) and KO (B2), showing treatment comparison. (B3-B5) Genotype and treatment comparison in P1, N1 and P2 amplitudes. In both cortical regions, N1 amplitudes were larger in *Fmr1* KO mice, compared to WT mice regardless of treatment. There were no significant differences in P1 or P2 amplitudes. Full statistics report is in Table 3.3. *p < 0.05, **p < 0.01, ***p < 0.001, ****p < 0.0001. Error bars show standard deviation.

Table 3.3. Event related potentials P1, N1, P2 amplitude statistics at P30

Cortical Region	ERP component	Factor	Genotype/Treatment	Mann-Whitney U	Adjusted P Value
Auditory Cortex	P1 Amplitude	Treatment	WT	145	0.2663
			KO	211	0.8228
		Genotype	Saline	136	0.1062
			NLX-101	185	0.5268
	N1 Amplitude	Treatment	WT	146	0.2763
			KO	197	0.5667
		Genotype	**Saline**	**90**	**0.0027**
			NLX-101	**120**	**0.0184**
	P2 Amplitude	Treatment	WT	182	0.6395
			KO	142	0.0956
		Genotype	Saline	185	0.5268
			NLX-101	129	0.0683
Frontal Cortex	P1 Amplitude	Treatment	WT	192	0.8410
			KO	191	0.7188
		Genotype	Saline	161	0.3732
			NLX-101	188	0.5788
	N1 Amplitude	Treatment	WT	163	0.5474
			KO	212	0.8422
		Genotype	**Saline**	**92**	**0.0033**
			NLX-101	**103**	**0.0046**
	P2 Amplitude	Treatment	WT	173	0.7272
			KO	216	0.9207
		Genotype	Saline	196	0.9149
			NLX-101	195	0.9149

3.3.2 Elevated single trial power observed in Fmr1 KO mice was corrected by NLX-101 at P30, but not P21

A consistent phenotype in both humans with FXS and the *Fmr1* KO mice is elevated single trial power (STP) measured during acoustic stimulation (Human: (Ethridge et al., 2020; Ethridge et al., 2016). Mouse: (Jonak et al., 2020; Lovelace et al., 2018, 2020; Rais et al., 2022).) STP is a measure of background noise at different spectral bands and increased STP may disrupt temporal consistency in auditory responses during repeated stimulation. We tested if acute NLX-101 reduces STP in *Fmr1* KO mice at P21 and P30. Figure 3.3 A-B shows the genotype effect in saline-treated mice at P21. In the AC (Figure 3.3A) and in the FC (Figure 3.3B), significantly higher STP during ERP

measurements was found in saline treated *Fmr1* KO mice compared to WT mice. STP was increased across a broad range of frequencies centered around ~40 Hz in the KO mice (Figures 3.3 A-B). At P21, treatment with NLX-101 did not affect *Fmr1* KO (Figure 3.3 C-D) or WT mice (Figure 3.3 E-F) compared to saline in either cortical region.

At P30, however, NLX-101 had a suppressive effect on STP (Figure 3.4). In saline treated P30 mice, elevated STP was found in *Fmr1* KO mice in both AC (Figure 3.4A) and FC (Figure 3.4B) compared to WT mice. Acute NLX-101 administration significantly reduced STP in *Fmr1* KO mice compared to saline in both cortical regions (Figure 3.4 C-D). Comparison of NLX-101 treated KO mice to saline treated WT mice showed no difference in STP in both AC (Figure 3.4E) and FC (Figure 3.4F). NLX-101 did not affect STP in WT groups (Figure 3.4 G-H). Taken together, these data show significantly elevated background noise suggested by increased STP in both AC and FC at both P21 and P30. NLX-101 had no effect at P21, but significantly reduced this sensory phenotype at P30 to WT levels, suggesting this effect was specific to the *Fmr1* KO mice.

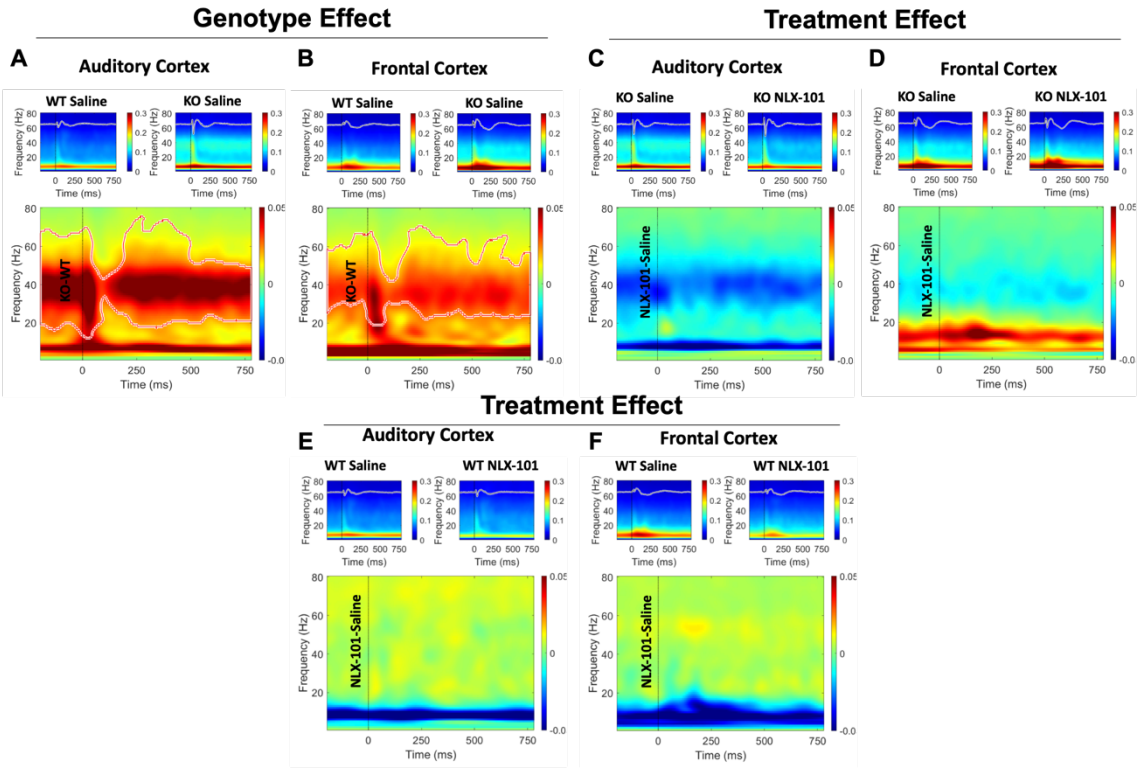

Figure 3.3 STP is significantly higher in Fmr1 KO compared with WT at P21, and NLX-101 failed to correct such phenotype.

(A-B) In each figure, two smaller panels at the top show grand averaged STP from each group. The larger panel at the bottom shows the STP difference between the two groups of mice. The vertical dashed line shows sound onset. The contoured area in the larger panels show regions of significant differences between the group being compared. Warm colors show elevated STP, and cool colors show a reduction in the difference plots. (A-B) Comparison of saline treated KO and WT mice shows a significant genotype effect on STP at P21. *Fmr1* KO mice have elevated STP in both auditory and frontal cortex compared with WT mice. (C-D) Comparison of NLX-101 and saline treated *Fmr1* KO mice shows there was no treatment effect in either cortical region at P21. (E-F) No treatment effect of NLX-101 was seen in WT mice either.

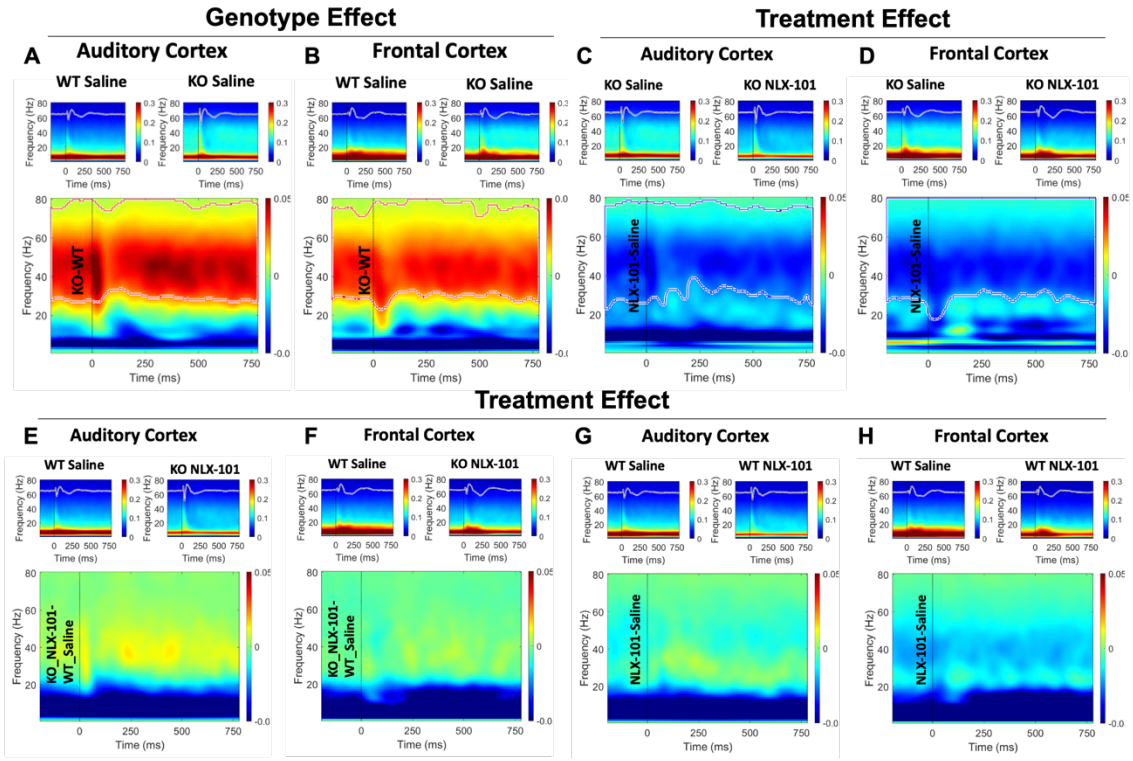

Figure 3.4. STP is significantly higher in Fmr1 KO mice compared with WT mice at P30, and NLX-101 reduced elevated STP in Fmr1 KO mice without affecting WT mice.

The details of this figure are similar to those described in Figure 3.3. (A-B) Comparison of saline treated KO and WT mice shows a significant genotype effect on STP at P30. *Fmr1* KO mice have elevated STP in both auditory and frontal cortex compared with WT mice. (C-D) STP in *Fmr1* KO mice was significantly reduced after NLX-101 compared with saline treated KO mice. (E-F) Comparison between KO NLX-101 treated group and WT saline treated group. No difference was seen, suggesting NLX-101 reduced elevated STP in *Fmr1* KO mice to the level that is indistinguishable from WT mice. (G-H) No treatment effect of NLX-101 was seen in WT mice in either cortical region suggesting NLX-101 effects on STP are specific to *Fmr1* KO mice.

3.3.3 NLX-101 improves temporal processing

The 40 Hz gap-ASSR is a paradigm in which EEG signals can be recorded in response to gaps presented at 40 Hz in noise. By varying the gap width, the fidelity with which the underlying neural generators phase lock to the temporal modulation across trials can be quantified as the inter-trial phase clustering (ITPC). Our previous study showed cortical deficits in ITPC in developing *Fmr1* KO mice (Croom et al., 2023, 2024). Here we tested whether NLX-101 improves ITPC in the KO mice.

Figure 3.5 shows gap-ASSR heat maps of ITPC from both AC and FC of representative mice under each condition at P21: saline treated WT (Figure 3.5A), NLX-101 treated WT (Figure 3.5B), saline treated KO (Figure 3.5C), and NLX-101 treated KO (Figure 3.5D). Each panel shows the ITPC at a specific gap width in a single mouse. The columns (left to right) show increasing gap widths. Warmer colors indicate higher ITPC, with the ITPC scale shown at the right end of each row of heat maps. Sound onset is at 0 msec. In these examples, ITPC is highest at 40 Hz as expected, given that the gap stimulus was inserted at 40 Hz in the background noise. As expected, ITPC improved with gap width. These illustrative examples suggest that NLX-101 treatment improved ITPC. The population data quantification (Figure 3.6) supports these suggestions. Figure 3.6A shows averaged ITPC in the AC across the gap widths of 3-9ms in saline treated P21 *Fmr1* WT and KO mice. No genotype effect was found (Repeated two-way ANOVA. $p= 0.1181$). Figure 3.6B shows analogous data from the FC in which no genotype differences were found (two-way ANOVA. $p= 0.8789$). Comparison of averaged ITPC between saline and NLX-101 treatment in the AC (Figure 3.6C) and FC (Figure 3.6D) in

WT mice showed no difference between treatments (AC: Repeated two-way ANOVA. p= 0.1394, FC: Repeated two-way ANOVA. p= 0.7999). However, acute NLX-101 administration significantly increased ITPC in the AC, but not the FC, in *Fmr1* KO group (Figure 3.6 E-F AC: Repeated two-way ANOVA. p= 0.0336; FC: Repeated two-way ANOVA. p= 0.1968). Therefore, NLX-101 showed specific improvement of temporal processing in the *Fmr1* KO mice at P21.

Figure 3.7 shows gap-ASSR heat maps of ITPC from both AC and IC of representative mice under each condition at P30: saline treated WT (Figure 3.7A), NLX-101 treated WT (Figure 3.7B), saline treated KO (Figure 3.7C), and NLX-101 treated KO (Figure 3.7D). NLX-101 improves ITPC in these mice, compared to saline. Across the population of mice, at P30, ITPC during gap-ASSR stimuli was significantly reduced in *Fmr1* KO mice compared to WT controls in the FC (Figure 3.8B, repeated two-way ANOVA. p= 0.0117), but not in the AC (Figure 3.8A, repeated two-way ANOVA. p=0.7237). Acute NLX-101 administration significantly increased ITPC in both the AC and the FC in *Fmr1* KO group (Figure 3.8 E-F). Besides, NLX-101 treatment also significantly improved ITPC in the FC in WT mice (Figure 3.8D), indicating broad benefits to temporal processing in developing mice. In WT mice, no treatment effect was observed in the AC (Figure 3.8C, repeated two-way ANOVA. p=0.2052). However, in the FC, NLX-101 treatment significantly increased ITPC (Figure 3.8D, repeated two-way ANOVA. p=0.0023). In *Fmr1* KO mice acute treatment of NLX-101 significantly increased ITPC in the AC (Figure 3.8E, repeated two-way ANOVA. p=0.0006) and the FC (Figure 3.8F, repeated two-way ANOVA. p<0.0001). Taken together, significant

deficits in temporal processing were seen in saline treated *Fmr1* KO mice at P30. Temporal processing at P30 was improved in both cortical regions in the *Fmr1* KO mice with NLX-101.

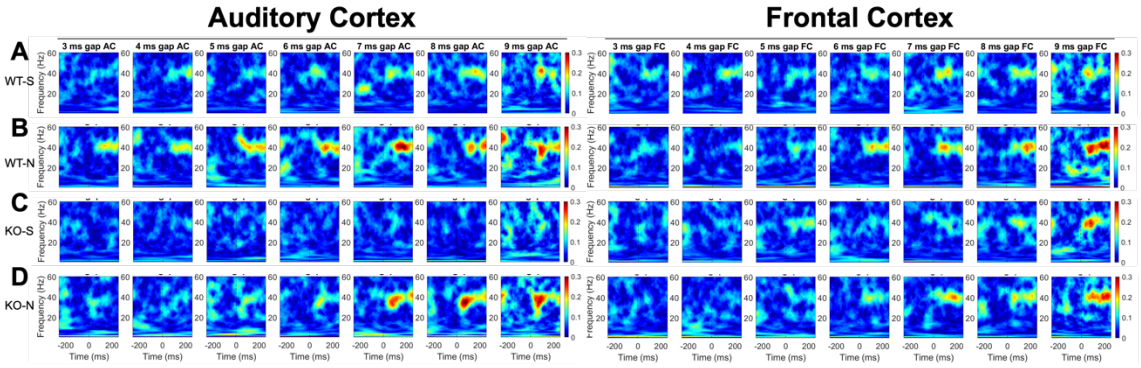

Figure 3.5. Representative gap-ASSR ITPC heatmaps from auditory and frontal cortex of Fmr1 WT and KO mice at P21.

Each panel shows the ITPC (scale is seen at the right edge of the last panel in AC and FC data, warmer colors mean greater ITPC) obtained from individual animals at a specific gap width. Each column shows ITPC for the same gap width, with the gap width increasing from left to right. As expected, ITPC increases with increasing gap width. The y-axis of each panel is the range of frequencies analyzed for ITPC. Not surprisingly, ITPC is maximum around 40 Hz, which was the frequency of gap-ASSR stimulus. The data shown for AC and FC in each row is from the same mice, with different example mice shown in the different rows. (A) WT saline. (B) WT NLX-101. (C) KO saline. (D) KO NLX-101. In these examples, mice treated with NLX-101 show higher ITPCs.

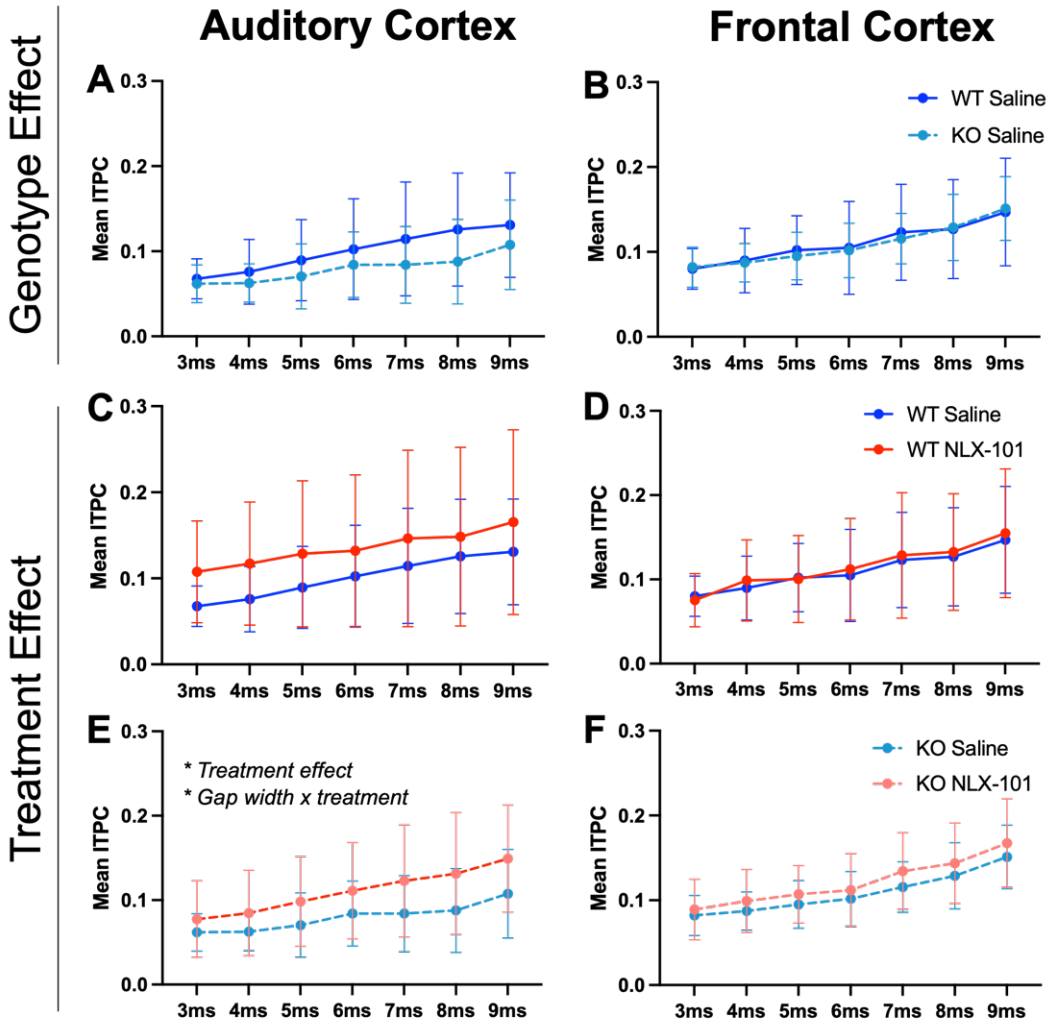

Figure 3.6. No genotype difference in ITPC was found at P21, but NLX-101 treatment increased ITPC in KO mice in the auditory cortex.

(A-B) No significant difference in ITPC for gap-ASSR was seen between *Fmr1* WT and KO mice in the auditory and frontal cortex. (C-D) No treatment effect of NLX-101 was seen in WT mice. (E-F) Treatment effect of NLX-101 in *Fmr1* KO mice. NLX-101 significantly increased ITPC in KO group in the auditory, but not the frontal, cortex. Besides, NLX-101 increased ITPC as gap width increases in the auditory cortex (treatment × gap width interaction). Full statistics report is in Table 3.4 and Table 3.6. *p < 0.05, **p < 0.01, ***p < 0.001, ****p < 0.0001. Error bars show standard deviation.

Table 3.4. Gap-ASSR treatment statistics at P21

Genotype	Cortical Region	Factor/ Interaction	ANOVA Results	P Value
WT	Auditory Cortex	Gap width x Treatment	F (6, 222) = 0.6361	0.7013
		Gap Width	**F (2.510, 92.86) = 27.97**	**<0.0001**
		Treatment	F (1, 37) = 2.281	0.1394
	Frontal Cortex	Gap width x Treatment	F (6, 222) = 0.4216	0.8642
		Gap Width	**F (3.171, 117.3) = 37.42**	**<0.0001**
		Treatment	F (1, 37) = 0.06521	0.7999
KO	Auditory Cortex	**Gap width x Treatment**	**F (6, 240) = 2.220**	**0.0419**
		Gap Width	**F (2.781, 111.2) = 34.44**	**<0.0001**
		Treatment	**F (1, 40) = 4.844**	**0.0336**
	Frontal Cortex	Gap width x Treatment	F (6, 240) = 0.3996	0.8789
		Gap Width	**F (4.427, 177.1) = 70.54**	**<0.0001**
		Treatment	F (1, 40) = 1.723	0.1968

Table 3.6. Gap-ASSR genotype statistics at P21

Cortical Region	Factor/ Interaction	ANOVA Results	P Value
Auditory Cortex	Gap width x Genotype	F (6, 228) = 2.008	0.0656
	Gap Width	**F (2.590, 98.44) = 28.37**	**<0.0001**
	Genotype	F (1, 38) = 2.556	0.1181
Frontal Cortex	Gap width x Genotype	F (6, 228) = 0.4566	0.8398
	Gap Width	**F (4.164, 158.2) = 48.31**	**<0.0001**
	Genotype	F (1, 38) = 0.02353	0.8789

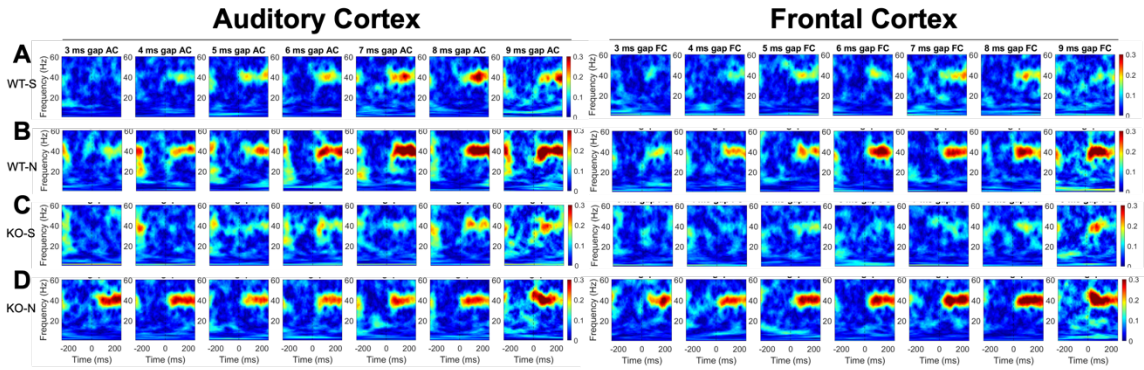

Figure 3.7. Representative gap-ASSR ITPC heatmaps from auditory and frontal cortex of Fmr1 WT and KO mice at P30.

(A) WT saline. (B) WT NLX-101. (C) KO saline. (D) KO NLX-101. Details as in Figure 3.5.

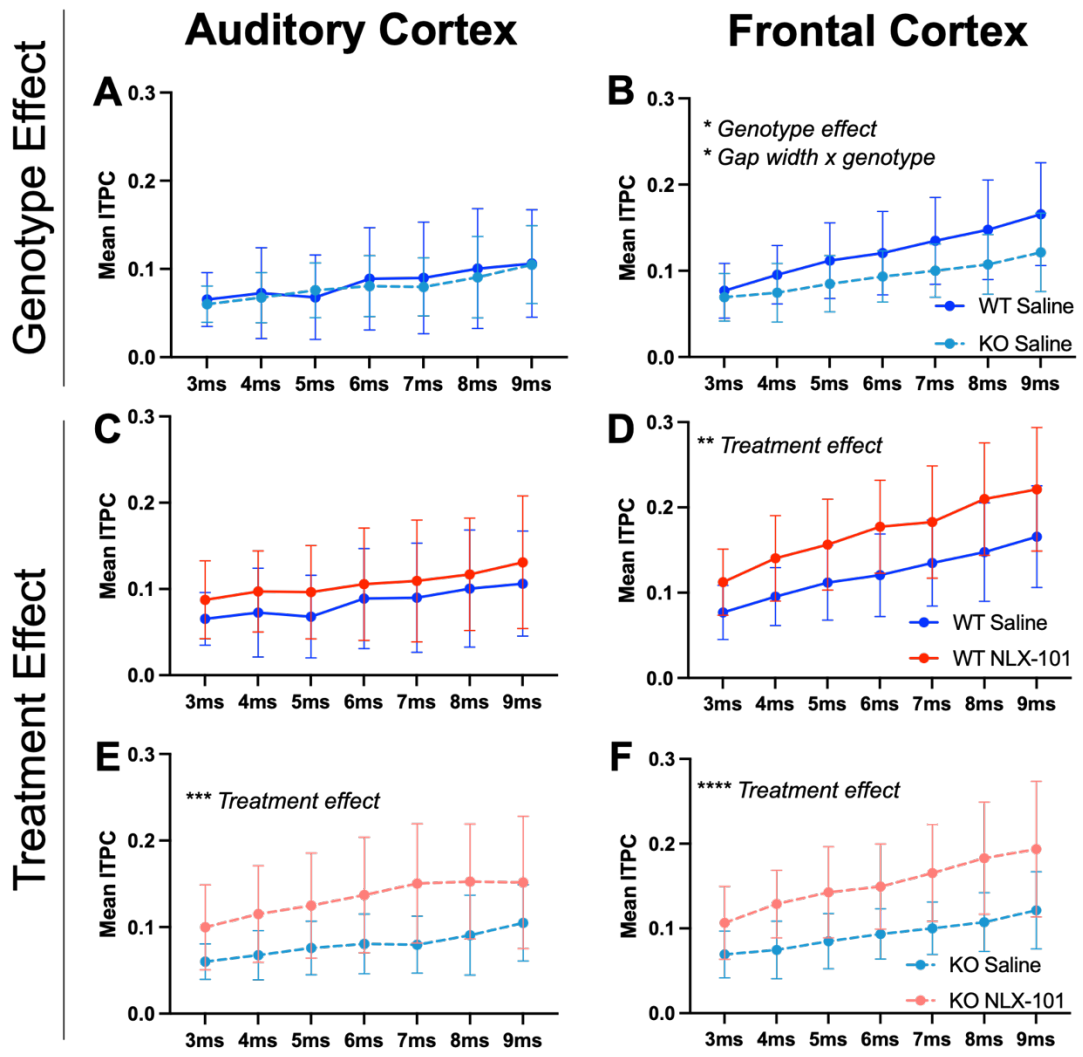

Figure 3.8. Genotype difference in ITPC was found in frontal, but not auditory, cortex at P30. NLX-101 increased ITPC in Fmr1 WT and KO mice.

(A-B) No genotype difference in gap-ASSR ITPC was found in the auditory cortex, but ITPC was significantly lower in the frontal cortex of *Fmr1* KO mice compared with WT controls. (C-D) Treatment effect of NLX-101 on *Fmr1* WT mice. NLX-101 significantly increased ITPC in the frontal cortex but not the auditory cortex. (E-F) Acute NLX-101 administration significantly increased ITPC in both auditory and frontal cortex of the *Fmr1* KO mice. Full statistics report is in Table 3.5 and Table 3.7. *$p < 0.05$, **$p < 0.01$, ***$p < 0.001$, ****$p < 0.0001$. Error bars show standard deviation.

Table 3.5. Gap-ASSR treatment statistics at P30

Genotype	Cortical Region	Factor/ Interaction	ANOVA Results	P Value
WT	Auditory Cortex	Gap width x Treatment	F (6, 228) = 0.2886	0.9420
		Gap Width	**F (3.105, 118.0) = 13.59**	**<0.0001**
		Treatment	F (1, 38) = 1.661	0.2052
	Frontal Cortex	Gap width x Treatment	F (6, 228) = 1.354	0.2343
		Gap Width	**F (4.233, 160.8) = 77.05**	**<0.0001**
		Treatment	**F (1, 38) = 10.69**	**0.0023**
KO	Auditory Cortex	Gap width x Treatment	F (6, 240) = 1.873	0.0862
		Gap Width	**F (3.645, 145.8) = 19.67**	**<0.0001**
		Treatment	**F (1, 40) = 13.99**	**0.0006**
	Frontal Cortex	**Gap width x Treatment**	**F (6, 240) = 2.847**	**0.0107**
		Gap Width	**F (3.327, 133.1) = 40.83**	**<0.0001**
		Treatment	**F (1, 40) = 22.11**	**<0.0001**

Table 3.7. Gap-ASSR genotype statistics at P30

Cortical Region	Factor/ Interaction	ANOVA Results	P Value
Auditory Cortex	Gap width x Genotype	F (6, 234) = 0.7458	0.6133
	Gap Width	**F (3.637, 141.9) = 17.44**	**<0.0001**
	Genotype	F (1, 39) = 0.1268	0.7237
Frontal Cortex	**Gap width x Genotype**	**F (6, 234) = 2.806**	**0.0118**
	Gap Width	**F (4.306, 167.9) = 43.35**	**<0.0001**
	Genotype	**F (1, 39) = 6.991**	**0.0117**

3.3.4 Sex Differences in temporal processing was observed in WT group

Sex difference in temporal processing was only found in WT group at both P21 (Figure S1) and P30 (Figure S2), but not in the KO group at either age (Figure S3 and

Figure S4). At P21, saline treated WT females showed significantly higher ITPC in the FC than the male counterpart (Figure S1 B, repeated two-way ANOVA. Sex effect: $p=0.0266$). At P21, the NLX-101 treated WT females exhibited higher ITPC at longer gap width than the male counterpart (Figure S1 D, repeated two-way ANOVA. Gap width × Sex: $p=0.0249$). At P30, sex difference in ITPC was only found in the treatment group where NLX-101 treated males had higher ITPC than female counterpart (Figure S2 D, repeated two-way ANOVA. $p=0.0299$). Taken together, the effect of NLX-101 in improving temporal processing is not specific to FXS, instead, there might be a shared underlying circuit of temporal processing under serotonin modulation. Such modulation may differ in male and female at early age point (P21). This finding is different from our previous report (Croom et al., 2023, 2024), which could be potentially due to handling and injection involved in this study.

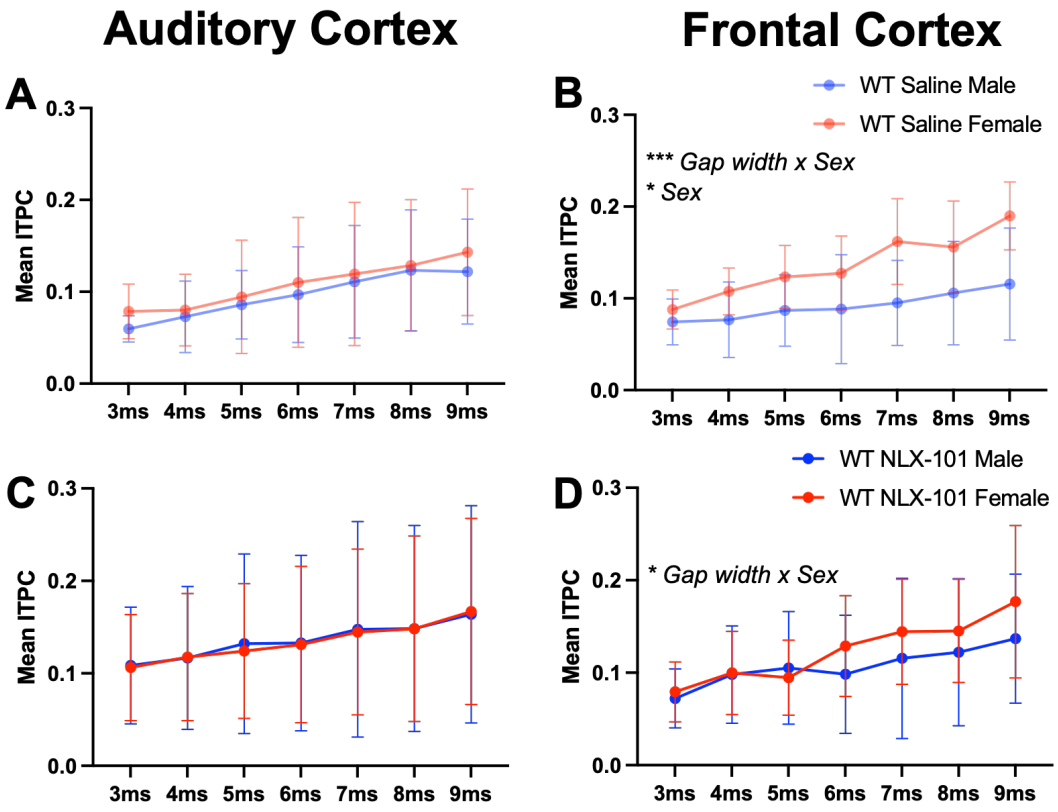

Figure S3.1. Sex differences in ITPC was found in Fmr1 WT mice at P21.

(A-B) Sex difference was found in the frontal cortex in *Fmr1* WT saline treated mice. ITPC at different gap widths was significantly affected by sex. Female has significantly higher ITPC compared with male counterparts. Besides, female also has higher ITPC at longer gaps. (C-D) Interaction between sex and gap width was found significant in the frontal cortex in Fmr1 WT mice after NLX-101 treatment. Full statistics report is in Table S3.1. *$p < 0.05$, **$p < 0.01$, ***$p < 0.001$, ****$p < 0.0001$. Error bars show standard deviation.

Table S3.1. WT gap-ASSR sex differences statistics at P21

Group	Cortical Region	Factor/ Interaction	ANOVA Results	P Value
WT_Saline_P21	Auditory Cortex	Gap width x Sex	F (6, 102) = 0.2516	0.9576
		Gap Width	**F (2.084, 35.44) = 16.06**	**<0.0001**
		Sex	F (1, 17) = 0.2682	0.6112
	Frontal Cortex	**Gap width x Sex**	**F (6, 102) = 4.321**	**0.0006**
		Gap Width	**F (3.476, 59.08) = 23.92**	**<0.0001**
		Sex	**F (1, 17) = 5.892**	**0.0266**
WT_NLX-101_P21	Auditory Cortex	Gap width x Sex	F (6, 108) = 0.08309	0.9978
		Gap Width	**F (2.582, 46.47) = 10.84**	**<0.0001**
		Sex	F (1, 18) = 0.001554	0.9690
	Frontal Cortex	**Gap width x Sex**	**F (6, 108) = 2.530**	**0.0249**
		Gap Width	**F (3.153, 56.76) = 22.31**	**<0.0001**
		Sex	F (1, 18) = 0.4625	0.5051

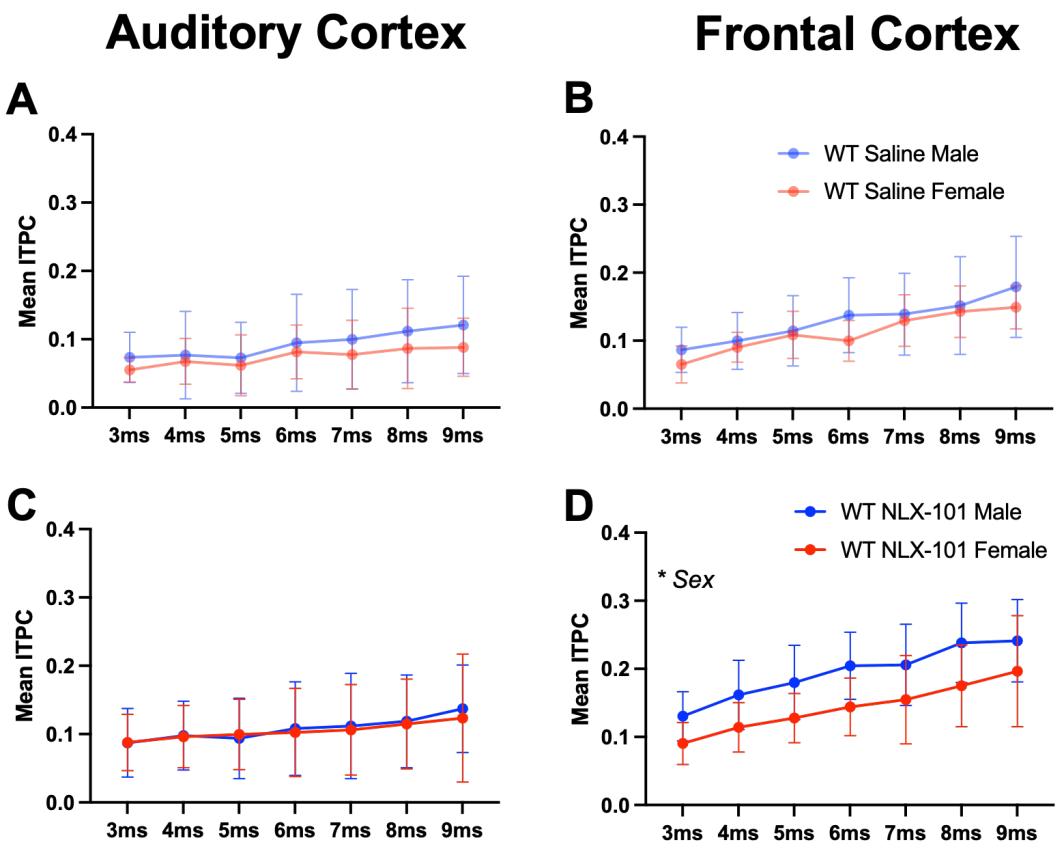

Figure S3.2. Sex differences in ITPC was found in Fmr1 WT mice at P30.

(A-B) No sex differences were found in either auditory cortex or frontal cortex in saline treated groups. (C-D) Sex differences were found in NLX-101 treated WT mice only in the frontal cortex (D) but not in the auditory cortex (C). NLX-101 treated WT males showed significantly higher ITPC than female counterparts. Full statistics report is in Table S3.2. *p < 0.05, **p < 0.01, ***p < 0.001, ****p < 0.0001. Error bars show standard deviation.

Table S3.2. WT gap-ASSR sex differences statistics at P30

Group	Cortical Region	Factor/ Interaction	ANOVA Results	P Value
WT_Saline_P30	Auditory Cortex	Gap width x Sex	F (6, 108) = 0.5677	0.7552
		Gap Width	**F (3.231, 58.16) = 7.810**	**<0.0001**
		Sex	F (1, 18) = 0.6768	0.4215
	Frontal Cortex	Gap width x Sex	F (6, 108) = 1.172	0.3269
		Gap Width	**F (3.892, 70.05) = 28.30**	**<0.0001**
		Sex	F (1, 18) = 0.8938	0.3570
WT_NLX-101_P30	Auditory Cortex	Gap width x Sex	F (6, 108) = 0.2326	0.9651
		Gap Width	**F (2.550, 45.91) = 5.232**	**0.0052**
		Sex	F (1, 18) = 0.01807	0.8946
	Frontal Cortex	Gap width x Sex	F (6, 108) = 0.5645	0.7577
		Gap Width	**F (3.487, 62.76) = 49.25**	**<0.0001**
		Sex	**F (1, 18) = 5.557**	**0.0299**

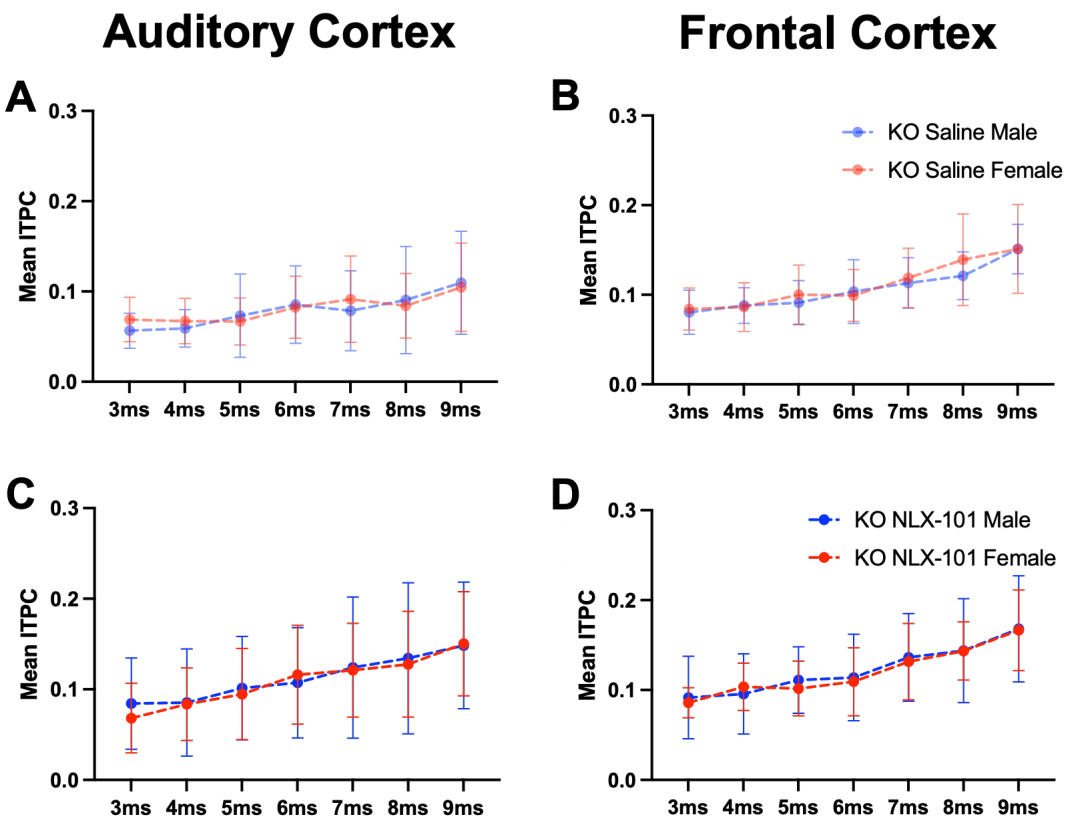

Figure S3.3. Sex differences in ITPC was not found in Fmr1 KO mice at P21.

(A-B) Sex differences were not observed in saline-treated KO mice in either cortex. (C-D) Sex differences were not seen in NLX-101-treated KO mice in either cortex. Full statistics report is in Table S3.3. *p < 0.05, **p < 0.01, ***p < 0.001, ****p < 0.0001. Error bars show standard deviation.

Table S3.3. KO gap-ASSR sex differences statistics at P21

Group	Cortical Region	Factor/ Interaction	ANOVA Results	P Value
KO_Saline_P21	Auditory Cortex	Gap width x Sex	F (6, 114) = 0.8582	0.5281
		Gap Width	**F (2.682, 50.95) = 16.06**	**<0.0001**
		Sex	F (1, 19) = 0.01326	0.9095
	Frontal Cortex	Gap width x Sex	F (6, 114) = 0.7417	0.6171
		Gap Width	**F (4.397, 83.58) = 32.47**	**<0.0001**
		Sex	F (1, 19) = 0.1451	0.7075
KO_NLX-101_P21	Auditory Cortex	Gap width x Sex	F (6, 114) = 0.5142	0.7966
		Gap Width	**F (2.354, 44.72) = 23.28**	**<0.0001**
		Sex	F (1, 19) = 0.01842	0.8935
	Frontal Cortex	Gap width x Sex	F (6, 114) = 0.3490	0.9092
		Gap Width	**F (3.508, 66.66) = 35.58**	**<0.0001**
		Sex	F (1, 19) = 0.02423	0.8779

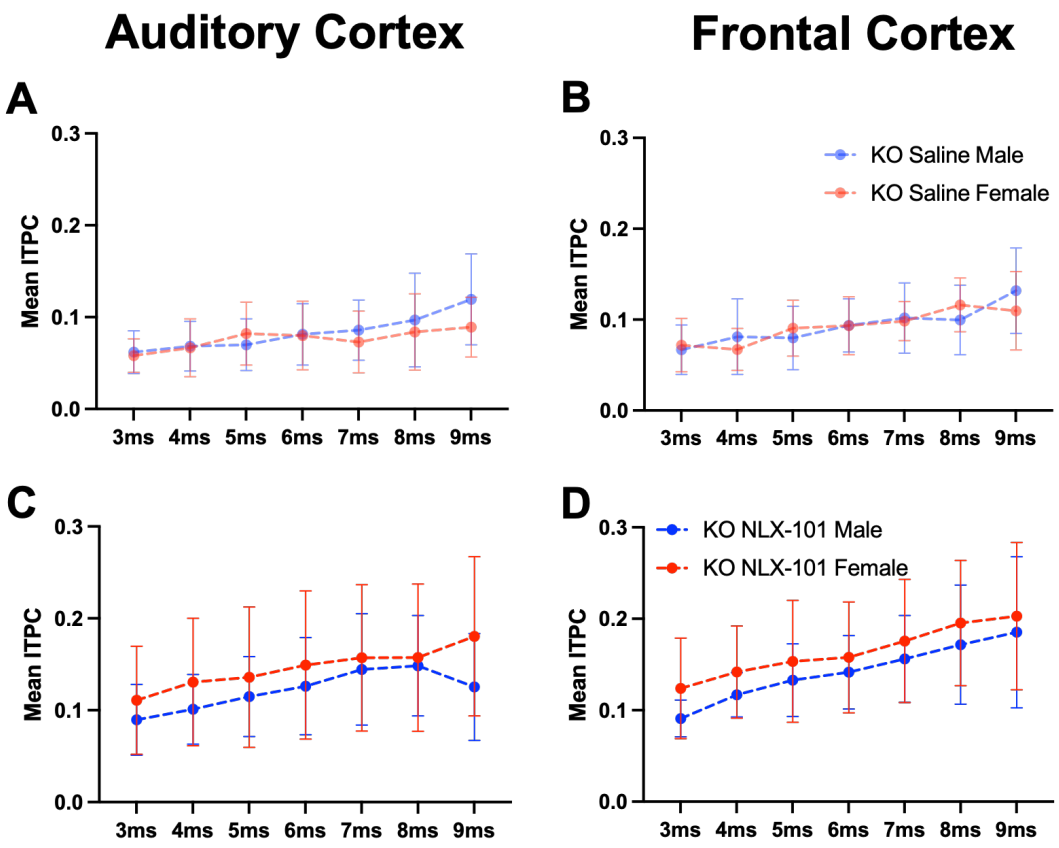

Figure S3.4. Sex differences in ITPC was not found in Fmr1 KO mice at P30.

(A-B) Sex differences were not found in saline-treated KO mice in either cortex. (C-D) Sex differences were not recorded in NLX-101-treated KO in either cortex. Full statistics report is in Table S3.4. *p < 0.05, **p < 0.01, ***p < 0.001, ****p < 0.0001. Error bars show standard deviation.

Table S3.4. KO gap-ASSR sex differences statistics at P30

Group	Cortical Region	Factor/ Interaction	ANOVA Results	P Value
KO_Saline_P30	Auditory Cortex	Gap width x Sex	F (6, 114) = 2.090	0.0597
		Gap Width	**F (3.698, 70.26) = 10.07**	**<0.0001**
		Sex	F (1, 19) = 0.3268	0.5742
	Frontal Cortex	Gap width x Sex	F (6, 114) = 2.145	0.0535
		Gap Width	**F (3.579, 68.01) = 15.57**	**<0.0001**
		Sex	F (1, 19) = 0.007057	0.9339
KO_NLX-101_P30	Auditory Cortex	Gap width x Sex	F (6, 114) = 1.569	0.1625
		Gap Width	**F (3.132, 59.51) = 11.62**	**<0.0001**
		Sex	F (1, 19) = 0.9161	0.3505
	Frontal Cortex	Gap width x Sex	F (6, 114) = 0.2151	0.9714
		Gap Width	**F (2.373, 45.09) = 25.09**	**<0.0001**
		Sex	F (1, 19) = 0.9769	0.3354

3.3.5 C-Fos activation in the IC or AC was not affected by NLX-101 treatment

To study if NLX-101 reduces STP by reducing activation in the IC and/ or AC, c-Fos expression in the IC and AC was examined in male *Fmr1* KO mice (P21-P23) following saline/NLX-101 i.p. treatment and sub-convulsive sound exposure (Figure 3.9). To avoid confounding audiogenic seizure (AGS)-induced motor activation, we used a 85dB SPL sound stimulus, which in our previous study revealed enhanced c-Fos activation in the IC of *Fmr1* KO mice, compared to WT mice (Nguyen et al., 2020). Behavior was videotaped and analyzed offline to ensure AGS were absent. Difference regrading c-Fos positive cell density between saline and NLX-101 groups was not observed in either the IC (Figure 3.9E, saline: n=6, NLX-101: n=6. P=0.6991, Mann-Whitney test) or in the AC (Figure 3.9F, saline: n=6, NLX-101: n=6. P=0.2403, Mann-

Whitney test), suggesting NLX-101 did not significantly impact general cell activation in response to a sound stimulus. But it is worth noticing c-Fos activation alone gives very little information about cell types. Future studies should investigate if NLX-101 treatment affects excitatory and inhibitory neuronal activation differently.

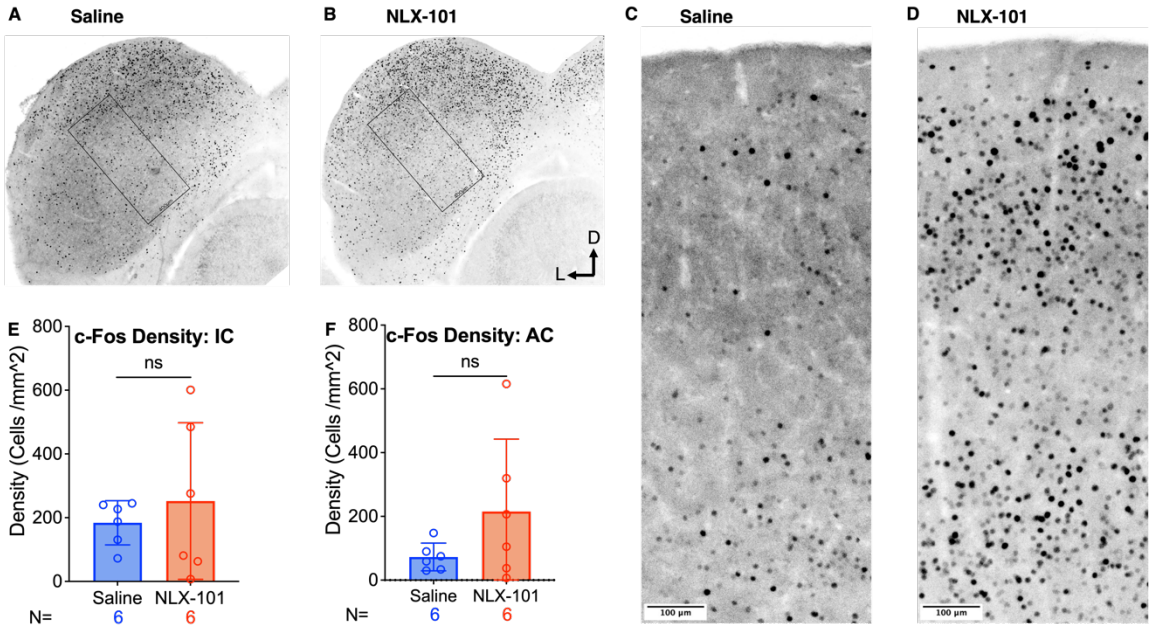

Figure 3.9. NLX-101 i.p. treatment did not affect c-Fos activation in either the IC or AC.

C-Fos activation was examined in male *Fmr1* KO mice at P21-P23 after either saline or NLX-101 treatment and sound exposure. (A-B) Representative c-Fos images obtained from the IC of the animals injected with saline (A) or NLX-101(B). Windows for counting are shown by angled rectangular boxes of 400 µm width. (C-D) Representative c-Fos images acquired from the AC of the animals treated with either saline (C) or NLX-101 (D). Scale bar is 100 µm. (E-F) Difference of c-Fos activation was not presented between saline and NLX-101 treated groups in either the IC (Figure 3.9E Saline: n=6, NLX-101: n=6. P=0.6991, Mann-Whitney test) or the AC (Figure 3.9F Saline: n=6, NLX-101: n=6. P=0.2403, Mann-Whitney test). The bars present the mean with standard deviation (SD).

3.4 Discussion

This study investigated the effects of acute, single dose injection of NLX-101, a selective serotonin-1A receptor biased agonist, on EEG phenotypes in *Fmr1* KO mice. Consistent with previously published studies (reviewed in Razak et al., 2021), EEG phenotypes in *Fmr1* KO mice including elevated ERP amplitudes, enhanced STP and reduced ITPC were found in this study in saline-treated *Fmr1* KO mice. These data add support to the robust and replicable nature of the EEG phenotypes in *Fmr1* KO mice across several studies and mouse strains (Increased ERP amplitudes: (Jonak et al., 2020; Lovelace et al., 2018; Wen et al., 2019). Increased STP: (Lovelace et al., 2018; Wen et al., 2019). Decreased ITPC: (Jonak et al., 2020; Lovelace et al., 2018; Pirbhoy et al., 2020). Following injection of NLX-101, ITPC in both *Fmr1* WT and KO was improved in both P21 and P30 groups; STP in *Fmr1* KO group was significantly reduced to the level that was indistinguishable to the WT control at P30, but not at P21; ERP in both age groups were not affected by the treatment. These data show that the EEG phenotypes are present from early development. NLX-101 shows robust EEG effects with specificity to alter STP and gap-ASSR measures, without affecting ERP amplitudes. Taken together, these data suggest a promising clinical treatment pathway in FXS by targeting 5-HT_{1A} receptors in early development either alone, or in combination with other treatments that may reduce ERP hypersensitivity.

Broadband noise was used to evoke auditory ERP responses in the present study. Background non-phase locked brain activity during noise stimulation was measured as single trial power (STP). Elevated ERP N1 amplitude and increased STP are consistent

phenotypes in FXS studies across species (Ethridge et al., 2019; Lovelace et al., 2018; Wen et al., 2019). ERP N1 amplitudes reflect cortical processing with increased amplitudes occurring due to increased neural responses and/ or increased synchrony of responses in the population (Näätänen & Picton, 1987). In the auditory cortex, inferior colliculus and superior olive of *Fmr1* KO mice, there is elevated sound driven neural activity and background activity (Garcia-Pino et al., 2017; Nguyen et al., 2020; S. Rotschafer & Razak, 2013; Wen et al., 2018). Indeed, enhanced evoked responses have been reported in other sensory cortices as well. In primary somatosensory cortex (S1), tactile stimulation of the hind paw produced significantly higher EPSP amplitudes and spiking rates in *Fmr1* KO mice than in WT mice (Bhaskaran et al., 2023). Increased synchrony of neurons is also seen in sensory cortex of *Fmr1* KO mice (Gonçalves et al., 2013). Together, increased sound-driven spiking response and synchrony may explain increased N1 amplitude in FXS.

The increased STP in *Fmr1* KO mice reflect elevated non-phase locked power in the background during acoustic stimulus presentation and is the summed single trial power both during and in-between stimuli. Such elevated background cortical activity will reduce signal to noise ratio during acoustic processing. In humans with FXS, elevated STP is correlated with distractibility and communication measures, suggesting potential clinical implications (Ethridge et al., 2019). Increased background activity has been observed in *Fmr1* KO mice in other sensory cortices as well. In S1, the percentage of neurons firing action potentials spontaneously is significantly higher in *Fmr1* KO mice than in WT mice (Bhaskaran et al., 2023). Visual cortex in *Fmr1* KO rats was found to

maintain “active” states even in the absence of arousal and attention (Berzhanskaya et al., 2016). Traditionally, background neural activity is viewed as “noise”, but spontaneous cortical activity interacts with external stimulation to produce behavioral responses toward sensory stimuli (Kwon, 2018; Ringach, 2009). Given that cortical responses are shaped by both external stimuli and spontaneous activity (Kwon, 2018), elevated evoked ERP amplitudes seen in *Fmr1* KO group in this study may also be partially explained by the increased STP in *Fmr1* KO mice. However, the differential impact of NLX-101 on ERP amplitude versus STP suggests they are generated by relatively independent mechanisms, most likely elevated synchrony playing a role in N1 amplitudes, and elevated responses playing a role in STP.

Single unit recording work in the inferior colliculus suggests how NLX-101 may reduce STP in *Fmr1* KO mice (Hurley, 2007). The target of NLX-101, 5-HT_{1A} receptors, are the predominant inhibitory 5-HT receptor subtype, decreasing cAMP production via activation of $G\alpha_i$ proteins (Albert & Vahid-Ansari, 2019), a process that is dysregulated in FXS (Kelley et al., 2007). Consistent with the hyperpolarizing effect of 5-HT_{1A} activation, in the inferior colliculus, activation of 5-HT_{1A}R with 8-OH-DPAT narrowed the response window of individual neurons by suppressing the latter spikes in response to sounds (Hurley, 2006, 2007). Indeed, *Fmr1* KO mouse single unit recordings show that ongoing responses after the stimulus, but not onset responses, are elevated in the KO mice compared to WT mice (Wen et al., 2018). Besides, neurons with longer latencies have a higher tendency to be suppressed by 8-OH-DPAT than those with shorter latencies (Hurley, 2007). By narrowing the response window, and by reducing overall spiking in

the midbrain, NLX-101 may reduce STP recorded in the auditory cortex. However, the drug appears to have minimal effect on cortical synchrony, leaving ERP amplitudes unchanged. The notion that NLX-101 has main effect in the midbrain is also supported by the data that showed the drug essentially abolished audiogenic seizures, a phenotype that potentially originates in the midbrain of *Fmr1* KO mice (Gonzalez et al., 2019). The improved effect of the drug on STP at P30, compared with P21, may reflect developmental regulation of 5-HT_{1A} receptors and/ or reduction of neural activity in the midbrain between P21 and P30. Future studies should examine P21 STP with a higher acute dose of NLX-101 and evaluate effects following chronic dosing.

Varied behavioral responses in autism have been broadly reported in human studies, manifested by significantly increased trial-by-trial variability in multiple sensory modalities (Auditory: (Dinstein et al., 2012; Latinus, 2019). Visual: (Dinstein et al., 2012; Kovarski et al., 2019; Milne, 2011). Somatosensory: (Dinstein et al., 2012; Haigh et al., 2016).). In this study, we examined temporal fidelity of the auditory cortex in *Fmr1* KO and WT mice with a modified auditory-steady-state responses (ASSR) paradigm. ASSR measures the capability of the auditory system to accurately phase lock to temporally modulated sound stimuli (Baltus & Herrmann, 2016). A previous study suggested trial-by-trial variability tends to be higher when sensory stimulus is more complex (Haigh, 2018). Therefore, instead of using 40-Hz click-train stimulus to induce 40Hz auditory oscillations in the conventional ASSR (Ogyu et al., 2023), we inserted gaps at 40Hz in the continuous background noise to make the stimuli more challenging to synchronize with (at short gaps, in particular), to better assess temporal processing acuity of the

auditory system (Rumschlag & Razak, 2021). The consistency of auditory responses can be measured using the inter-trial phase clustering (ITPC) which quantifies phase locking fidelity across trials. In line with published studies that used different spectrotemporally modulated stimuli (Jonak et al., 2020; Lovelace et al., 2018; Pirbhoy et al., 2020), reduced ITPC was observed in KO group compared with the WT group. Such reduced ITPC, or increased variability from trial to trial, at the neural network level, can be traced back to the variability at the cellular level such as variable resting membrane potentials of individual neurons in the *Fmr1* KO mice (Bhaskaran et al., 2023). Cortical recordings to sounds also showed increased variability across trials in terms of latency (Rotschafer & Razak, 2013), which will lead to variable representation of temporal responses. Consistent behavior output largely relies on reliable sensory perception. In speech comprehension, variable auditory processing will lead to unstable perception and is likely to underlie speech and language differences in FXS and other sensory-related cognition measures (Haigh, 2018).

We found that NLX-101 improved ITPC in response to gap-ASSR stimulation, suggesting that targeting cortical 5-HT_{1A} receptors with a selective biased agonist may be a potentially useful approach to reduce sensory variability. Both WT and KO mice, and at both ages tested, showed improved ITPC with NLX-101, suggesting serotonin modulation helped to reduce trial-by-trial variability. As mentioned above, 5-HT_{1A} receptor activation regulates temporal characteristics of evoked auditory responses in the IC (Hurley, 2007). By reducing overall response windows, NLX-101 may improve response reliability across trials.

Our data on the utility of modulating serotonin signaling in *Fmr1* KO mice is consistent with the notion that the serotonin system may provide potentially useful therapeutic pathways to treat FXS (reviewed in (Hanson & Hagerman, 2014)). Hessl et al.(2008) demonstrated that the serotonin transporter (5-HTTLPR) genotype correlated with most aggressive, destructive, and stereotypic behaviors in humans with FXS (ages 8-24 years). A recent study revealed that juvenile *Fmr1* KO mice had lower whole-brain 5-HT_{1A} receptor expression than WT mice (Saraf et al., 2024). Costa et al. (2012, 2018) found that stimulation of $5HT_{7A}$ receptors reversed the consistently exaggerated hippocampal mGluR5-mediated synaptic plasticity defects in *Fmr1* KO mice to WT range, and improved learning outcomes. Lim et al. (2014) showed that psychoactive drugs that act on 5-HT and dopamine receptors improved learning in Y-maze and fear-conditioning paradigms in the *Fmr1* KO mice. Importantly they suggested low-dose activation of both receptor types to be beneficial, setting the stage to examine if NLX-101 in combination with other drugs may reduce most, if not all, of the EEG phenotypes. Saraf et al. (2022) found that FPT, a non-selective agonist of several 5-HT_1 and 5-HT_{7A} receptors engaged spectral band changes EEG recordings from *Fmr1* KO mice (alpha and delta power changes, but not in the gamma band), reduced audiogenic seizures and improved social behaviors (Armstrong et al., 2020; Saraf et al., 2024). Fluoxetine, a selective serotonin reuptake inhibitor (SSRI), has some anxiolytic effect in *Fmr*1 KO mice, and reduces hyperactivity. Developmental changes in the serotonin transporter and BDNF/ TrkB signaling may underlie some differences in effects in WT versus Fmr1 KO

mice (Uutela et al., 2014). Sertraline, another SSRI, also shows off-label efficacy to improve language function in FXS (Indah Winarni et al., 2012).

Several future studies are suggested by our results. Here, NLX-101 was applied systemically, so it is unclear whether the observed improvement is contributed predominantly by one or more brain regions, although previous studies on NLX-101 indicate that it preferentially targets 5-HT_{1A} receptors in cortical and brainstem regions. Future studies that specifically administer 5-HT_{1A} receptor agonists and/ or antagonists in the inferior colliculus or auditory cortex will identify regional effects. The present study was done with an acute single injection of NLX-101, and studies are warranted to determine whether its effects are maintained upon chronic administration. In terms of audiogenic seizures, multiple days of NLX-101 administration did not reduce the beneficial effects, but it is unclear how EEG responses may be affected with longer term treatments. The expression levels of 5-HT_{1A} receptors may change with age, leading to specific optimal treatment windows, so future studies will examine expression of 5-HT_{1A} receptors across development, regions, and age.

3.5 Conclusions

Our findings are consistent with other studies that suggest serotonin modulation as a useful therapeutic approach in FXS. NLX-101 has specific properties that may be of use in treatment of sensory variability and background noise in FXS. Unlike NLX-101, the more commonly used agonist of 5-HT_{1A} receptors, 8-OH-DPAT, also activates

autoreceptors in the raphe nuclei (Rojas & Fiedler, 2016) and causes hypothermia (Martin et al., 1992). In contrast, NLX-101 has much higher selectivity compared with 8-OH-DPAT (Newman-Tancredi et al., 2022) and preferentially activates 5-HT_{1A} heteroreceptors (Newman-Tancredi et al., 2009), leaving autoreceptors in the raphe nuclei unaffected. The unique neuropharmacology of such biased agonists may make them more suitable for therapeutic approaches, and future studies should determine if NLX-101 or other biased selective 5-HT_{1A} receptor agonists are beneficial in children with FXS.

References

Albert, P. R., & Vahid-Ansari, F. (2019). The 5-HT1AR eceptor: Signaling to behavior. *Biochimie*, *161*, 34–45. https://doi.org/10.1016/j.biochi.2018.10.015

An, W. W., Nelson, C. A., & Wilkinson, C. L. (2022). Neural response to repeated auditory stimuli and its association with early language ability in male children with Fragile X syndrome. *Frontiers in Integrative Neuroscience*, *16*, 987184. https://doi.org/10.3389/fnint.2022.987184

Armstrong, J. L., Casey, A. B., Saraf, T. S., Mukherjee, M., Booth, R. G., & Canal, C. E. (2020). (S)-5-(2′-Fluorophenyl)- N , N -dimethyl-1,2,3,4-tetrahydronaphthalen-2-amine, a Serotonin Receptor Modulator, Possesses Anticonvulsant, Prosocial, and Anxiolytic-like Properties in an Fmr1 Knockout Mouse Model of Fragile X Syndrome and Autism Spectrum. *ACS Pharmacology & Translational Science*. https://doi.org/10.1021/acsptsci.9b00101

Baltus, A., & Herrmann, C. S. (2016). The importance of individual frequencies of endogenous brain oscillations for auditory cognition – A short review. *Brain Research*, *1640*, 243–250. https://doi.org/10.1016/j.brainres.2015.09.030

Bankhead, P., Loughrey, M. B., Fernández, J. A., Dombrowski, Y., McArt, D. G., Dunne, P. D., McQuaid, S., Gray, R. T., Murray, L. J., Coleman, H. G., James, J. A., Salto-Tellez, M., & Hamilton, P. W. (2017). QuPath: Open source software for digital pathology image analysis. *Scientific Reports*, *7*(1), 16878. https://doi.org/10.1038/s41598-017-17204-5

Berzhanskaya, J., Phillips, M. A., Gorin, A., Lai, C., Shen, J., & Colonnese, M. T. (2016). Disrupted Cortical State Regulation in a Rat Model of Fragile X Syndrome. *Cerebral Cortex*, bhv331. https://doi.org/10.1093/cercor/bhv331

Bhaskaran, A. A., Gauvrit, T., Vyas, Y., Bony, G., Ginger, M., & Frick, A. (2023). Endogenous noise of neocortical neurons correlates with atypical sensory response variability in the Fmr1−/y mouse model of autism. *Nature Communications*, *14*(1), 7905. https://doi.org/10.1038/s41467-023-43777-z

Canal, C. E., Felsing, D. E., Liu, Y., Zhu, W., Wood, J. T., Perry, C. K., Vemula, R., & Booth, R. G. (2015). An Orally Active Phenylaminotetralin-Chemotype Serotonin 5-HT $_{7}$ and 5-HT $_{1A}$ Receptor Partial Agonist That Corrects Motor Stereotypy in Mouse Models. *ACS Chemical Neuroscience*, *6*(7), 1259–1270. https://doi.org/10.1021/acschemneuro.5b00099

Chen, L., & Toth, M. (2001). Fragile X mice develop sensory hyperreactivity to auditory stimuli. *Neuroscience*, *103*(4), 1043–1050. https://doi.org/10.1016/S0306-4522(01)00036-7

Cohen, M. X. (2014). *Analyzing Neural Time Series Data: Theory and Practice*. MIT Press.

Cordeiro, L., Ballinger, E., Hagerman, R., & Hessl, D. (2010). Clinical assessment of DSM-IV anxiety disorders in fragile X syndrome: Prevalence and characterization. *Journal of Neurodevelopmental Disorders*, *3*(1), 57–67. https://doi.org/10.1007/s11689-010-9067-y

Costa, L., Sardone, L. M., Bonaccorso, C. M., D'Antoni, S., Spatuzza, M., Gulisano, W., Tropea, M. R., Puzzo, D., Leopoldo, M., Lacivita, E., Catania, M. V., & Ciranna, L. (2018). Activation of Serotonin 5-HT7 Receptors Modulates Hippocampal Synaptic Plasticity by Stimulation of Adenylate Cyclases and Rescues Learning and Behavior in a Mouse Model of Fragile X Syndrome. *Frontiers in Molecular Neuroscience*, *11*, 353. https://doi.org/10.3389/fnmol.2018.00353

Costa, L., Spatuzza, M., D'Antoni, S., Bonaccorso, C. M., Trovato, C., Musumeci, S. A., Leopoldo, M., Lacivita, E., Catania, M. V., & Ciranna, L. (2012). Activation of 5-HT7 Serotonin Receptors Reverses Metabotropic Glutamate Receptor-Mediated Synaptic Plasticity in Wild-Type and Fmr1 Knockout Mice, a Model of Fragile X Syndrome. *Biological Psychiatry*, *72*(11), 924–933. https://doi.org/10.1016/j.biopsych.2012.06.008

Croom, K., Rumschlag, J. A., Erickson, M. A., Binder, D. K., & Razak, K. A. (2023). Developmental delays in cortical auditory temporal processing in a mouse model of Fragile X syndrome. *Journal of Neurodevelopmental Disorders*, *15*(1), 23. https://doi.org/10.1186/s11689-023-09496-8

Croom, K., Rumschlag, J. A., Erickson, M. A., Binder, D., & Razak, K. A. (2024). Sex differences during development in cortical temporal processing and event related potentials in wild-type and fragile X syndrome model mice. *Journal of Neurodevelopmental Disorders*, *16*(1), 24. https://doi.org/10.1186/s11689-024-09539-8

Dinstein, I., Heeger, D. J., Lorenzi, L., Minshew, N. J., Malach, R., & Behrmann, M. (2012). Unreliable Evoked Responses in Autism. *Neuron*, *75*(6), 981–991. https://doi.org/10.1016/j.neuron.2012.07.026

Ethridge, L. E., De Stefano, L. A., Schmitt, L. M., Woodruff, N. E., Brown, K. L., Tran, M., Wang, J., Pedapati, E. V., Erickson, C. A., & Sweeney, J. A. (2019). Auditory EEG Biomarkers in Fragile X Syndrome: Clinical Relevance. *Frontiers in Integrative Neuroscience*, *13*, 60. https://doi.org/10.3389/fnint.2019.00060

Ethridge, L. E., White, S. P., Mosconi, M. W., Wang, J., Byerly, M. J., & Sweeney, J. A. (2016). Reduced habituation of auditory evoked potentials indicate cortical hyper-excitability in Fragile X Syndrome. *Translational Psychiatry*, *6*(4), e787–e787. https://doi.org/10.1038/tp.2016.48

Ethridge, L. E., White, S. P., Mosconi, M. W., Wang, J., Pedapati, E. V., Erickson, C. A., Byerly, M. J., & Sweeney, J. A. (2017). Neural synchronization deficits linked to cortical hyper-excitability and auditory hypersensitivity in fragile X syndrome. *Molecular Autism*, *8*(1), 22. https://doi.org/10.1186/s13229-017-0140-1

Ethridge, L., Thaliath, A., Kraff, J., Nijhawan, K., & Berry-Kravis, E. (2020). Development of Neural Response to Novel Sounds in Fragile X Syndrome: Potential Biomarkers. *American Journal on Intellectual and Developmental Disabilities*, *125*(6), 449–464. https://doi.org/10.1352/1944-7558-125.6.449

Euler, M. J., Weisend, M. P., Jung, R. E., Thoma, R. J., & Yeo, R. A. (2015). Reliable activation to novel stimuli predicts higher fluid intelligence. *NeuroImage*, *114*, 311–319. https://doi.org/10.1016/j.neuroimage.2015.03.078

Galambos, R., Makeig, S., & Talmachoff, P. J. (1981). A 40-Hz auditory potential recorded from the human scalp. *Proceedings of the National Academy of Sciences*, *78*(4), 2643–2647. https://doi.org/10.1073/pnas.78.4.2643

Garcia-Pino, E., Gessele, N., & Koch, U. (2017). Enhanced Excitatory Connectivity and Disturbed Sound Processing in the Auditory Brainstem of Fragile X Mice. *The Journal of Neuroscience*, *37*(31), 7403–7419. https://doi.org/10.1523/JNEUROSCI.2310-16.2017

Gonçalves, J. T., Anstey, J. E., Golshani, P., & Portera-Cailliau, C. (2013). Circuit level defects in the developing neocortex of Fragile X mice. *Nature Neuroscience*, *16*(7), 903–909. https://doi.org/10.1038/nn.3415

Gonzalez, D., Tomasek, M., Hays, S., Sridhar, V., Ammanuel, S., Chang, C., Pawlowski, K., Huber, K. M., & Gibson, J. R. (2019). Audiogenic Seizures in the *Fmr1* Knock-Out Mouse Are Induced by *Fmr1* Deletion in Subcortical, VGlut2-Expressing Excitatory Neurons and Require Deletion in the Inferior Colliculus. *The Journal of Neuroscience*, *39*(49), 9852–9863. https://doi.org/10.1523/JNEUROSCI.0886-19.2019

Hagerman, R. J., & Hagerman, P. J. (2002). *Fragile X Syndrome: Diagnosis, Treatment, and Research*. Taylor & Francis US.

Haigh, S. M. (2018). Variable sensory perception in autism. *European Journal of Neuroscience*, *47*(6), 602–609. https://doi.org/10.1111/ejn.13601

Haigh, S. M., Minshew, N., Heeger, D. J., Dinstein, I., & Behrmann, M. (2016). Over-Responsiveness and Greater Variability in Roughness Perception in Autism. *Autism Research*, *9*(3), 393–402. https://doi.org/10.1002/aur.1505

Hanson, A. C., & Hagerman, R. J. (2014). Serotonin dysregulation in Fragile X Syndrome: Implications for treatment. *Intractable & Rare Diseases Research*, *3*(4), 110–117. https://doi.org/10.5582/irdr.2014.01027

Hessl, D., Tassone, F., Cordeiro, L., Koldewyn, K., McCormick, C., Green, C., Wegelin, J., Yuhas, J., & Hagerman, R. J. (2008). Brief Report: Aggression and Stereotypic Behavior in Males with Fragile X Syndrome—Moderating Secondary Genes in a "Single Gene" Disorder. *Journal of Autism and Developmental Disorders*, *38*(1), 184–189. https://doi.org/10.1007/s10803-007-0365-5

Heydari, A., & Davoudi, S. (2017). The effect of sertraline and 8-OH-DPAT on the PTZ_induced seizure threshold: Role of the nitrergic system. *Seizure*, *45*, 119–124. https://doi.org/10.1016/j.seizure.2016.12.005

Holley, A. J., Shedd, A., Boggs, A., Lovelace, J., Erickson, C., Gross, C., Jankovic, M., Razak, K., Huber, K., & Gibson, J. R. (2022). A sound-driven cortical phase-locking change in the Fmr1 KO mouse requires Fmr1 deletion in a subpopulation of brainstem neurons. *Neurobiology of Disease*, *170*, 105767. https://doi.org/10.1016/j.nbd.2022.105767

Hunter, J., Rivero-Arias, O., Angelov, A., Kim, E., Fotheringham, I., & Leal, J. (2014). Epidemiology of fragile X syndrome: A systematic review and meta-analysis.

American Journal of Medical Genetics Part A, *164*(7), 1648–1658. https://doi.org/10.1002/ajmg.a.36511

Hurley, L. M. (2006). Different Serotonin Receptor Agonists Have Distinct Effects on Sound-Evoked Responses in Inferior Colliculus. *Journal of Neurophysiology*, *96*(5), 2177–2188. https://doi.org/10.1152/jn.00046.2006

Hurley, L. M. (2007). Activation of the serotonin 1A receptor alters the temporal characteristics of auditory responses in the inferior colliculus. *Brain Research*, *1181*, 21–29. https://doi.org/10.1016/j.brainres.2007.08.053

Hwang, E., Brown, R. E., Kocsis, B., Kim, T., McKenna, J. T., McNally, J. M., Han, H.-B., & Choi, J. H. (2019). Optogenetic stimulation of basal forebrain parvalbumin neurons modulates the cortical topography of auditory steady-state responses. *Brain Structure and Function*, *224*(4), 1505–1518. https://doi.org/10.1007/s00429-019-01845-5

Indah Winarni, T., Chonchaiya, W., Adams, E., Au, J., Mu, Y., Rivera, S. M., Nguyen, D. V., & Hagerman, R. J. (2012). Sertraline May Improve Language Developmental Trajectory in Young Children with Fragile X Syndrome: A Retrospective Chart Review. *Autism Research and Treatment*, *2012*, 1–8. https://doi.org/10.1155/2012/104317

Jonak, C. R., Lovelace, J. W., Ethell, I. M., Razak, K. A., & Binder, D. K. (2020). Multielectrode array analysis of EEG biomarkers in a mouse model of Fragile X Syndrome. *Neurobiology of Disease*, *138*, 104794. https://doi.org/10.1016/j.nbd.2020.104794

Juczewski, K., von Richthofen, H., Bagni, C., Celikel, T., Fisone, G., & Krieger, P. (2016). Somatosensory map expansion and altered processing of tactile inputs in a mouse model of fragile X syndrome. *Neurobiology of Disease*, *96*, 201–215. https://doi.org/10.1016/j.nbd.2016.09.007

Kagaya, A., Tanra, A. J., Shinno, H., Kugaya, A., Muraoka, M., Oyamada, T., Uchitomi, Y., & Yamawaki, S. (1996). TJS-010, a new prescription of oriental medicine, enhances 8-OH-DPAT-induced effects in rats. *Journal of Neural Transmission*, *103*(1), 69–75. https://doi.org/10.1007/BF01292617

Kaufmann, W. E., Cortell, R., Kau, A. S. M., Bukelis, I., Tierney, E., Gray, R. M., Cox, C., Capone, G. T., & Stanard, P. (2004). Autism spectrum disorder in fragile X syndrome: Communication, social interaction, and specific behaviors. *American Journal of Medical Genetics Part A*, *129A*(3), 225–234. https://doi.org/10.1002/ajmg.a.30229

Kelley, D. J., Davidson, R. J., Elliott, J. L., Lahvis, G. P., Yin, J. C. P., & Bhattacharyya, A. (2007). The Cyclic AMP Cascade Is Altered in the Fragile X Nervous System. *PLoS ONE*, *2*(9), e931. https://doi.org/10.1371/journal.pone.0000931

Kim, T., Thankachan, S., McKenna, J. T., McNally, J. M., Yang, C., Choi, J. H., Chen, L., Kocsis, B., Deisseroth, K., Strecker, R. E., Basheer, R., Brown, R. E., & McCarley, R. W. (2015). Cortically projecting basal forebrain parvalbumin neurons regulate cortical gamma band oscillations. *Proceedings of the National Academy of Sciences*, *112*(11), 3535–3540. https://doi.org/10.1073/pnas.1413625112

Koerner, T. K., & Zhang, Y. (2015). Effects of background noise on inter-trial phase coherence and auditory N1–P2 responses to speech stimuli. *Hearing Research*, *328*, 113–119. https://doi.org/10.1016/j.heares.2015.08.002

Koerner, T. K., Zhang, Y., Nelson, P. B., Wang, B., & Zou, H. (2017). Neural indices of phonemic discrimination and sentence-level speech intelligibility in quiet and noise: A P3 study. *Hearing Research*, *350*, 58–67. https://doi.org/10.1016/j.heares.2017.04.009

Kovarski, K., Malvy, J., Khanna, R. K., Arsène, S., Batty, M., & Latinus, M. (2019). Reduced visual evoked potential amplitude in autism spectrum disorder, a variability effect? *Translational Psychiatry*, *9*(1), 341. https://doi.org/10.1038/s41398-019-0672-6

Kwon, S. E. (2018). The Interplay Between Cortical State and Perceptual Learning: A Focused Review. *Frontiers in Systems Neuroscience*, *12*, 47. https://doi.org/10.3389/fnsys.2018.00047

Latinus, M. (2019). Atypical Sound Perception in ASD Explained by Inter-Trial (In)consistency in EEG. *Frontiers in Psychology*, *10*.

Lim, C.-S., Hoang, E. T., Viar, K. E., Stornetta, R. L., Scott, M. M., & Zhu, J. J. (2014). Pharmacological rescue of Ras signaling, GluA1-dependent synaptic plasticity, and learning deficits in a fragile X model. *Genes & Development*, *28*(3), 273–289. https://doi.org/10.1101/gad.232470.113

Lladó-Pelfort, L., Assié, M.-B., Newman-Tancredi, A., Artigas, F., & Celada, P. (2010). Preferential in vivo action of F15599, a novel 5-HT1AR eceptor agonist, at

postsynaptic 5-HT1AR eceptors: Actions of F15599 at 5-HT1AR eceptors. *British Journal of Pharmacology*, *160*(8), 1929–1940. https://doi.org/10.1111/j.1476-5381.2010.00738.x

Llinás, R. R. (1988). The Intrinsic Electrophysiological Properties of Mammalian Neurons: Insights into Central Nervous System Function. *Science*, *242*(4886), 1654–1664. https://doi.org/10.1126/science.3059497

Lovelace, J. W., Ethell, I. M., Binder, D. K., & Razak, K. A. (2018). Translation-relevant EEG phenotypes in a mouse model of Fragile X Syndrome. *Neurobiology of Disease*, *115*, 39–48. https://doi.org/10.1016/j.nbd.2018.03.012

Lovelace, J. W., Rais, M., Palacios, A. R., Shuai, X. S., Bishay, S., Popa, O., Pirbhoy, P. S., Binder, D. K., Nelson, D. L., Ethell, I. M., & Razak, K. A. (2020). Deletion of Fmr1 from Forebrain Excitatory Neurons Triggers Abnormal Cellular, EEG, and Behavioral Phenotypes in the Auditory Cortex of a Mouse Model of Fragile X Syndrome. *Cerebral Cortex*, *30*(3), 969–988. https://doi.org/10.1093/cercor/bhz141

Maris, E., & Oostenveld, R. (2007). Nonparametric statistical testing of EEG- and MEG-data. *Journal of Neuroscience Methods*, *164*(1), 177–190. https://doi.org/10.1016/j.jneumeth.2007.03.024

Martin, K. F., Phillips, I., Hearson, M., Prow, M. R., & Heal, D. J. (1992). Characterization of 8-OH-DPAT-induced hypothermia in mice as a 5-HT1A autoreceptor response and its evaluation as a model to selectively identify

antidepressants. *British Journal of Pharmacology*, *107*(1), 15–21. https://doi.org/10.1111/j.1476-5381.1992.tb14457.x

Miller, L. J., McIntosh, D. N., McGrath, J., Shyu, V., Lampe, M., Taylor, A. K., Tassone, F., Neitzel, K., Stackhouse, T., & Hagerman, R. J. (1999). Electrodermal responses to sensory stimuli in individuals with fragile X syndrome: A preliminary report. *American Journal of Medical Genetics*, *83*(4), 268–279. https://doi.org/10.1002/(SICI)1096-8628(19990402)83:4<268::AID-AJMG7>3.0.CO;2-K

Milne, E. (2011). Increased Intra-Participant Variability in Children with Autistic Spectrum Disorders: Evidence from Single-Trial Analysis of Evoked EEG. *Frontiers in Psychology*, *2*. https://doi.org/10.3389/fpsyg.2011.00051

Näätänen, R., & Picton, T. (1987). The N1 Wave of the Human Electric and Magnetic Response to Sound: A Review and an Analysis of the Component Structure. *Psychophysiology*, *24*(4), 375–425. https://doi.org/10.1111/j.1469-8986.1987.tb00311.x

Newman-Tancredi, A., Depoortère, R. Y., Kleven, M. S., Kołaczkowski, M., & Zimmer, L. (2022). Translating biased agonists from molecules to medications: Serotonin 5-HT1AR eceptor functional selectivity for CNS disorders. *Pharmacology & Therapeutics*, *229*, 107937. https://doi.org/10.1016/j.pharmthera.2021.107937

Newman-Tancredi, A., Martel, J.-C., Assié, M.-B., Buritova, J., Lauressergues, E., Cosi, C., Heusler, P., Bruins Slot, L., Colpaert, F., Vacher, B., & Cussac, D. (2009). Signal transduction and functional selectivity of F15599, a preferential post-

synaptic 5-HT $_{1A}$ receptor agonist. *British Journal of Pharmacology*, *156*(2), 338–353. https://doi.org/10.1111/j.1476-5381.2008.00001.x

Nguyen, A. O., Binder, D. K., Ethell, I. M., & Razak, K. A. (2020a). Abnormal development of auditory responses in the inferior colliculus of a mouse model of Fragile X Syndrome. *Journal of Neurophysiology*, *123*(6), 2101–2121. https://doi.org/10.1152/jn.00706.2019

Nguyen, A. O., Binder, D. K., Ethell, I. M., & Razak, K. A. (2020b). Abnormal development of auditory responses in the inferior colliculus of a mouse model of Fragile X Syndrome. *Journal of Neurophysiology*, *123*(6), 2101–2121. https://doi.org/10.1152/jn.00706.2019

Ogyu, K., Matsushita, K., Honda, S., Wada, M., Tamura, S., Takenouchi, K., Tobari, Y., Kusudo, K., Kato, H., Koizumi, T., Arai, N., Koreki, A., Matsui, M., Uchida, H., Fujii, S., Onaya, M., Hirano, Y., Mimura, M., Nakajima, S., & Noda, Y. (2023). Decrease in gamma-band auditory steady-state response in patients with treatment-resistant schizophrenia. *Schizophrenia Research*, *252*, 129–137. https://doi.org/10.1016/j.schres.2023.01.011

Pastor, M. A., Artieda, J., Arbizu, J., Marti-Climent, J. M., Peñuelas, I., & Masdeu, J. C. (2002). Activation of Human Cerebral and Cerebellar Cortex by Auditory Stimulation at 40 Hz. *The Journal of Neuroscience*, *22*(23), 10501–10506. https://doi.org/10.1523/JNEUROSCI.22-23-10501.2002

Pieretti, M., Zhang, F., Fu, Y.-H., Warren, S. T., Oostra, B. A., Caskey, C. T., & Nelson, D. L. (1991). Absence of expression of the *FMR-1* gene in fragile X syndrome. *Cell*, *66*(4), 817–822. https://doi.org/10.1016/0092-8674(91)90125-I

Pirbhoy, P. S., Rais, M., Lovelace, J. W., Woodard, W., Razak, K. A., Binder, D. K., & Ethell, I. M. (2020). Acute pharmacological inhibition of matrix metalloproteinase-9 activity during development restores perineuronal net formation and normalizes auditory processing in Fmr1 KO mice. *Journal of Neurochemistry*, *155*(5), 538–558. https://doi.org/10.1111/jnc.15037

Rais, M., Lovelace, J. W., Shuai, X. S., Woodard, W., Bishay, S., Estrada, L., Sharma, A. R., Nguy, A., Kulinich, A., Pirbhoy, P. S., Palacios, A. R., Nelson, D. L., Razak, K. A., & Ethell, I. M. (2022). Functional consequences of postnatal interventions in a mouse model of Fragile X syndrome. *Neurobiology of Disease*, *162*, 105577. https://doi.org/10.1016/j.nbd.2021.105577

Razak, K. A., Binder, D. K., & Ethell, I. M. (2021). Neural Correlates of Auditory Hypersensitivity in Fragile X Syndrome. *Frontiers in Psychiatry*, *12*. https://www.frontiersin.org/article/10.3389/fpsyt.2021.720752

Rigoulot, S., Knoth, I. S., Lafontaine, M., Vannasing, P., Major, P., Jacquemont, S., Michaud, J. L., Jerbi, K., & Lippé, S. (2017). Altered visual repetition suppression in Fragile X Syndrome: New evidence from ERPs and oscillatory activity. *International Journal of Developmental Neuroscience*, *59*(1), 52–59. https://doi.org/10.1016/j.ijdevneu.2017.03.008

Ringach, D. L. (2009). Spontaneous and driven cortical activity: Implications for computation. *Current Opinion in Neurobiology*, *19*(4), 439–444. https://doi.org/10.1016/j.conb.2009.07.005

Rojas, D. C., Benkers, T. L., Rogers, S. J., Teale, P. D., & Reite, M. L. (2001). *Auditory evoked magnetic Æelds in adults with fragile X syndrome*. 4.

Rojas, P. S., & Fiedler, J. L. (2016). What Do We Really Know About 5-HT1AR eceptor Signaling in Neuronal Cells? *Frontiers in Cellular Neuroscience*, *10*. https://doi.org/10.3389/fncel.2016.00272

Rosanova, M., Casali, A., Bellina, V., Resta, F., Mariotti, M., & Massimini, M. (2009). Natural Frequencies of Human Corticothalamic Circuits. *Journal of Neuroscience*, *29*(24), 7679–7685. https://doi.org/10.1523/JNEUROSCI.0445-09.2009

Rotschafer, S. E., & Razak, K. A. (2014). Auditory Processing in Fragile X Syndrome. *Frontiers in Cellular Neuroscience*, *8*. https://doi.org/10.3389/fncel.2014.00019

Rotschafer, S., & Razak, K. (2013). Altered auditory processing in a mouse model of fragile X syndrome. *Brain Research*, *1506*, 12–24. https://doi.org/10.1016/j.brainres.2013.02.038

Rumschlag, J. A., Lovelace, J. W., & Razak, K. A. (2021). Age- and movement-related modulation of cortical oscillations in a mouse model of presbycusis. *Hearing Research*, *402*, 108095. https://doi.org/10.1016/j.heares.2020.108095

Rumschlag, J. A., & Razak, K. A. (2021). Age-related changes in event related potentials, steady state responses and temporal processing in the auditory cortex of mice with

severe or mild hearing loss. *Hearing Research*, *412*, 108380. https://doi.org/10.1016/j.heares.2021.108380

Saraf, T. S., Chen, Y., Tyagi, R., & Canal, C. E. (2024). Altered brain serotonin 5-HT1AR eceptor expression and function in juvenile Fmr1 knockout mice. *Neuropharmacology*, *245*, 109774. https://doi.org/10.1016/j.neuropharm.2023.109774

Schneider, C. A., Rasband, W. S., & Eliceiri, K. W. (2012). NIH Image to ImageJ: 25 years of image analysis. *Nature Methods*, *9*(7), 671–675. https://doi.org/10.1038/nmeth.2089

Seymour, R. A., Rippon, G., Gooding-Williams, G., Sowman, P. F., & Kessler, K. (2020). Reduced auditory steady state responses in autism spectrum disorder. *Molecular Autism*, *11*(1), 56. https://doi.org/10.1186/s13229-020-00357-y

Sinclair, D., Oranje, B., Razak, K. A., Siegel, S. J., & Schmid, S. (2017). Sensory processing in autism spectrum disorders and Fragile X syndrome—From the clinic to animal models. *Neuroscience & Biobehavioral Reviews*, *76*, 235–253. https://doi.org/10.1016/j.neubiorev.2016.05.029

Tao, X., Newman-Tancredi, A., Varney, M. A., & Razak, K. A. (2023). Acute and Repeated Administration of NLX-101, a Selective Serotonin-1A Receptor Biased Agonist, Reduces Audiogenic Seizures in Developing Fmr1 Knockout Mice. *Neuroscience*, *509*, 113–124. https://doi.org/10.1016/j.neuroscience.2022.11.014

Thuné, H., Recasens, M., & Uhlhaas, P. J. (2016). The 40-Hz Auditory Steady-State Response in Patients With Schizophrenia: A Meta-analysis. *JAMA Psychiatry*, *73*(11), 1145. https://doi.org/10.1001/jamapsychiatry.2016.2619

Tupal, S., & Faingold, C. L. (2019). Fenfluramine, a serotonin-releasing drug, prevents seizure-induced respiratory arrest and is anticonvulsant in the DBA /1 mouse model of SUDEP. *Epilepsia*, epi.14658. https://doi.org/10.1111/epi.14658

Uutela, M., Lindholm, J., RantamÃ¤ki, T., Umemori, J., Hunter, K., VÃµikar, V., & CastrÃ©n, M. L. (2014). Distinctive behavioral and cellular responses to fluoxetine in the mouse model for Fragile X syndrome. *Frontiers in Cellular Neuroscience*, *8*. https://doi.org/10.3389/fncel.2014.00150

Van der Molen, M. J. W., Van der Molen, M. W., Ridderinkhof, K. R., Hamel, B. C. J., Curfs, L. M. G., & Ramakers, G. J. A. (2012a). Auditory and visual cortical activity during selective attention in fragile X syndrome: A cascade of processing deficiencies. *Clinical Neurophysiology*, *123*(4), 720–729. https://doi.org/10.1016/j.clinph.2011.08.023

Van der Molen, M. J. W., Van der Molen, M. W., Ridderinkhof, K. R., Hamel, B. C. J., Curfs, L. M. G., & Ramakers, G. J. A. (2012b). Auditory change detection in fragile X syndrome males: A brain potential study. *Clinical Neurophysiology*, *123*(7), 1309–1318. https://doi.org/10.1016/j.clinph.2011.11.039

Wen, T. H., Afroz, S., Reinhard, S. M., Palacios, A. R., Tapia, K., Binder, D. K., Razak, K. A., & Ethell, I. M. (2018). Genetic Reduction of Matrix Metalloproteinase-9 Promotes Formation of Perineuronal Nets Around Parvalbumin-Expressing

Interneurons and Normalizes Auditory Cortex Responses in Developing Fmr1 Knock-Out Mice. *Cerebral Cortex*, *28*(11), 3951–3964. https://doi.org/10.1093/cercor/bhx258

Wen, T. H., Lovelace, J. W., Ethell, I. M., Binder, D. K., & Razak, K. A. (2019). Developmental Changes in EEG Phenotypes in a Mouse Model of Fragile X Syndrome. *Neuroscience*, *398*, 126–143. https://doi.org/10.1016/j.neuroscience.2018.11.047

Yu, L., Wang, S., Huang, D., Wu, X., & Zhang, Y. (2018). Role of inter-trial phase coherence in atypical auditory evoked potentials to speech and nonspeech stimuli in children with autism. *Clinical Neurophysiology*, *129*(7), 1374–1382. https://doi.org/10.1016/j.clinph.2018.04.599

Zhang, H., Zhao, H., Zeng, C., Van Dort, C., Faingold, C. L., Taylor, N. E., Solt, K., & Feng, H.-J. (2018). Optogenetic activation of 5-HT neurons in the dorsal raphe suppresses seizure-induced respiratory arrest and produces anticonvulsant effect in the DBA/1 mouse SUDEP model. *Neurobiology of Disease*, *110*, 47–58. https://doi.org/10.1016/j.nbd.2017.11.003

Chapter 4: Serotonin-1A receptor mRNA level in the auditory cortex and inferior colliculus in *Fmr1* KO mice

Abstract

Fragile X syndrome (FXS) is a leading known genetic cause of intellectual disability and autism spectrum disorders (ASD)-like behaviors. A consistent and debilitating phenotype of FXS is auditory hypersensitivity that may lead to delayed language and high anxiety. In our previous studies, we found that a selective serotonin-1A receptor biased agonist, NLX-101, reduced auditory hypersensitivity, background noise and improved temporal processing. This suggests that abnormal 5-HT_{1A}R expression may be present in the auditory pathway of *Fmr1* KO mice. However, the expression of 5-HT_{1A} mRNA pattern in the auditory regions, mainly in the auditory cortex (AC) and the inferior colliculus (IC), in *Fmr1* WT and KO mice during early development has not been studied. Here, we quantified 5-HT_{1A}R mRNA in two cell types (GAD+ and GAD-) in *Fmr1* WT and KO mice (male and female) in all layers of the AC and the central IC (ICC) at two age points, postnatal (P) 21 and 30 days. Overall, we found that most 5-HT_{1A}R puncta was found in non-GAD expressing (GAD-) cells. In the AC layer 2/3 of *Fmr1* KO mice there was a surprisingly higher level of 5-HT_{1A}R mRNA compared with WT mice. There were no other genotype differences. We also found that in all layers of the AC, expression level of 5-HT_{1A} mRNA showed an increase from P21 to P30, suggesting developmental regulation. Comparing the percentage of GAD+ cells across age, genotype and sex showed no genotype differences. The percentage of GAD+ cells in the ICC is higher at P30 than at P21, but no differences were seen in the AC. Only ICC showed sex difference at P21 with males showing a higher percentage of GAD+ cells than females. Because 5-HT_{1A}R activation causes hyperpolarization in the

post-synaptic neurons, these results suggest that mostly GAD- cells, many of which are putative excitatory neurons, are hyperpolarized with the selective agonists, and this causes a reduction in auditory hypersensitivity in *Fmr1* KO mice.

4.1 Introduction

Fragile X Syndrome (FXS) is caused by the lack of fragile X messenger ribonucleoprotein (FMRP) and affects approximately 1 in 4000 males and 1 in 8000 female (Hunter et al., 2014). FXS is the leading known genetic cause of intellectual disability and autism spectrum disorder (ASD)-like behaviors. FMRP is expressed from the *Fmr1* gene, at the promotor region of which are several CGG trinucleotide repeats. The full mutation occurs when the CGG repeat number exceeds 200, leading to transcriptional silencing of the *Fmr1* gene and the loss of FMRP (Pieretti et al., 1991). Children with FXS show intellectual impairments, repetitive behaviors, anxiety, hyperactivity, seizure susceptibility and sensory hypersensitivity (Cordeiro et al., 2010; Hagerman & Hagerman, 2002; Kaufmann et al., 2004). Strong and consistent auditory hypersensitivity impairs daily functioning and may lead to delayed language, high anxiety, and social impairments in FXS. Currently, there are no effective treatments to reduce sensory hypersensitivity in FXS, or other forms of ASD.

Children with FXS consistently exhibit various sensory processing issues including tactile, visual, and auditory hypersensitivity [Tactile: (Miller et al., 1999). Visual: (Miller et al., 1999; Rigoulot et al., 2017; Van der Molen et al., 2012a). Auditory:

(Ethridge et al., 2016, 2019; Rojas et al., 2001; Van der Molen et al., 2012b, 2012a)]. The *Fmr1* knockout (KO) mouse shows many of the sensory phenotypes seen in humans [Tactile: (Juczewski et al., 2016). Visual: (Rigoulot et al., 2017). Auditory: (Rotschafer & Razak, 2013); reviewed in (Sinclair et al., 2017)], making it a useful animal model for FXS research. Activating 5-HT_{1A} may be a potentially useful therapeutic approach in FXS. Previous studies have shown that activating serotonin signaling by targeting serotonin receptors is beneficial in reducing auditory hypersensitivity in *Fmr1* KO mice. Armstrong et al., 2020 showed reduced audiogenic seizures (AGS) in *Fmr1* KO mice after administration of FPT ((S)-5-(2'-fluorophenyl)-N,N-dimethyl-1,2,3,4-tetrahydronaphthalen-2-amine), a partial agonist for 5-HT_{1A}, 5-HT_{2C} and 5-HT_7 receptors (Armstrong et al., 2020; Canal et al., 2015). We showed that a more specific agonist of 5-HT_{1A} Receptor, NLX-101, caused a major reduction in AGS-induced death and tonic-clonic seizures (Tao et al., 2023). Besides, unpublished electroencephalogram (EEG) recordings (Chapter 3) from our lab showed that acute administration of NLX-101 improved temporal processing in *Fmr1* KO mice at both P21 and P30, and reduced background power in *Fmr1* KO mice only at P30 but not at P21. These findings suggest that developmental regulation of 5-HT_{1A}R signaling plays a major role in the development of auditory processing, and 5-HT_{1A}R activity may be abnormal in *Fmr1* KO mice.

The expression pattern of 5-HT_{1A}R across auditory regions and during early development in *Fmr1* WT and KO mice remains unclear. Thompson et al.,1994 showed the central auditory system is innervated by serotonergic fibers that originate from the

raphe nuclei (Thompson et al., 1994). Among auditory brain regions, the heaviest 5-HT_{1A}R binding was found in the IC (Thompson et al., 1994). Besides, more than half of GABAergic neurons in the IC were found to be associated with 5-HT_{1A}R (Peruzzi & Dut, 2004), which is also similar to what we found in this study (~60%). Therefore, NLX-101, as a 5-HT_{1A}R agonist, may ameliorate auditory hypersensitivity and improve cortical auditory temporal processing by enhancing serotonin signaling through activating 5-HT_{1A}Rs in the auditory system. The hypothesis above assumed that serotonin signaling is impaired in *Fmr1* KO mice due to lack of sufficient expression level of 5-HT_{1A}Rs. Indeed, recent findings showed that the whole brain 5-HT_{1A}R expression level was significantly reduced in juvenile *Fmr1* KO mice compared with the control mice, manifested by reduced 5-HT_{1A}R radioactive ligand binding (Saraf et al., 2024). They also attempted to examine the 5-HT_{1A}R level in the IC and the AC with binding density and found no genotype difference in the IC. Genotype effect was only found in AC in female group. However, they failed to provide cortical layer- and cell-type specific expression information. Therefore, in this study we investigated the mRNA level of 5-HT_{1A}R in both IC and AC in *Fmr1* WT and KO mice (males and females) across two age points—P21 and P30. To quantify 5-HT_{1A}R mRNA expression level in different cell types, we used a GAD probe to mark the GABAergic neurons.

4.2 Methods

4.2.1 Mice

All procedures were approved by the Institutional Animal Care and Use Committee at the University of California, Riverside. Mice were obtained from an in-house breeding colony that originated from Jackson Laboratory (Bar Harbor, ME). The mice used for the study are sighted FVB wild-type (Jax, stock# 004828; WT) and sighted FVB *Fmr1* knock-out (Jax, stock# 004624; *Fmr1* KO). The choice of FVB background strain (as opposed to the C57bl6/J strain) for the WT and *Fmr1* KO mice was guided by developmental auditory sensitivity and processing deficits (Croom et al., 2023; Nguyen et al., 2020; Wen et al., 2019) and the effects of NLX-101 in reducing auditory hypersensitivity (Tao et al., 2023) and improving temporal processing (Chapter 3) in *Fmr1* KO mice on this background strain.

For mice at P21, they were housed in home cage with the dam until they were used. For mice at P30, one to five mice were housed in each cage post-weaning under a 12:12-h light-dark cycle and fed ad libitum. This study examines 5-HT_{1A}R mRNA levels across genotypes (WT and KO), sex (male and female), and ages (P21 and P30). Three mice under each condition were used (24 mice in total). Two brain regions, the central inferior colliculus (ICC) and the auditory cortex (AC), were examined in each mouse.

4.2.2 In situ hybridization

We examined the central IC (ICC) and the auditory cortex (AC) to determine if there are genotypic (WT, KO), age (P21, P30), sex (male, female) differences in 5-HT_{1A}R mRNA expression across groups. In the AC, we also quantified layer-specific expression across genotype, age, and sex. Mice were euthanized with sodium pentobarbital (Fatal-Plus, 125 mg/kg ip) for perfusion. Transcardial perfusion was done with cold 0.1 M PBS (pH 7.4) followed by cold 4% PFA (pH 7.6). The brain tissues were extracted and postfixed overnight in 4% PFA before storage in 0.1 M PBS at 4°C until further tissue processing. The brains were cryoprotected in 30% sucrose for 2 days before being sectioned (CM 1860, Leica Biosystems) in the coronal plane at 15µm thickness. Sections were directly collected on the charged glass slides (Fisherbrand™ Superfrost™ Plus Microscope Slides) and were allowed to sit under room temperature for 2 hours before being stored at -80°C. Single molecule in situ hybridization was performed using Advanced Cell Diagnostics (ACD) RNAscope Multiplex Fluorescent Reagent kit v2 (REF 323100) with probes against 5-HT_{1A}R (Mm-Htr1a, REF 312301) and GAD (Mm-Gad1-C2, REF 400951-C2). The whole procedure lasted for 2 days.

One the first day, slides were first thawed at room temperature for 5~10 minutes before being washed with PBS for 5~10 minutes. Slides were then baked at 60°C in the ACD HybEZ™ oven for 30 minutes, followed by immersion in 4% PFA (diluted with PBS from 16% Formaldehyde Solution (w/v), Methanol-free, Thermo Scientific REF 28908). The slides were later immersed in 50%, 70%, 100% and 100% ethanol for 5 minutes each, followed by 5-minutes of air drying. To prepare target retrieval dilution,

RNAscope Target Retrieval Reagent (REF 322000) was diluted with MiliQ water at 1:10 and was heated on the hot plate stirrer (VWR cat# 7042-634). The temperature of the target retrieval dilution was maintained between 90-95°C throughout. After air drying, the slides were immersed in heated target retrieval dilution for 5 minutes and quickly dipped in distilled water twice before they were covered by RNAscope Hydroperoxide Reagent (REF 322381) under the room temperature for 10 minutes. After two quick dips in DI water, the slides were transferred in 100% ethanol for 3 minutes, followed by air drying. Hydrophobic barriers were drawn around the tissue sections on the slides with a PAP pen (ImmEdge® Pen Cat. no. H-4000). The slides were then covered by RNAscope Protease Plus Reagent (REF 322381) and moved to ACD HybEZ™ oven at 40°C for 30 minutes (humidified paper towel was used to cover the bottom of the slides chamber to prevent liquid from drying out). Protease plus reagent was washed off by dipping the slides in DI water twice. Probe mixture was made by mixing probe 1 (5-HT_{1A}R) and probe 2 (GAD67) at 1:50. After sections were covered by the probe mixtures, they were moved to ACD HybEZ™ oven at 40°C for 120 minutes (humidified paper towel was used to cover the bottom of the slides chamber to prevent liquid from drying out). After hybridization, the slides were washed twice (2 minutes each) in RNAscope Wash Buffer Reagent (REF 310091), diluted with DI water at 1:50. Slides were later stored in 5x SSC (saline-sodium citrate, diluted from 20x stock with DEPC distilled water) buffer at the room temperature overnight. 20x SSC stock was made by dissolving 175.3 g of NaCl and 88.2 g of sodium citrate in 1L of distilled water with the pH adjusted to 7.0, followed by

autoclave. The final concentrations of the ingredients are 3.0 M NaCl and 0.3 M sodium citrate.

On the second day, slides were taken out of the SSC buffer, and sections were covered by Amp 1, 2 and 3 reagents for 30, 30 and 15 minutes respectively for signal amplification. All amplification steps were done at 40°C in ACD HybEZ™ oven with humidifying paper in the slides chamber. After each step, slides were washed twice (2 minutes each) with the wash buffer. After amplification, fluorescence labeling was done to each channel (probe) at 40°C in ACD HybEZ™ oven following the process (humidifying paper towel was used to prevent liquid from drying out): HRP reagent incubation for 15 minutes, TSA vivid Fluorophore incubation for 30 minutes and HRP blocker incubation for 15 minutes. After each step, slides were washed twice (2 x 2 minutes) with the wash buffer. TSA vivid Fluorophore was diluted with TSA buffer (REF 322809) at 1:750 for 650nm (REF 323273) and 1:1500 for 520nm (REF 323271). Channel 1 (5-HT_{1A}R probe) and Channel 2 (GAD67 probe) were labeled with fluorophore 650 nm and 520 nm, respectively. DAPI staining was done after RNAscope procedures. After the last step of washing, slides were taken out and sections were covered by DAPI dilution (1:250, ThermoFisher Cat. No. 62248) for 10 minutes at the room temperature, followed by 3 times wash with PBS (3 x 10 minutes). After the last PBS wash, slides were mounted with Fluoro Gel (Electron Microscopy Sciences Cat. #17985-03), covered and sealed with coverslip (ThorLabs CG15KH1) and nail polish respectively. Sealed slides were stored in the non-transparent slides' boxes under 4°C until imaging.

4.2.3 Imaging and quantification

Stained sections were imaged using a confocal microscope (Zeiss 880 Inverted) with 20x objective and a stack of 10-15 optical images was collected with optimal resolution at 0.797 µm z-steps. Image quantification was performed using HALO software (Indica Labs) FISH v. 3.2.3 module. A 420 µm square window in the middle of the central nucleus of the inferior colliculus (ICC) was used as the counting window for the ICC. Because the auditory cortex (AC) is composed of multiple layers with different functions, we did quantification in three categories respectively based on cell organization structures: L2/3 (for cortico-cortical projections), L4 (receiving input from subcortical regions), and L5 & L6 (sending output from cortical region to the subcortical regions). The dimensions of the counting window vary from section to section, so quantification is normalized to total cell number in each category. In HALO software FISH module: DAPI was set to nuclear dye; 2 FISH probes were analyzed: GAD and 5-HT_{1A}. We were interested in two nuclear phenotypes: GAD+ 5-HT_{1A} + and GAD- 5-HT_{1A} +. The detailed parameter settings are listed in the Table 4.1 and Table 4.2 ("*" marked the parameters that were subjected to fine tuning from image to image based on staining quality. The goal was to make the real-time tuning markup be as close as possible to the real image.). Once parameters were set, cell counting and colocalization counting were done automatically by HALO. %GAD+5-HT_{1A} 5-HT_{1A} +, %GAD-5-HT_{1A} +, %5-HT_{1A} +, %GAD+ were directly extracted from the summary table in the results section. To further characterize the expression profile of 5-HT_{1A} mRNA, 5-HT_{1A} H-Scores for GAD+ and GAD- categories were computed respectively. Object data in

HALO were copied and pasted in Excel: if number of GAD copies was bigger than zero, they were classified in GAD+ category; otherwise in GAD- category. Under each category, cells were classified into 5 bins based on how many 5-HT_{1A} mRNA copies were detected: zero copies detected (bin-0); 1-3 copies detected (bin-1); 4-9 copies detected (bin-2); 10-15 copies detected (bin-3) and 16 or more copies detected (bin-4). 5-HT_{1A} H-score was computed in both categories as sum of the multiplication of bin number and percentage of cells of the bin (H-score = Σ (bin number x percentage of cells per bin)) (Musser et al., 2022).

Table 4.1. Cell detection settings in HALO software

Settings	Parameters
Nuclear contrast threshold	0.5
Minimum nuclear intensity	*
Nuclear segmentation aggressiveness	0.33
Nuclear size	*
Minimum nuclear roundness	0
Maximum cytoplasm radius	2.5

** Indicates that parameters vary from image to image based on staining quality*

Table 4.2. Probe detection settings in HALO software

	5HT1A	GAD
Probe contrast threshold	0.52	0.5
Probe signal minimum intensity	0.04	0.04
Probe spot size	0.1-20	*
Probe copy intensity	0.15	0.15
Spot segmentation aggressiveness	0.95	0.95

** Indicates that parameters vary from image to image based on staining quality*

4.2.4 Experiment design and statistics

This study investigates 5-HT_{1A}R mRNA expression pattern across sex (male and female), genotypes (*Fmr1* WT and KO) and ages (P21 and P30). 3 animals under each condition were used, and total 24 animals were used. 2-5 sections were taken from each animal for each brain region. We used multilevel model to examine the mouse-level variables but also consider of the sections within mice. We examined the main effects of genotype, age, sex, and interactions between main effects. Effects of $p < 0.05$ were considered statistically significant, and denoted as *$p < 0.05$, **$p < 0.01$, ***$p < 0.001$, ****$p < 0.0001$.

4.3 Results

In this study, we investigated the pattern of 5-HT_{1A}R mRNA in *Fmr1* WT and KO mice during early development by performing RNAscope at two age points, P21 and P30. In the previous studies, we observed significant reduction in auditory hyperactivity (Tao

et al., 2023) and improvement in auditory temporal processing (chapter 3) after 5-HT_{1A}R activation by NLX-101. Therefore, we specifically examined the 5-HT_{1A}R mRNA expression levels in the AC and the ICC which have been reported to be implicated in auditory hyperactivity and temporal processing (Gonzalez et al., 2019; Holley et al., 2022; Lovelace et al., 2020). To further explore the expression pattern in different cell types, we utilized a GAD probe to mark GABAergic neurons. Fig. 4.1 and Fig. 4.2 showed representative images from the AC and the ICC respectively in *Fmr1* WT and KO at P21 and P30. In Fig. 4.1 and Fig. 4.2, DAPI staining is shown in blue, each magenta puncta represents one copy of 5-HT_{1A}R mRNA, and green fluorescence represent GAD+ cells. We adopted two quantification methods to study the 5-HT_{1A}R mRNA level in each cell type. We first quantified the percentage of cells that express 5-HT_{1A} mRNA. Then we scored each positive cell based on its number of 5-HT_{1A}R mRNA copies to acquire an expression profile. The summed score was noted as H-Score which captures the general expression profile of 5-HT_{1A}R mRNA positive cells in each brain section (Musser et al., 2022).

In the following sections, we first report the 5-HT_{1A}R mRNA expression level in all cells. Then we classify the cells into GAD- and GAD+ based on GAD detection and report 5-HT_{1A}R mRNA expression level in each category. Lastly, we report the percentage of GAD+ cells across genotypes, sex, and ages. Analysis was done in each brain regions separately: AC layer 2/3, AC layer 4, AC layer 5 & 6, and ICC.

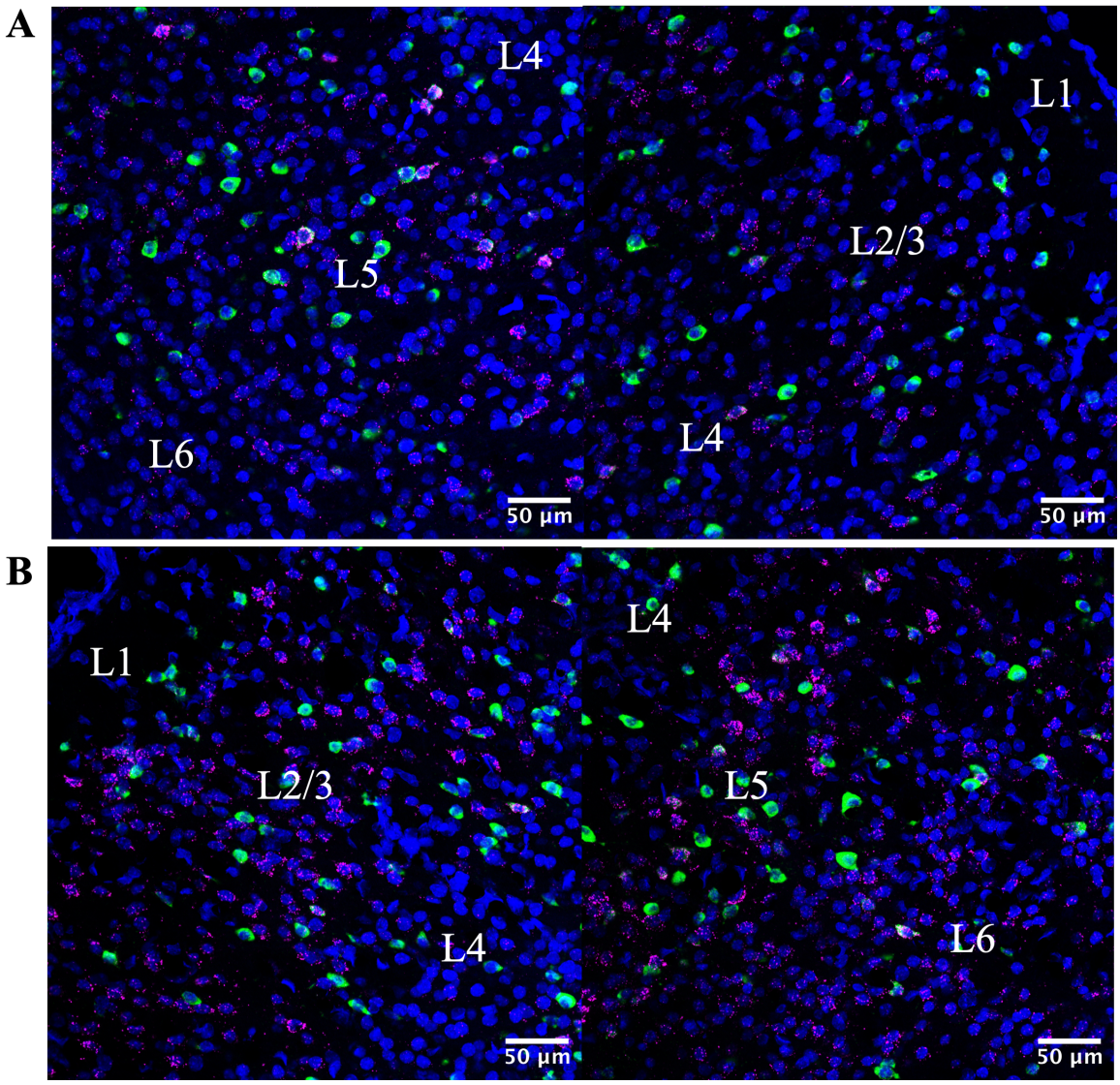
A
L4
L5
L6
50 µm
L1
L2/3
L4
50 µm
B
L1
L2/3
L4
50 µm
L4
L5
L6
50 µm

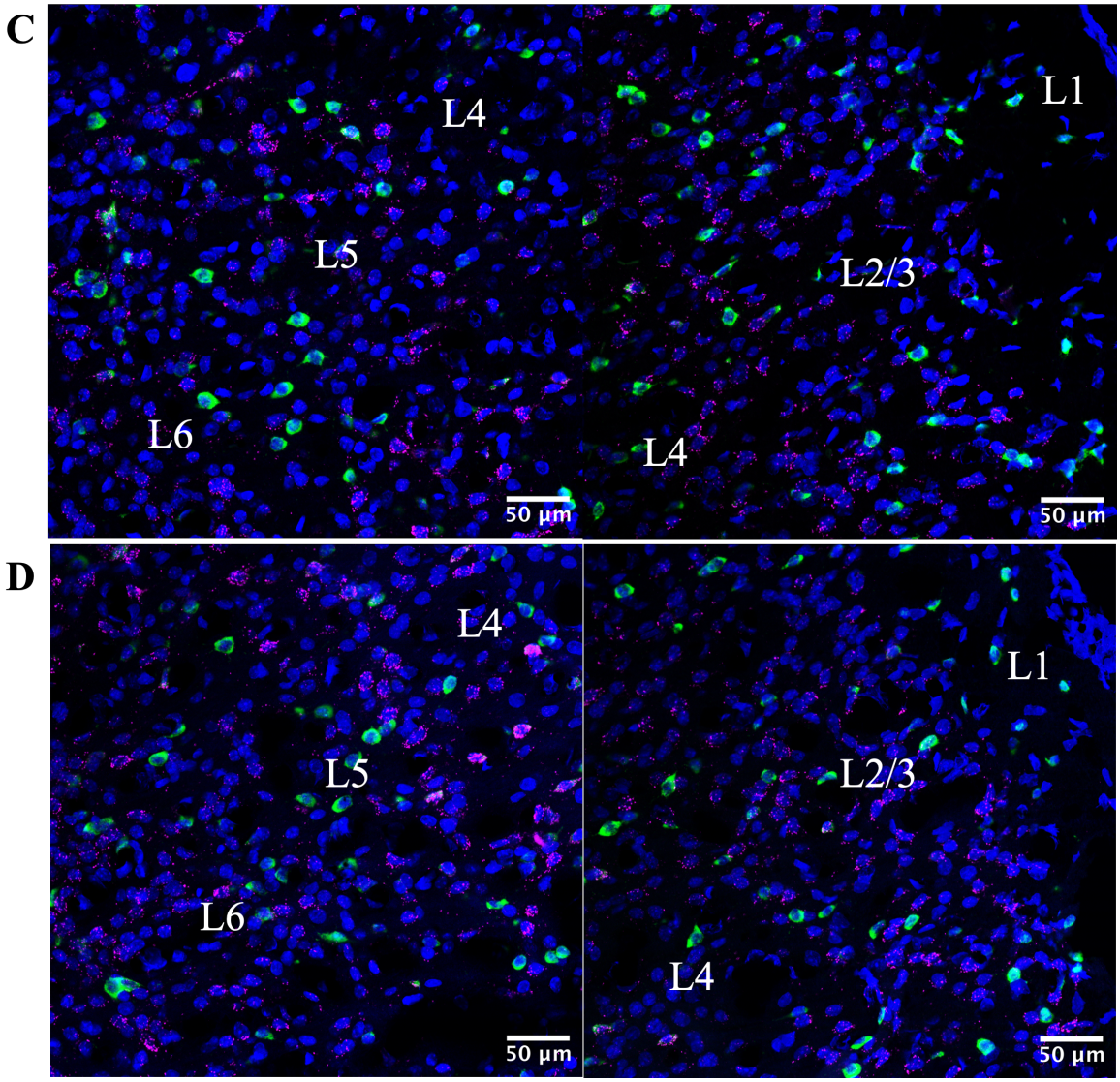

Figure 4.1. Representative images from the AC.

Bule stain: DAPI; green halo: GAD; magenta puncta: 5-HT_{1A}. The edge of the AC indicates the orientation of the section. Scale bar represents 50µm. (A) *Fmr1* WT P21 (right); (B) *Fmr1* KO P21 (left) ; (C) *Fmr1* WT P30 (right); (D) *Fmr1* KO P30 (right).

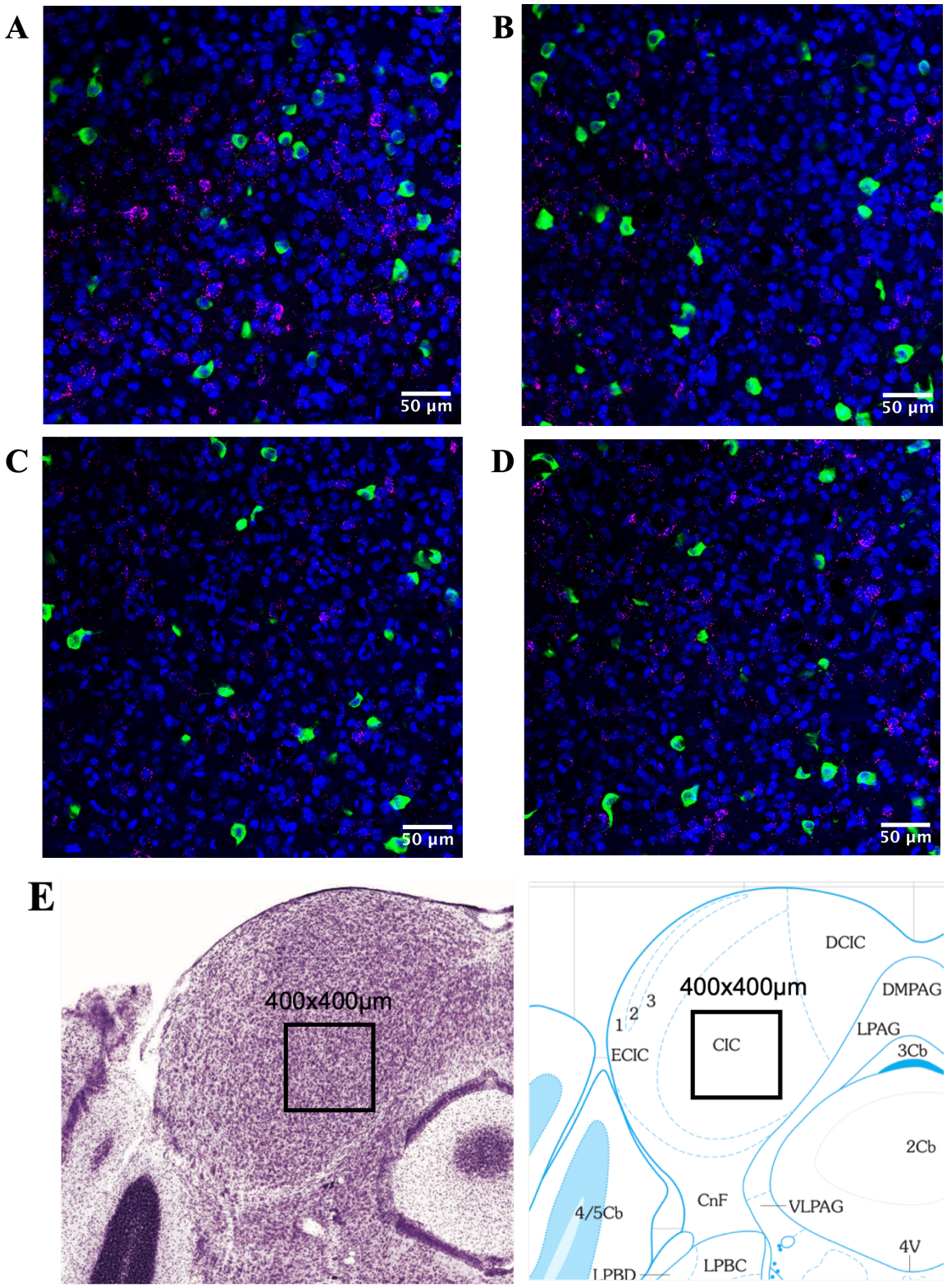
A
50 µm
B
50 µm
C
50 µm
D
50 µm
E
400x400µm
400x400µm
DCIC
DMPAG
1
2
3
ECIC
CIC
LPAG
3Cb
2Cb
4/5Cb
CnF
VLPAG
4V
LPBD
LPBC

Figure 4.2. Representative images from the ICC.

Bule stain: DAPI; green halo: GAD; magenta puncta: 5-HT_{1A}. The counting window covers the entire image. Scale bar represents 50μm. (A) *Fmr1* WT P21; (B) *Fmr1* KO P21; (C) *Fmr1* WT P30; (D) *Fmr1* KO P30. (E) Schematic graph showing the counting window of the ICC, 400μm x 400μm. Images modified from Allen Mouse Brain Atlas.

4.3.1 Percentage of 5-HT_{1A} positive cells and H-Score in all cells

The first quantification was done by comparing percentage of 5-HT_{1A} positive cells (Figure 4.3). In AC layer 2/3, a genotype effect was revealed, but surprisingly, *Fmr1* KO mice showed significantly higher expression level of 5-HT_{1A}R mRNA than WT ($p=0.0349$, KO mean=77.6803, WT mean=75.1820). Besides, the 5-HT_{1A}R mRNA level is significantly higher at P30 than at P21 ($p=0.0005$, P21 mean=67.3487, P30 mean=80.9250). No sex effect was found ($p=0.3257$). In AC layer 4, only an age effect was found, with higher 5-HT_{1A}R mRNA at P30 than at P21 ($p=0.017$, P21 mean=61.0399, P30 mean=78.5854). No genotype ($p=0.9367$) or sex effect ($p=0.4786$) was observed. In AC layer 5 and 6, 5-HT_{1A}R mRNA expression level is significantly higher at P30 than at P21 ($p=0.0205$. P21 mean=54.2275, P30 mean=64.1407). No genotype ($p=0.3845$) or sex effect ($p=0.5140$) was observed. In the ICC, there was no genotype ($p=0.6073$), sex (0.8059) or age effect (0.1171).

The second quantification was done by comparing 5-HT_{1A} H-scores of the region of interest (Figure 4.4). In layer 2/3, KO mice had higher H-Score than WT ($p=0.01162$. KO mean=187.8847, WT mean=152.6753), and P30 mice showed higher H-Score than P21 mice ($p=0.00934$. P21 mean=152.0097 and P30 mean=188.5503). But sex effect was

not significant (p=0.94128). Age effect (p=0.0202. P21 mean=118.4710. P30 mean=155.5587) was found to be significant in layer 4, but not genotype (p=0.9115) or sex effect (p=0.4225). In layer 5 and 6, only age effect was seen (p=0.02805. P21 mean=107.7523. P30 mean=138.3257), but not genotype (p=0.25949) or sex effect (p=0.58850). We did not find any significant main effects in the ICC (Genotype: p=0.5905; sex: p=0.5007; age: p=0.2227).

Together, in AC layer 2/3, KO group showed higher percentage of 5-HT_{1A} positive cells than WT, and each cell in KO group tends to have higher copy number of 5-HT_{1A} than in WT. Besides, as age increases, more cells started to express 5-HT_{1A}R mRNA, rendering higher percentage of 5-HT_{1A} positive at age of P30 than at P21. For individual 5-HT_{1A} positive cells, the copy number tends to increase with age as well.

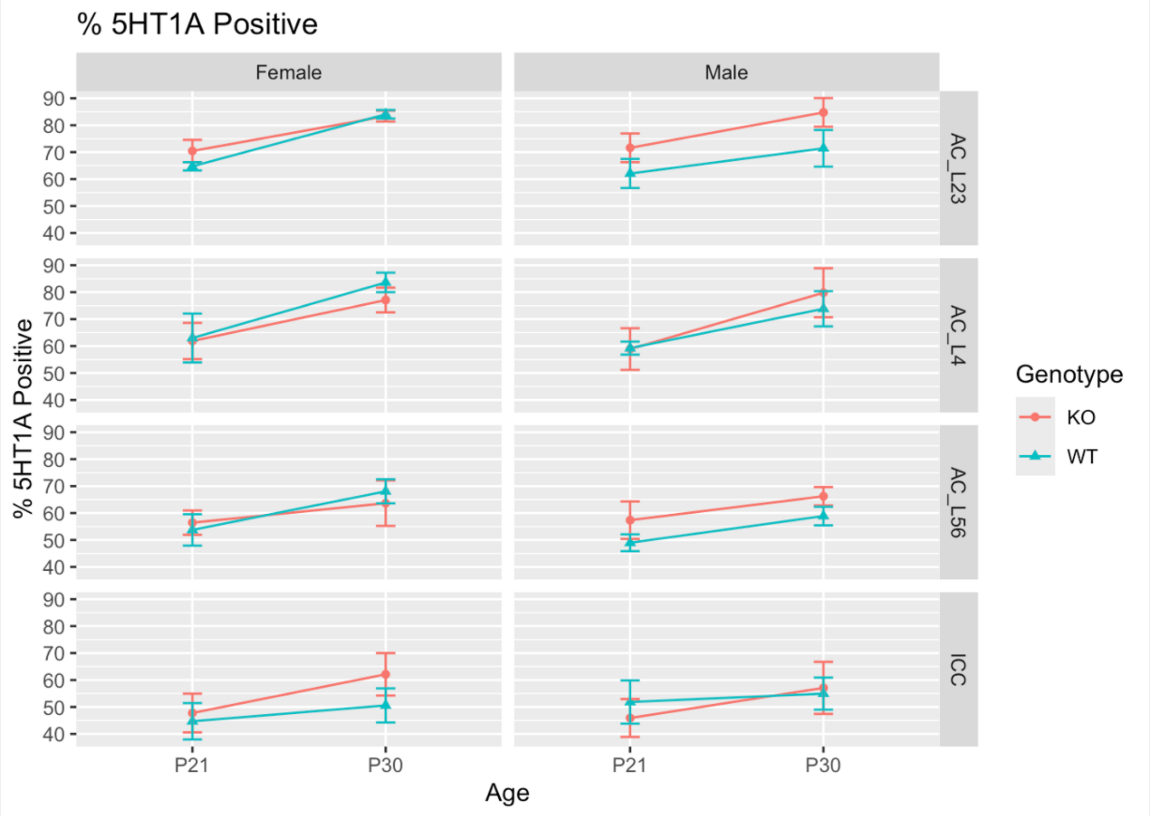

Figure 4.3. Percentage of cells that are positive for 5-HT_{1A}R egardless of GAD expression in males and females in four regions of interest at two age points P21 and P30.

Genotype effect (p=0.0349216) and age effect (p=0.0004671) were found significant in AC_L23. Age effect was also significant in AC_L4 (p=0.001674) and AC_L56 (p=0.02048). Full statistics results are in Table S4.1. AC_L23: auditory cortex layer 2/3; AC_L4: auditory cortex layer 4; AC_L56: auditory layer 5 and 6; ICC: central inferior colliculus.

Table S4.1. Percentage of 5-HT1A positive cells

Region of interest	Effects	F value	P-value
AC Layer 2/3	Genotype	5.3651	**0.0349216**
	Sex	0.9808	0.3375240
	Age	19.6887	**0.0004671**
AC Layer 4	Genotype	0.0065	0.936731
	Sex	0.5271	0.478608
	Age	14.3674	**0.001674**
AC Layer 5 and 6	Genotype	0.7970	0.3845
	Sex	0.4444	0.51397
	Age	6.5346	**0.02048**
ICC	Genotype	0.2747	0.6073
	Sex	0.0624	0.8059
	Age	2.7432	0.1171

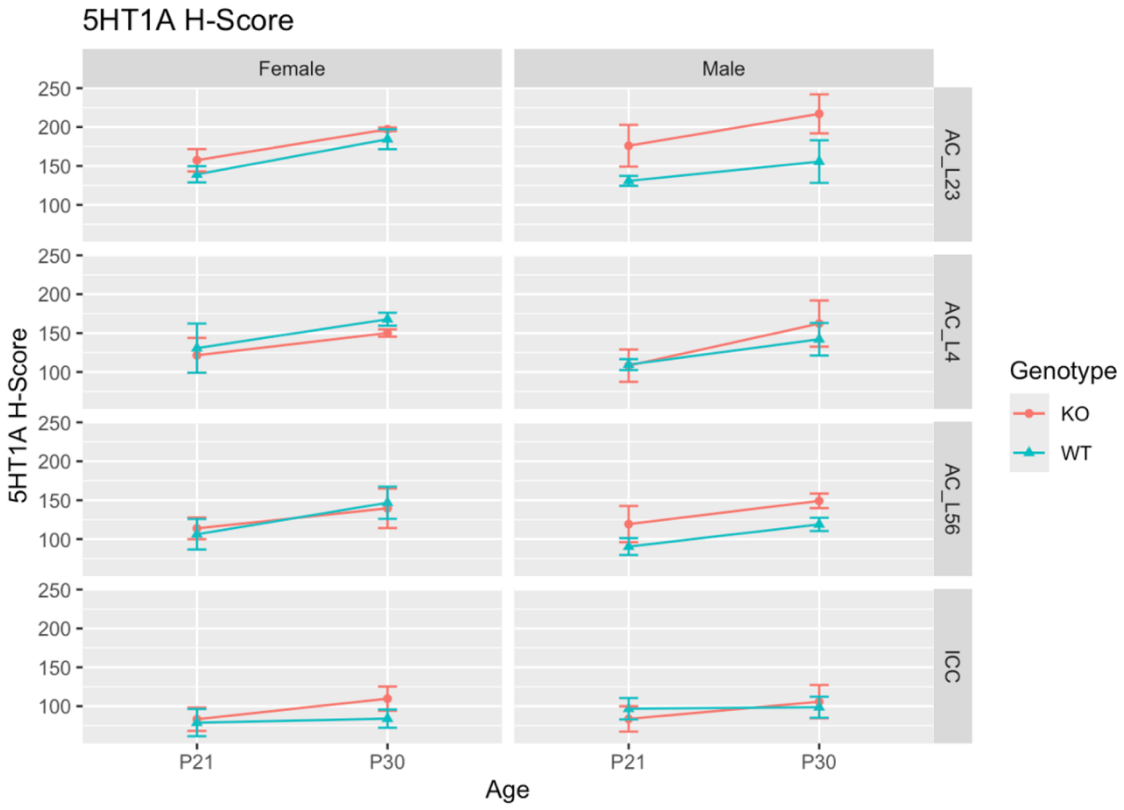

Figure 4.4. 5-HT$_{1A}$ H-Score in males and females in four regions of interest at two age points P21 and P30.

H-Score was computed based on 5-HT$_{1A}$ expression profile of individual neurons (details are in method). Genotype effect (p=0.01162) and age effect (p=0.00934) were found significant in AC_L23. Age effect was also significant in AC_L4 (p=0.0202) and AC_L56 (p=0.02805). Full statistics results are in Table S4.2. AC_L23: auditory cortex layer 2/3; AC_L4: auditory cortex layer 4; AC_L56: auditory layer 5 and 6; ICC: central inferior colliculus.

Table S4.2. 5-HT1A H-Score

Region of interest	Effects	F value	P-value
AC Layer 2/3	Genotype	8.3397	**0.01162**
	Sex	0.0056	0.94128
	Age	8.9822	**0.00934**
AC Layer 4	Genotype	0.0128	0.9115
	Sex	0.6788	0.4225
	Age	6.6923	**0.0202**
AC Layer 5 and 6	Genotype	1.3623	0.25949
	Sex	0.3043	0.58850
	Age	5.7827	**0.02805**
ICC	Genotype	0.3015	0.5905
	Sex	0.4746	0.5007
	Age	1.6092	0.2227

4.3.2 Percentage of 5-HT$_{1A}$ positive cells and H-Score in GAD- cells

To quantify cell type specific 5-HT$_{1A}$R mRNA we examined the genotype, sex, and age effects on the expression level of 5-HT$_{1A}$R mRNA in GAD- cells in AC and IC. The results of this analysis were largely like those seen with overall 5-HT$_{1A}$R mRNA because most of the mRNA was seen in the GAD- cells. We first compared percentage of 5-HT$_{1A}$ positive cells in GAD- category (Figure 4.5). In AC layer 2/3, a genotype effect was revealed, and KO mice showed significantly higher expression level of 5-HT$_{1A}$R mRNA than WT (p=0.01674. KO mean=69.7187, WT mean=62.3020). Besides, 5-HT$_{1A}$R mRNA level is significantly higher at P30 than at P21 (p=0.00034. P21 mean=59.696, P30 mean=72.3246). No sex effect was found (p=0.3489). In AC layer 4, only age effect was found, and expression level is higher at P30 than at P20 (p=0.0021. P21

mean=55.3263, P30 mean=71.2730). No genotype (p=0.9205) or sex effect (p=0.4692) revealed. In AC layer 5 and 6, 5-HT_{1A}R mRNA expression level is significantly higher at P30 than at P21 (p=0.0172. P21 mean=48.4746, P30 mean=57.8709). No genotype (p=0.34170) or sex effect (p=0.40518) was observed. In the ICC, there was no genotype (p=0.59595), sex (0.86077) or age effect (0.09944) was found.

We then compared the H-scores of GAD- cells in all regions of interest (Figure 4.6). In layer 2/3, genotype (p=0.01160, KO mean=187.5323, WT mean=151.8149) and age effect (p=0.01252, P21 mean=152.0497, P30 mean=187.2975) were found to be significant: KO mice showed higher H-Score than WT mice, and 5-HT_{1A} H-Score is higher at P30 than at P21. We did not see any sex effect (p=0.87752). In layer 4, only age effect was observed (p=0.02573, P21 mean=115.7904, P30 mean=151.5573): 5-HT_{1A} H-Score for GAD- cells is significantly higher at P30 than at P21. Neither genotype (p=0.91869) nor sex effect (0.36750) was found. Similarly, age effect (p=0.02631, P21 mean=104.7107, P30 mean=135.9917) was also found significant in Layer 5 and 6, and 5-HT_{1A} H-Score for GAD- cells was higher at P30 than P21. No genotype (p=24290) or sex effect (p=52502) was found.

In GAD- cells from AC layer 2/3, KO group showed higher percentage of 5-HT_{1A} positive cells than WT, and each cell in KO group tends to have higher copy number of 5-HT_{1A} than in WT. Besides, as age increases, more GAD- cells started to express 5-HT_{1A} mRNA, rendering higher percentage of 5-HT_{1A} positive at age of P30 than at P21. For individual GAD- but 5-HT_{1A} positive cells, the copy number tends to increase with age as well.

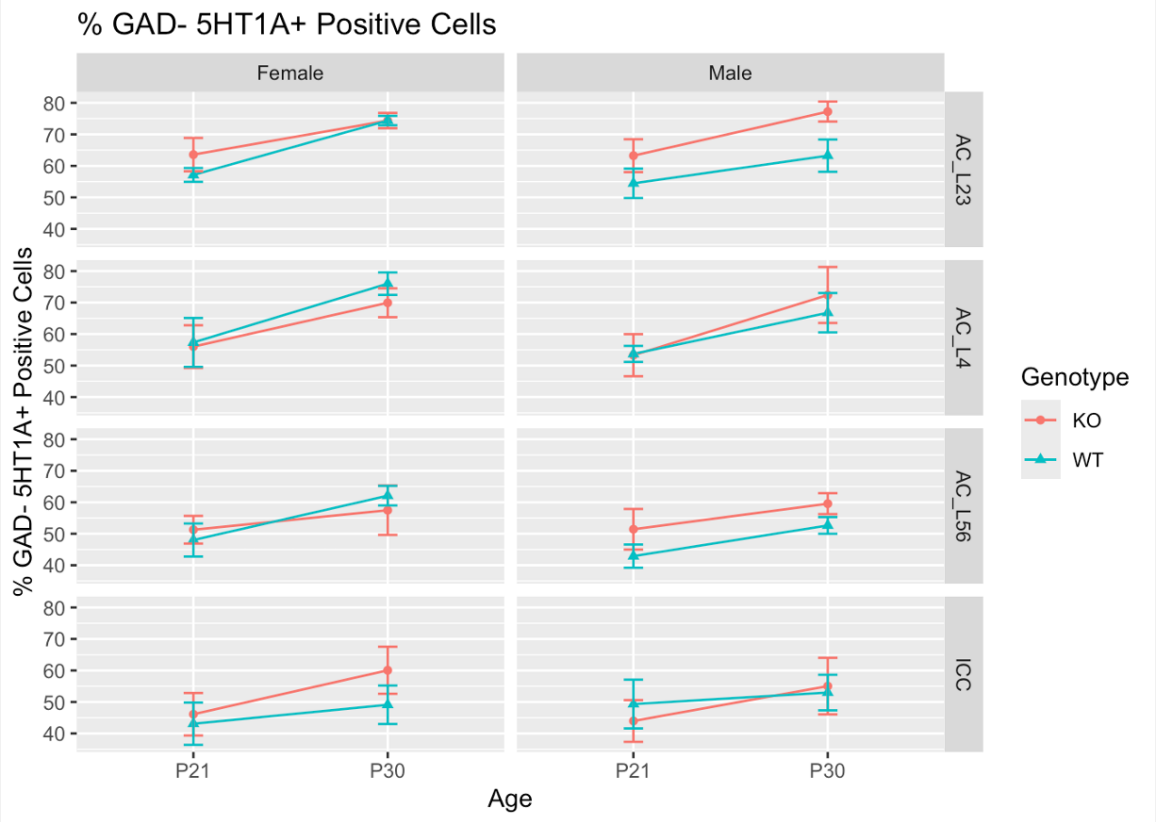

Figure 4.5. Percentage of cells that are only positive for 5-HT$_{1A}$ but not GAD in males and females in four regions of interest at two age points P21 and P30.

Genotype effect (p=0.0167353) and age effect (p=0.0003401) were found significant in AC_L23. Age effect was also significant in AC_L4 (p=0.002132) and AC_L56 (p=0.01721). Full statistics results are in Table S4.3. AC_L23: auditory cortex layer 2/3; AC_L4: auditory cortex layer 4; AC_L56: auditory layer 5 and 6; ICC: central inferior colliculus.

Table S4.3. Percentage of 5-HT1A + and GAD- cells

Region of interest	Effects	F value	P-value
AC Layer 2/3	Genotype	7.1754	**0.0167353**
	Sex	0.9326	0.3489057
	Age	20.8037	**0.0003401**
AC Layer 4	Genotype	0.0103	0.920533
	Sex	0.5503	0.469200
	Age	13.4820	**0.002132**
AC Layer 5 and 6	Genotype	0.9569	0.34170
	Sex	0.7288	0.40518
	Age	6.9700	**0.01721**
ICC	Genotype	0.2927	0.59595
	Sex	0.0318	0.86077
	Age	3.0582	0.09944

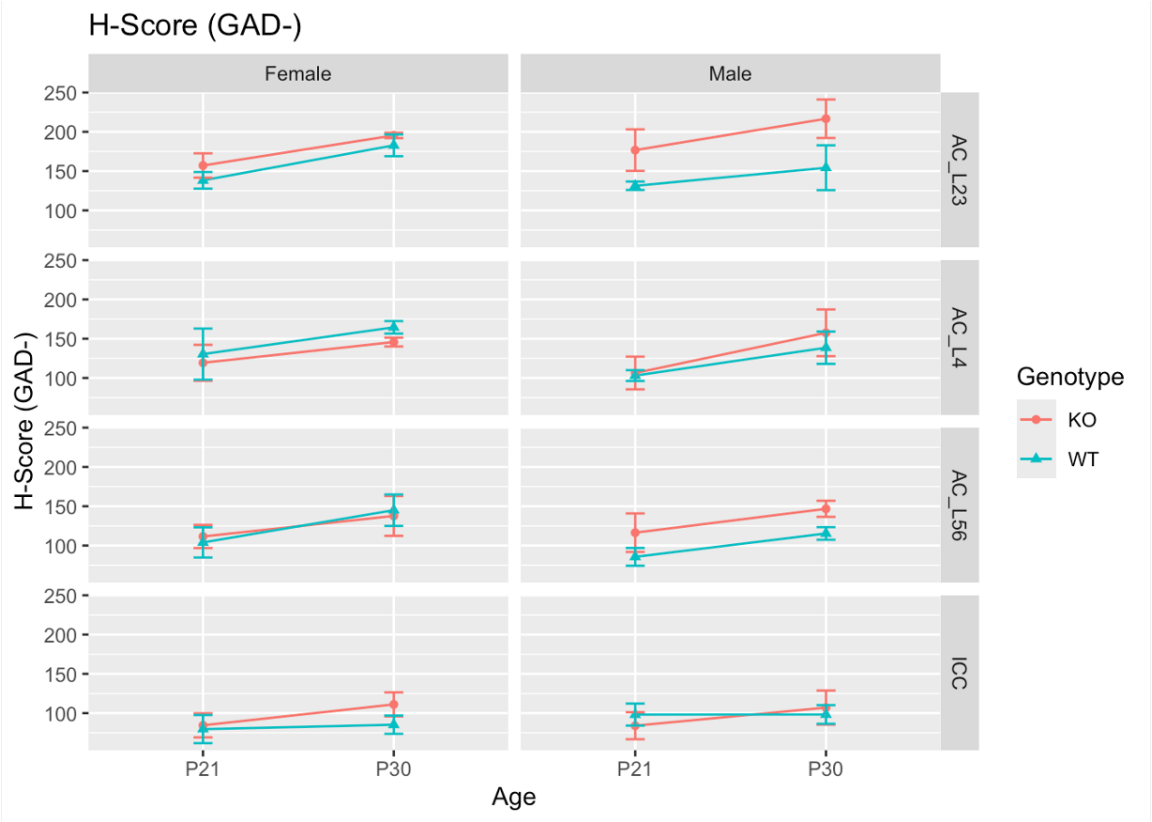

Figure 4.6. 5-HT$_{1A}$ H-Score for GAD- cells in males and females in four regions of interest at two age points P21 and P30.

5-HT$_{1A}$ H-Score (GAD-) was computed based on 5-HT$_{1A}$ expression profile of individual GAD- neurons (details are in method). Genotype effect (p=0.01160) and age effect (p=0.01252) were found significant in AC_L23. Age effect was also significant in AC_L4 (p=0.02578) and AC_L56 (p=0.02631). Full statistics results are in Table S4.4. AC_L23: auditory cortex layer 2/3; AC_L4: auditory cortex layer 4; AC_L56: auditory layer 5 and 6; ICC: central inferior colliculus.

Table S4.4. 5-HT1A H-Score (GAD-)

Region of interest	Effects	F value	P-value
AC Layer 2/3	Genotype	8.3458	**0.01160**
	Sex	0.0246	0.87752
	Age	8.1278	**0.01252**
AC Layer 4	Genotype	0.0108	0.91869
	Sex	0.8615	0.36750
	Age	6.0743	**0.02578**
AC Layer 5 and 6	Genotype	1.4655	0.24290
	Sex	0.4215	0.52502
	Age	5.9381	**0.02631**
ICC	Genotype	0.3346	0.5710
	Sex	0.4072	0.5324
	Age	1.5691	0.2283

4.3.3 Percentage of 5-HT$_{1A}$ positive cells and H-Score in GAD+ cells

For neurons that were positive for both 5-HT$_{1A}$ and GAD, no significant effect was found in any region of interest in terms of percentage of cells (Figure 4.7. Layer 2/3: genotype: p=0.7428, sex: p=0.7240, age: p=0.3477. Layer 4: genotype: p=0.9207, sex: p=0.8930, age: p=0.0966. Layer 5 and 6: genotype: p=0.9875, sex: p=0.6066, age: p=0.5429. ICC: genotype: p=0.8409, sex: p=0.1685, age: p=0.8869.) For 5-HT$_{1A}$ H-Score of GAD+ cells (Figure 4.8.) AC layer 2/3, *Fmr1* KO mice GAD+ cells showed higher 5-HT$_{1A}$ H-Score than WT mice (p=0.026748 KO mean=194.3770, WT mean=164.8264). 5-HT$_{1A}$ H-Score was higher at P30 than P21 (p=0.001987. P21

mean=156.7305, P30 mean=202.4729). No significant sex difference was found (p=0.586583). In layer 5 and 6, no significant effects were found (Genotype: p=0.46655, sex: 0.66548, age: 0.06512).

Together, the percentage of cells that are positive for both GAD and 5-HT_{1A} did not differ across genotypes, sex, or ages in all brain regions examined. However, for individual dual positive cells, the copy number of 5-HT_{1A} is significantly higher in KO than WT and it increases as age in almost all layers of the AC except for layer 5 and 6.

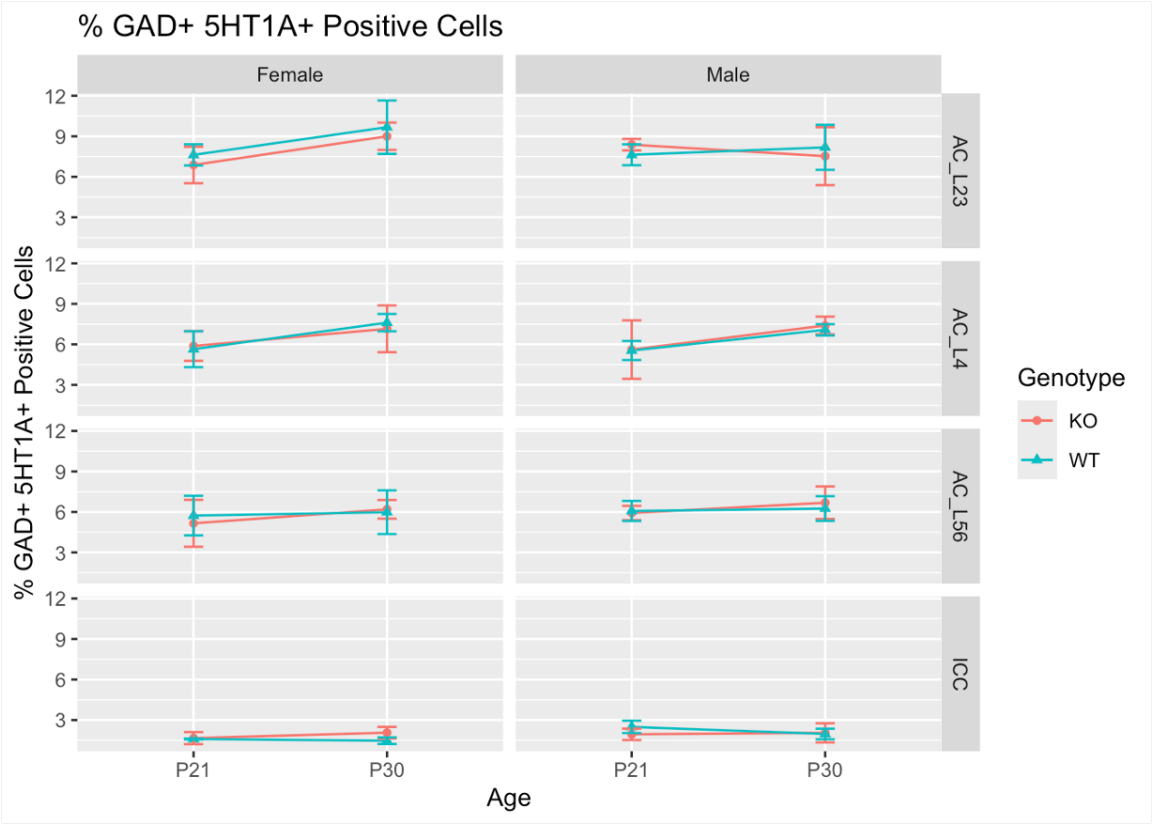

Figure 4.7. Percentage of cells that are positive for both 5-HT$_{1A}$ and GAD in males and females in four regions of interest at two age points P21 and P30.

No significant effect was found in any region of interest. Full statistics results are in Table S4.5. AC_L23: auditory cortex layer 2/3; AC_L4: auditory cortex layer 4; AC_L56: auditory layer 5 and 6; ICC: central inferior colliculus.

Table S4.5. Percentage of 5-HT1A + and GAD+ cells

Region of interest	Effects	F value	P-value
AC Layer 2/3	Genotype	0.1116	0.7428
	Sex	0.1293	0.7240
	Age	0.9373	0.3477
AC Layer 4	Genotype	0.0102	0.9207
	Sex	0.0187	0.8930
	Age	3.1071	0.0966
AC Layer 5 and 6	Genotype	0.0003	0.9875
	Sex	0.2760	0.6066
	Age	0.3867	0.5429
ICC	Genotype	0.0417	0.8409
	Sex	2.0815	0.1685
	Age	0.0209	0.8869

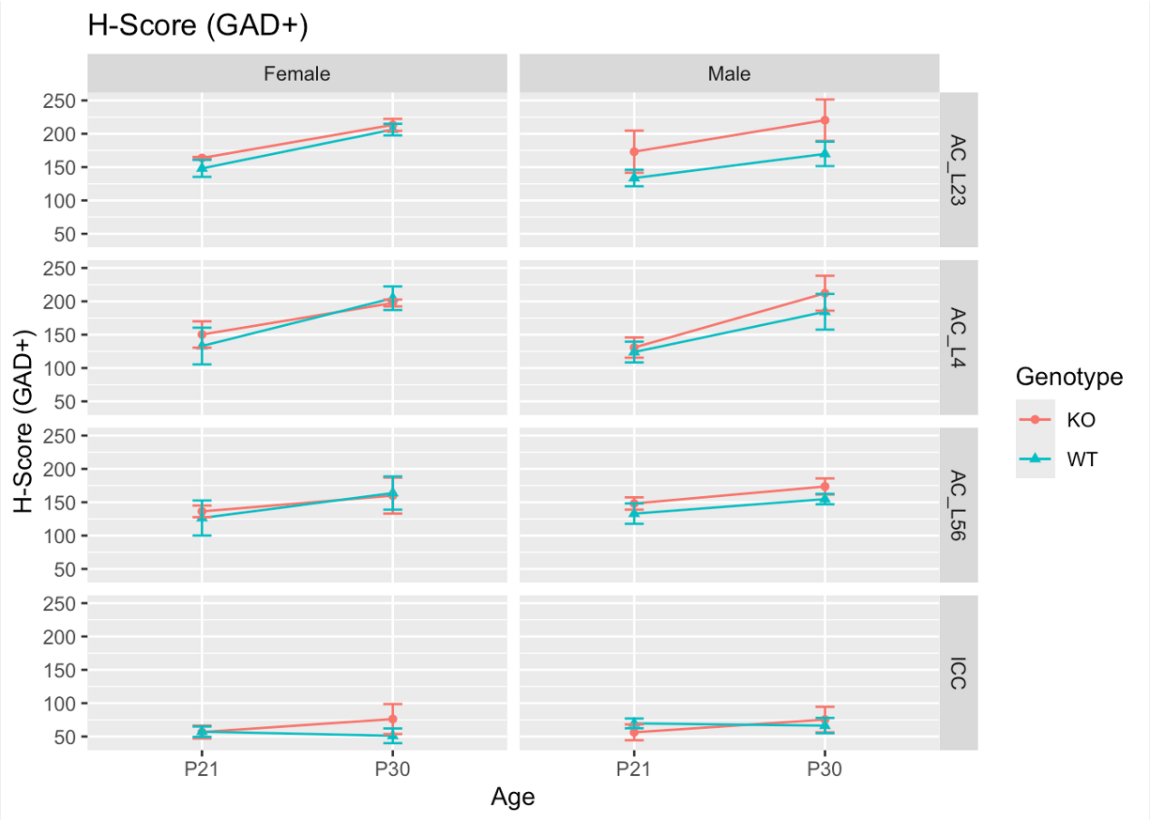

Figure 4.8. 5-HT$_{1A}$ H-Score for GAD+ cells in males and females in four regions of interest at two age points P21 and P30.

5-HT$_{1A}$ H-Score (GAD+) was computed based on 5-HT$_{1A}$ expression profile of individual GAD+ neurons (details are in method). Genotype effect (p=0.026748) and age effect (p=0.001987) were found significant in AC_L23. Age effect was also significant in AC_L4 (p=0.0004212). Full statistics results are in Table S4.6. AC_L23: auditory cortex layer 2/3; AC_L4: auditory cortex layer 4; AC_L56: auditory layer 5 and 6; ICC: central inferior colliculus.

Table S4.6. 5-HT1A H-Score (GAD+)

Region of interest	Effects	F value	P-value
AC Layer 2/3	Genotype	6.2686	**0.026748**
	Sex	0.3113	0.586583
	Age	15.0203	**0.001987**
AC Layer 4	Genotype	0.6544	0.4307283
	Sex	0.3063	0.5877981
	Age	19.8921	**0.0004212**
AC Layer 5 and 6	Genotype	0.5547	0.46655
	Sex	0.1936	0.66548
	Age	3.8876	0.06512
ICC	Genotype	0.3073	0.5870
	Sex	0.5697	0.4613
	Age	0.6082	0.4468

4.3.4 Percentage of GAD positive cells

We quantified the percentage of GAD+ cells in the AC and IC (Figure 4.9). There were no significant main effects found on the percentage of GAD+ cells in all layers of the AC (Layer 2/3: genotype: p=0.3063, sex: p=0.6804, age: p=0.2921. Layer 4: genotype: p=0.9582, sex: p=0.8651, age: p=0.8635. Layer 5 and 6: genotype: p=0.7336, sex: p=0.6747, age: p=0.6265). In the ICC, sex effect was found such that males had higher percentage of GAD+ cells than females (p=0.02693. Female mean=4.0818, Male mean= 4.9612). The percentage of GAD positive cells was higher at P21 than at P30 (p=0.02465. P21 mean=4.9692, P30 mean=4.0738). There was no genotype effect

(p=0.8382). Together, GAD exhibited development and sex- dependent expression pattern in the ICC but not any layers of the AC.

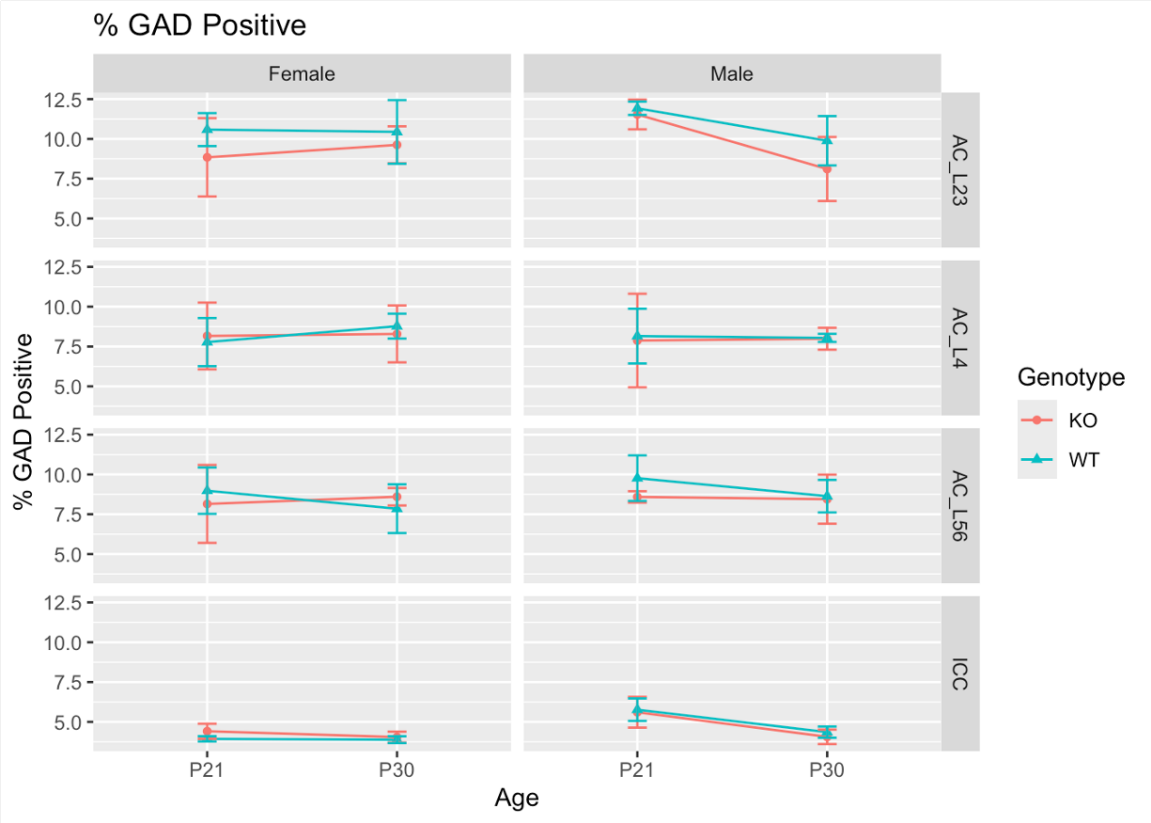

Figure 4.9. The percentage of cells that positive for GAD regardless of 5-HT$_{1A}$ expression in males and females in four regions of interest at two age points P21 and P30.

No significant effect was found in any layer of the AC. Sex effect (p=0.02693) and age effect (p=0.02465) was found significant in the ICC. Full statistics results are in Table S4.7. AC_L23: auditory cortex layer 2/3; AC_L4: auditory cortex layer 4; AC_L56: auditory layer 5 and 6; ICC: central inferior colliculus.

Table S4.7. Percentage of GAD+ cells

Region of interest	Effects	F value	P-value
AC Layer 2/3	Genotype	1.1160	0.3063
	Sex	0.1760	0.6804
	Age	1.1863	0.2921
AC Layer 4	Genotype	0.0028	0.9582
	Sex	0.0298	0.8651
	Age	0.0305	0.8635
AC Layer 5 and 6	Genotype	0.1199	0.7336
	Sex	0.1828	0.6747
	Age	0.2461	0.6265
ICC	Genotype	0.0432	0.83820
	Sex	6.0284	**0.02693**
	Age	6.2511	**0.02465**

4.4 Discussion

In this study, we examined the effects of genotypes, sex, and age on 5-HT_{1A}R mRNA in the AC and the ICC. Our main findings are: 1) 5-HT_{1A}R mRNA transcripts were found in both GAD+ and GAD- cell types, but predominately associate with GAD- cells in both brain regions; 2) The number of 5-HT_{1A}R mRNA transcripts increases with age in the AC, suggesting developmental regulation; 3) In AC layer 2/3, *Fmr1* KO mice showed a surprisingly higher expression level of 5-HT_{1A} mRNA transcripts than WT mice. Overall, counter to our hypothesis, we did not see a reduction in *Fmr1* KO mouse AC or IC in terms of 5-HT_{1A}R mRNA transcripts, but an age-dependent increase was the main outcome.

Fmr1 KO mice on the FVB background show severe audiogenic susceptibility at ~P21. Activating 5-HT_{1A}R with partial agonist FPT significantly reduced seizure-induced death rate in *Fmr1* KO mice (Armstrong et al., 2020). With more selective 5-HT_{1A}R agonist, NLX-101, we showed activating 5-HT_{1A} strongly protected *Fmr1* KO mice from having audiogenic seizures (Tao et al., 2023) and improved temporal processing (chapter 3). Activating 5-HT_{2B} R in *Fmr1* KO mouse enhanced Ras-PI3K/ PKB signaling input and GluA1-dependent synaptic plasticity and partially rescued the learning deficits (Lim et al., 2014). These results suggested that *Fmr1* KO mice have abnormal expression or signaling of serotonin receptors. Consistent with this idea, a recent study showed juvenile *Fmr1* KO mice had lower whole-brain 5-HT_{1A} receptor expression than WT mice (Saraf et al., 2024). However, specifically in the AC and the IC of the auditory system, our data does not show a reduction at the 5-HT_{1A}R mRNA level.

This suggests, perhaps that signaling through the receptor, or the expression of the receptor on the cell membrane may be impaired. Another possibility is that there is no difference in 5-HT_{1A}R expression or signaling, but a selective agonist of this receptor reduces auditory hypersensitivity and improves temporal processing in both WT and *Fmr1* KO mice, and in the latter group, the reduced activity is in the sub-convulsive range. WT mice do not show audiogenic seizures for the sound levels we tested, so the effects of NLX-101 on seizure activity was not studied. In our EEG study (chapter 3) we observed improvement in temporal processing in both WT and KO mice at P30, suggesting the effects of NLX-101 may be in the absence of genotype differences in receptor expression.

Serotonin release in the cortex increases during seizures (Deng et al., 2024). Therefore, a possible dysfunction in the *Fmr1* KO mice is that serotonin release is not as robust as in WT mice with loud sounds. Tangentially supportive of this idea is a study by (Uutela et al., 2014), who showed that the SSRI, fluoxetine improved cellular and behavioral responses in *Fmr1* KO mice, although auditory function was not tested. Altered serotonin synthesis has also been reported in humans with FXS (Boccuto et al., 2013; Chugani, 2002), prompting treatment strategies that modulate serotoninergic system. Sertraline, an FDA approved selective serotonin reuptake inhibitor (SSRI), showed various improvement in humans with FXS especially during development [Improvement in expressive and receptive language: (Indah Winarni et al., 2012). Improvement in cognition: (Winarni et al., 2012). Improvement in motor and visual perception: (Greiss Hess et al., 2016).] Future studies will measure serotonin release in the AC and IC with increasing sound levels using fiber photometry and grab sensors.

The central auditory system is under innervation of serotoninergic fibers originating from the raphe nuclei (Thompson et al., 1994). As expected, we found expression of 5-HT_{1A} mRNA in both AC and ICC. Besides, 5-HT_{1A}R mRNA transcripts were found in both cell types, GAD+ and GAD-, which is also consistent with published findings by others (Aznar et al., 2003; Cervantes-Ramírez et al., 2019; García-Oscos et al., 2015; Peruzzi & Dut, 2004). Interestingly, we observed 5-HT_{1A} mRNA transcripts were predominately associated with GAD- cells in both AC and ICC. Similar pattern has been recorded in other cortices in rats. (Czyrak et al., 2003) reported that 5-HT_{1A}R s were abundant in pyramidal neurons in layer 2/3, layer 5 and layer 6 in the cingulate cortex

with immunohistostaining (Czyrak et al., 2003). Similarly, with in situ hybridization, Santana (2004) found about 60% of pyramidal neurons are colocalized with 5-HT_{1A}R mRNA transcripts and only about 25% of GABAergic neurons were positive for 5-HT_{1A}R mRNA in prefrontal cortex (Santana, 2004).

Another interesting result that stood out in this study is we found genotype difference only in the AC layer 2/3 but no other layers of AC or ICC. In current study, we saw 5-HT_{1A}R mRNA transcripts were expressed in both GAD+ and GAD- cells. Given that not only neurons, glial cells also express 5-HT_{1A}Rs (Azmitia et al., 1996). Future studies are needed to further characterize the expression pattern of 5-HT_{1A}R in excitatory neurons in both AC and ICC with triple labeling. It has been well established that 5-HT_{1A}R is coupled with Gi protein and exerts hyperpolarizing effects on cells (Albert & Vahid-Ansari, 2019). However, depending on the subcellular locations of 5-HT_{1A}R , they can give rise to different effects in different cell types (Azmitia et al., 1996; Cervantes-Ramírez et al., 2019; García-Oscos et al., 2015; Llado-Pelfort et al., 2012). (Azmitia et al., 1996) characterized two distinct expression patterns of 5-HT_{1A}R: somatodentric pattern and axon hillock pattern. Somatodentic pattern, where the dendritic shaft, branches and spiks are labeled, was found in the midbrain and medullary raphe nuclei, locus coeruleus nucleus, and large reticular neurons in the pons, and some interneurons in the CA. Axon hillock pattern, where labeled areas are the initial segment of the axon, was found cortical and hippocampal pyramidal neurons and brainstem motoneurons. (Azmitia et al., 1996). Given such differences, the activation of 5-HT_{1A}R on GAD+ or GAD- cells may lead to different effects. Activating 5-HT_{1A}R located on somatodendritic areas cause

pronounced hyperpolarization mediated events; but activating those located on axon hillocks may lead to a nonsynaptically mediated inhibition of the initiation of the action potential (Azmitia et al., 1996). These differences have important clinic implications: 5-HT_{1A}Rs on axon hillocks are less susceptible to receptor down regulation in response to 5-HT_{1A}R agonist compared with those located on somatodendritic areas, making them ideal targets for clinic treatment. Indeed, it has been reported that application of 5-HT_{1A}R agonist induces dose-dependent effects on firing rates in pyramidal neurons in the prefrontal cortex, which was due to the preferential activation of 5-HT_{1A}Rs on GABAergic neurons followed by 5-HT_{1A}R s activation on the pyramidal neurons (Llado-Pelfort et al., 2012). In the auditory cortex layer 2/3, (García-Oscos et al., 2015) found that the reduction of GABA release in response to serotonin application is mediated by 5-HT_{1A}R s through presynaptic mechanisms (García-Oscos et al., 2015). With the similar experiment setup, the same group revealed that reduced glutamatergic synaptic transmission following serotonin application in AC layer 2/3 is mediated by 5-HT_{1A}R s through post-synaptic mechanism (Cervantes-Ramírez et al., 2019). These findings suggest serotonin can exert diverse effects not only through its different receptor subtypes, but also by the unique subcellular locations of the same receptor subtype, making it even harder to predict the results of 5-HT receptor activation.

We found there were higher number of copies of 5-HT_{1A}R mRNA in *Fmr1* KO mice than WT in AC layer 2/3, suggesting there might be functional implications. In the primary somatosensory (S1), (Quiquempoix et al., 2018) found that pyramidal neurons in layer 2/3 amplifies sensory-evoked response from layer 5, making them a gain modulator

(Quiquempoix et al., 2018). Activating 5-HT_{1A}R s in pyramidal neurons in AC layer 2/3 leads to reduced glutamatergic synaptic transmission (Cervantes-Ramírez et al., 2019). If higher copy number of 5-HT_{1A}R mRNA transcripts seen in *Fmr1* KO mice in this study do imply higher number of 5-HT_{1A}R protein expression level, then increasing 5-HT_{1A}Rs in AC layer 2/3 could be a compensatory mechanism in *Fmr1* KO mice to decrease hyperactive cortical activity. Indeed, serotonin modulates sensory signal to noise ratio. In single unit recording work, application of 5-HT_{1A}R shortened the response window of neurons by suppressing those with longer latencies at the network level and later spikes at the cellular level (Hurley, 2007). Therefore, increasing expression of 5-HT_{1A}R in AC layer 2/3 might be potentially beneficial for *Fmr1* KO mice because it reduces unspecific intrinsic synaptic transmission and helps to enhance more specific and task relevant auditory signals from the thalamus.

4.5 Conclusions

By manipulating spatial and temporal expression pattern of 5-HT_{1A}Rs in transgenic mice, (Gross et al., 2002) found that expression of 5-HT_{1A}R during early development, but not adulthood, is necessary to establish normal anxiety behavior in adult, supporting the view that serotonin homeostasis during early development is critical to establish normal behavioral patterns in adulthood. Behavioral changes during adulthood can be partially attributed to mis-wiring in the brain circuits due to disturbance in serotonin modulation (Bar-Peled et al., 1991; Gross et al., 2002). There is a strong link between early developmental sensory hypersensitivity and anxiety phenotypes in ASD

(Saemundsen et al., 2007). The observations that there is a developmental regulation of 5-HT_{1A}R mRNA and that a selective agonist of this receptor reduces auditory hypersensitivity and improves temporal processing in the *Fmr1* KO mice suggests that serotonin modulation may be a useful therapeutic approach in FXS, and perhaps more broadly in ASD.

References

Albert, P. R., & Vahid-Ansari, F. (2019). The 5-HT1A receptor: Signaling to behavior. *Biochimie*, *161*, 34–45. https://doi.org/10.1016/j.biochi.2018.10.015

Armstrong, J. L., Casey, A. B., Saraf, T. S., Mukherjee, M., Booth, R. G., & Canal, C. E. (2020). (S)-5-(2′-Fluorophenyl)- N , N -dimethyl-1,2,3,4-tetrahydronaphthalen-2-amine, a Serotonin Receptor Modulator, Possesses Anticonvulsant, Prosocial, and Anxiolytic-like Properties in an Fmr1 Knockout Mouse Model of Fragile X Syndrome and Autism Spectrum. *ACS Pharmacology & Translational Science*. https://doi.org/10.1021/acsptsci.9b00101

Azmitia, E. C., Gannon, P. J., Kheck, N. M., & Whitaker-Azmitia, P. M. (1996). *Cellular Localization of the 5-HTIA Receptor in Primate Brain Neurons and Glial Cells*.

Aznar, S., Qian, Z., Shah, R., Rahbek, B., & Knudsen, G. M. (2003). The 5-HT1A serotonin receptor is located on calbindin- and parvalbumin-containing neurons in the rat brain. *Brain Research*, *959*(1), 58–67. https://doi.org/10.1016/S0006-8993(02)03727-7

Bar-Peled, O., Gross-Isseroff, R., Ben-Hur, H., Hoskins, I., Groner, Y., & Biegon, A. (1991). Fetal human brain exhibits a prenatal peak in the density of serotonin 5-HT1A receptors. *Neuroscience Letters*, *127*(2), 173–176. https://doi.org/10.1016/0304-3940(91)90787-T

Boccuto, L., Chen, C.-F., Pittman, A. R., Skinner, C. D., McCartney, H. J., Jones, K., Bochner, B. R., Stevenson, R. E., & Schwartz, C. E. (2013). Decreased

tryptophan metabolism in patients with autism spectrum disorders. *Molecular Autism*, *4*(1), 16. https://doi.org/10.1186/2040-2392-4-16

Canal, C. E., Felsing, D. E., Liu, Y., Zhu, W., Wood, J. T., Perry, C. K., Vemula, R., & Booth, R. G. (2015). An Orally Active Phenylaminotetralin-Chemotype Serotonin 5-HT7 and 5-HT1A Receptor Partial Agonist That Corrects Motor Stereotypy in Mouse Models. *ACS Chemical Neuroscience*, *6*(7), 1259–1270. https://doi.org/10.1021/acschemneuro.5b00099

Cervantes-Ramírez, V., Canto-Bustos, M., Aguilar-Magaña, D., Pérez-Padilla, E. A., Góngora-Alfaro, J. L., Pineda, J. C., Atzori, M., & Salgado, H. (2019). Citalopram reduces glutamatergic synaptic transmission in the auditory cortex via activation of 5-HT1A receptors. *NeuroReport*, *30*(18), 1316–1322. https://doi.org/10.1097/WNR.0000000000001366

Chugani, D. C. (2002). Role of altered brain serotonin mechanisms in autism. *Molecular Psychiatry*, *7*(S2), S16–S17. https://doi.org/10.1038/sj.mp.4001167

Cordeiro, L., Ballinger, E., Hagerman, R., & Hessl, D. (2010). Clinical assessment of DSM-IV anxiety disorders in fragile X syndrome: Prevalence and characterization. *Journal of Neurodevelopmental Disorders*, *3*(1), 57–67. https://doi.org/10.1007/s11689-010-9067-y

Croom, K., Rumschlag, J. A., Erickson, M. A., Binder, D. K., & Razak, K. A. (2023). Developmental delays in cortical auditory temporal processing in a mouse model of Fragile X syndrome. *Journal of Neurodevelopmental Disorders*, *15*(1), 23. https://doi.org/10.1186/s11689-023-09496-8

Czyrak, A., Czepiel, K., Maćkowiak, M., Chocyk, A., & Wędzony, K. (2003). Serotonin 5-HT1A receptors might control the output of cortical glutamatergic neurons in rat cingulate cortex. *Brain Research*, *989*(1), 42–51. https://doi.org/10.1016/S0006-8993(03)03352-3

Deng, F., Wan, J., Li, G., Dong, H., Xia, X., Wang, Y., Li, X., Zhuang, C., Zheng, Y., Liu, L., Yan, Y., Feng, J., Zhao, Y., Xie, H., & Li, Y. (2024). Improved green and red GRAB sensors for monitoring spatiotemporal serotonin release in vivo. *Nature Methods*, *21*(4), 692–702. https://doi.org/10.1038/s41592-024-02188-8

Ethridge, L. E., De Stefano, L. A., Schmitt, L. M., Woodruff, N. E., Brown, K. L., Tran, M., Wang, J., Pedapati, E. V., Erickson, C. A., & Sweeney, J. A. (2019). Auditory EEG Biomarkers in Fragile X Syndrome: Clinical Relevance. *Frontiers in Integrative Neuroscience*, *13*, 60. https://doi.org/10.3389/fnint.2019.00060

Ethridge, L. E., White, S. P., Mosconi, M. W., Wang, J., Byerly, M. J., & Sweeney, J. A. (2016). Reduced habituation of auditory evoked potentials indicate cortical hyper-excitability in Fragile X Syndrome. *Translational Psychiatry*, *6*(4), e787–e787. https://doi.org/10.1038/tp.2016.48

García-Oscos, F., Torres-Ramírez, O., Dinh, L., Galindo-Charles, L., Pérez Padilla, E. A., Pineda, J. C., Atzori, M., & Salgado, H. (2015). Activation of 5- HT receptors inhibits GABA ergic transmission by pre-and post-synaptic mechanisms in layer II/III of the juvenile rat auditory cortex. *Synapse*, *69*(3), 115–127. https://doi.org/10.1002/syn.21794

Gonzalez, D., Tomasek, M., Hays, S., Sridhar, V., Ammanuel, S., Chang, C., Pawlowski, K., Huber, K. M., & Gibson, J. R. (2019). Audiogenic Seizures in the *Fmr1* Knock-Out Mouse Are Induced by *Fmr1* Deletion in Subcortical, VGlut2-Expressing Excitatory Neurons and Require Deletion in the Inferior Colliculus. *The Journal of Neuroscience*, *39*(49), 9852–9863. https://doi.org/10.1523/JNEUROSCI.0886-19.2019

Greiss Hess, L., Fitzpatrick, S. E., Nguyen, D. V., Chen, Y., Gaul, K. N., Schneider, A., Lemons Chitwood, K., Eldeeb, M. A. A. A., Polussa, J., Hessl, D., Rivera, S., & Hagerman, R. J. (2016). A Randomized, Double-Blind, Placebo-Controlled Trial of Low-Dose Sertraline in Young Children With Fragile X Syndrome. *Journal of Developmental & Behavioral Pediatrics*, *37*(8), 619–628. https://doi.org/10.1097/DBP.0000000000000334

Gross, C., Zhuang, X., Stark, K., Ramboz, S., Oosting, R., Kirby, L., Santarelli, L., Beck, S., & Hen, R. (2002). Serotonin1A receptor acts during development to establish normal anxiety-like behaviour in the adult. *Nature*, *416*(6879), 396–400. https://doi.org/10.1038/416396a

Hagerman, R. J., & Hagerman, P. J. (2002). *Fragile X Syndrome: Diagnosis, Treatment, and Research*. Taylor & Francis US.

Holley, A. J., Shedd, A., Boggs, A., Lovelace, J., Erickson, C., Gross, C., Jankovic, M., Razak, K., Huber, K., & Gibson, J. R. (2022). A sound-driven cortical phase-locking change in the Fmr1 KO mouse requires Fmr1 deletion in a subpopulation

of brainstem neurons. *Neurobiology of Disease*, *170*, 105767. https://doi.org/10.1016/j.nbd.2022.105767

Hunter, J., Rivero-Arias, O., Angelov, A., Kim, E., Fotheringham, I., & Leal, J. (2014). Epidemiology of fragile X syndrome: A systematic review and meta-analysis. *American Journal of Medical Genetics Part A*, *164*(7), 1648–1658. https://doi.org/10.1002/ajmg.a.36511

Hurley, L. M. (2007). Activation of the serotonin 1A receptor alters the temporal characteristics of auditory responses in the inferior colliculus. *Brain Research*, *1181*, 21–29. https://doi.org/10.1016/j.brainres.2007.08.053

Indah Winarni, T., Chonchaiya, W., Adams, E., Au, J., Mu, Y., Rivera, S. M., Nguyen, D. V., & Hagerman, R. J. (2012). Sertraline May Improve Language Developmental Trajectory in Young Children with Fragile X Syndrome: A Retrospective Chart Review. *Autism Research and Treatment*, *2012*, 1–8. https://doi.org/10.1155/2012/104317

Juczewski, K., von Richthofen, H., Bagni, C., Celikel, T., Fisone, G., & Krieger, P. (2016). Somatosensory map expansion and altered processing of tactile inputs in a mouse model of fragile X syndrome. *Neurobiology of Disease*, *96*, 201–215. https://doi.org/10.1016/j.nbd.2016.09.007

Kaufmann, W. E., Cortell, R., Kau, A. S. M., Bukelis, I., Tierney, E., Gray, R. M., Cox, C., Capone, G. T., & Stanard, P. (2004). Autism spectrum disorder in fragile X syndrome: Communication, social interaction, and specific behaviors. *American*

Journal of Medical Genetics Part A, *129A*(3), 225–234. https://doi.org/10.1002/ajmg.a.30229

Lim, C.-S., Hoang, E. T., Viar, K. E., Stornetta, R. L., Scott, M. M., & Zhu, J. J. (2014). Pharmacological rescue of Ras signaling, GluA1-dependent synaptic plasticity, and learning deficits in a fragile X model. *Genes & Development*, *28*(3), 273–289. https://doi.org/10.1101/gad.232470.113

Llado-Pelfort, L., Santana, N., Ghisi, V., Artigas, F., & Celada, P. (2012). 5-HT1A Receptor Agonists Enhance Pyramidal Cell Firing in Prefrontal Cortex Through a Preferential Action on GABA Interneurons. *Cerebral Cortex*, *22*(7), 1487–1497. https://doi.org/10.1093/cercor/bhr220

Lovelace, J. W., Rais, M., Palacios, A. R., Shuai, X. S., Bishay, S., Popa, O., Pirbhoy, P. S., Binder, D. K., Nelson, D. L., Ethell, I. M., & Razak, K. A. (2020). Deletion of Fmr1 from Forebrain Excitatory Neurons Triggers Abnormal Cellular, EEG, and Behavioral Phenotypes in the Auditory Cortex of a Mouse Model of Fragile X Syndrome. *Cerebral Cortex*, *30*(3), 969–988. https://doi.org/10.1093/cercor/bhz141

Miller, L. J., McIntosh, D. N., McGrath, J., Shyu, V., Lampe, M., Taylor, A. K., Tassone, F., Neitzel, K., Stackhouse, T., & Hagerman, R. J. (1999). Electrodermal responses to sensory stimuli in individuals with fragile X syndrome: A preliminary report. *American Journal of Medical Genetics*, *83*(4), 268–279. https://doi.org/10.1002/(SICI)1096-8628(19990402)83:4<268::AID-AJMG7>3.0.CO;2-K

Musser, M. L., Viall, A. K., Phillips, R. L., Fasina, O., & Johannes, C. M. (2022). Prostaglandin EP4 receptor mRNA expression in canine lymphoma. *Veterinary and Comparative Oncology*, *20*(1), 127–133. https://doi.org/10.1111/vco.12753

Nguyen, A. O., Binder, D. K., Ethell, I. M., & Razak, K. A. (2020). Abnormal development of auditory responses in the inferior colliculus of a mouse model of Fragile X Syndrome. *Journal of Neurophysiology*, *123*(6), 2101–2121. https://doi.org/10.1152/jn.00706.2019

Peruzzi, D., & Dut, A. (2004). GABA, serotonin and serotonin receptors in the rat inferior colliculus. *Brain Research*, *998*(2), 247–250. https://doi.org/10.1016/j.brainres.2003.10.059

Pieretti, M., Zhang, F., Fu, Y.-H., Warren, S. T., Oostra, B. A., Caskey, C. T., & Nelson, D. L. (1991). Absence of expression of the *FMR-1* gene in fragile X syndrome. *Cell*, *66*(4), 817–822. https://doi.org/10.1016/0092-8674(91)90125-I

Quiquempoix, M., Fayad, S. L., Boutourlinsky, K., Leresche, N., Lambert, R. C., & Bessaih, T. (2018). Layer 2/3 Pyramidal Neurons Control the Gain of Cortical Output. *Cell Reports*, *24*(11), 2799-2807.e4. https://doi.org/10.1016/j.celrep.2018.08.038

Rigoulot, S., Knoth, I. S., Lafontaine, M., Vannasing, P., Major, P., Jacquemont, S., Michaud, J. L., Jerbi, K., & Lippé, S. (2017). Altered visual repetition suppression in Fragile X Syndrome: New evidence from ERPs and oscillatory activity. *International Journal of Developmental Neuroscience*, *59*(1), 52–59. https://doi.org/10.1016/j.ijdevneu.2017.03.008

Rojas, D. C., Benkers, T. L., Rogers, S. J., Teale, P. D., & Reite, M. L. (2001). *Auditory evoked magnetic Æelds in adults with fragile X syndrome*. 4.

Rotschafer, S., & Razak, K. (2013). Altered auditory processing in a mouse model of fragile X syndrome. *Brain Research*, *1506*, 12–24. https://doi.org/10.1016/j.brainres.2013.02.038

Saemundsen, E., Ludvigsson, P., Hilmarsdottir, I., & Rafnsson, V. (2007). Autism Spectrum Disorders in Children with Seizures in the First Year of Life-A Population-Based Study: *ASD FOLLOWING SEIZURES IN INFANCY*. *Epilepsia*, *48*(9), 1724–1730. https://doi.org/10.1111/j.1528-1167.2007.01150.x

Santana, N. (2004). Expression of Serotonin1A and Serotonin2A Receptors in Pyramidal and GABAergic Neurons of the Rat Prefrontal Cortex. *Cerebral Cortex*, *14*(10), 1100–1109. https://doi.org/10.1093/cercor/bhh070

Saraf, T. S., Chen, Y., Tyagi, R., & Canal, C. E. (2024). Altered brain serotonin 5-HT1A receptor expression and function in juvenile Fmr1 knockout mice. *Neuropharmacology*, *245*, 109774. https://doi.org/10.1016/j.neuropharm.2023.109774

Sinclair, D., Oranje, B., Razak, K. A., Siegel, S. J., & Schmid, S. (2017). Sensory processing in autism spectrum disorders and Fragile X syndrome—From the clinic to animal models. *Neuroscience & Biobehavioral Reviews*, *76*, 235–253. https://doi.org/10.1016/j.neubiorev.2016.05.029

Tao, X., Newman-Tancredi, A., Varney, M. A., & Razak, K. A. (2023). Acute and Repeated Administration of NLX-101, a Selective Serotonin-1A Receptor Biased

Agonist, Reduces Audiogenic Seizures in Developing Fmr1 Knockout Mice. *Neuroscience*, *509*, 113–124. https://doi.org/10.1016/j.neuroscience.2022.11.014

Thompson, G. C., Thompson, A. M., Garrett, K. M., & Britton, B. H. (1994). Serotonin and serotonin receptors in the central auditory system. *Otolaryngology–Head and Neck Surgery*, *110*(1), 93–102. https://doi.org/10.1177/019459989411000111

Uutela, M., Lindholm, J., RantamÃ¤ki, T., Umemori, J., Hunter, K., VÃµikar, V., & CastrÃ©n, M. L. (2014). Distinctive behavioral and cellular responses to fluoxetine in the mouse model for Fragile X syndrome. *Frontiers in Cellular Neuroscience*, *8*. https://doi.org/10.3389/fncel.2014.00150

Van der Molen, M. J. W., Van der Molen, M. W., Ridderinkhof, K. R., Hamel, B. C. J., Curfs, L. M. G., & Ramakers, G. J. A. (2012a). Auditory and visual cortical activity during selective attention in fragile X syndrome: A cascade of processing deficiencies. *Clinical Neurophysiology*, *123*(4), 720–729. https://doi.org/10.1016/j.clinph.2011.08.023

Van der Molen, M. J. W., Van der Molen, M. W., Ridderinkhof, K. R., Hamel, B. C. J., Curfs, L. M. G., & Ramakers, G. J. A. (2012b). Auditory change detection in fragile X syndrome males: A brain potential study. *Clinical Neurophysiology*, *123*(7), 1309–1318. https://doi.org/10.1016/j.clinph.2011.11.039

Wen, T. H., Lovelace, J. W., Ethell, I. M., Binder, D. K., & Razak, K. A. (2019). Developmental Changes in EEG Phenotypes in a Mouse Model of Fragile X Syndrome. *Neuroscience*, *398*, 126–143. https://doi.org/10.1016/j.neuroscience.2018.11.047

Winarni, T. I., Schneider, A., Borodyanskara, M., & Hagerman, R. J. (2012). Early Intervention Combined with Targeted Treatment Promotes Cognitive and Behavioral Improvements in Young Children with Fragile X Syndrome. *Case Reports in Genetics*, *2012*, 1–4. https://doi.org/10.1155/2012/280813

Chapter 5: Conclusion

Audiogenic seizures (AGS) are one of the most robust expressions of auditory hyperactivity in *Fmr1* KO mice. With a specific and highly selective serotonin-1A (5-HT_{1A}) post-synaptic receptor agonist, NLX-101, I found enhancing post-synaptic 5-HT_{1A} signaling is effective in reducing auditory hyperactive from the behavioral level: reducing AGS-induced death rate and decreasing general AGS severity in *Fmr1* KO in a dose-dependent manner. Besides, sex differences were revealed by the following evidence: 1) Untreated *Fmr1* KO females were less susceptible to AGS compared to male KOs; 2) *Fmr1* KO mice benefited from NLX-101 treatment at lower dose than male KOs. 3) Higher dose of 5-HT_{1A} receptor antagonists were needed to abolish beneficial effect of NLX-101 in *Fmr1* KO females than males. These data support for targeting post-synaptic 5-HT_{1A} receptors to reduce auditory hyperactivity in FXS at the behavioral level.

At the network level, auditory hyperacidity in *Fmr1* KO mice is marked by increased evoked auditory responses (indicated by increased N1 amplitude in ERP) toward auditory stimuli and increased non-phase locked power (shown by increased STP). Reduced temporal processing is manifestoed by decreased ITPC in response to temporally modulated auditory stimuli. Follow up on the previous finding, I found NLX-101 treatment improved temporal processing in *Fmr1* KO mice at both P21 and P30, suggested by increased ITPC in treatment groups. Besides, NLX-101 also reduced elevated STP in *Fmr1* KO mice but only at P30 not P21. However, no improvement was found regarding N1 amplitudes with NLX-101 treatment. These studies imply there might be an age-dependent effect on NLX-101 treatment. Besides, STP and ERP may have different mechanisms with most likely elevated synchrony playing a role in N1

amplitudes, and elevated responses playing a role in STP. Improved temporal processing at the network level following NLX-101 administration can be partially explained by finings in single unit recording where 5-HT_{1A} activation biased response more toward the timing that is close to stimulus onset (Hurley, 2007).

RNAscope was performed to examine 5-HT_{1A} receptor mRNA level in the AC and ICC across ages, sex, and genotypes. Data showed that 5-HT_{1A} mRNAs are predominately colocalized with non-GAD cells in both AC and ICC. Given that 5-HT_{1A} receptor is Gi protein coupled receptor and exerts hyperpolarizing effect on cells upon activation, I hypothesize NLX-101 reduces auditory hyperactivity by activating 5-HT_{1A} receptors on excitatory neurons. Besides, we also found 5-HT_{1A} receptor mRNA expression increases as age, suggesting a developmental regulation. Indeed, 5-HT_{1A} receptor modulation during early age is necessary to establish normal anxiety level in adulthood (Gross et al., 2002). Another interesting finding emerging from this study is *Fmr1* KO mice surprisingly showed higher level of 5-HT_{1A} receptor mRNA than WT specifically in AC layer 2/3, which implied a compensatory mechanism.

In conclusion, the presented results emphasized the importance of 5-HT_{1A} signaling in *Fmr1* KO mice during development and provided evidence for targeting post-synaptic 5-HT_{1A} receptor to ameliorate auditory hyperactivity and improve temporal processing in FXS or ASD generally.

There are several implications emerging from these studies. Firstly, EEG as a translational relevant technique can be used to evaluate potential treatment for FXS. The

manifestations of auditory hyperactivity and reduced temporal processing at the network level have widely and consistently reported in FXS individual and *Fmr1* KO mice. The promising results seen in the current studies with *Fmr1* KO mice have prompted future clinic trials in humans with FXS. Secondly, the presented studies have shown enhancing 5-HT_{1A} signaling during early development is beneficial for *Fmr1* KO mice. Besides, normal 5-HT_{1A} signaling during early development is necessary to establish normal anxiety level in adulthood (Gross et al., 2002). Together, the current studies and published work by others strongly appeal for early serotonin intervention in FXS to maximize benefits. Lastly, abnormal sensory processing has been implicated in sensory-related cognition decline (Haigh, 2018). In these studies, improved sensory processing has been observed in *Fmr1* KO mice following NLX-101 treatment, which suggests that early intervention with NLX-101 may not only improve sensory processing itself but may also prevent sensory related cognitive deficits.

Despite exciting results in the current research, the following limitations should be considered. In the studies presented in Chapter 2 and Chapter 3, NLX-101 was given systemically. Therefore, we could not point out which brain region(s) is(are) necessary for NLX-101 to show effects. In Chapter 4, RNAscope was performed in two cell types: GAD positive and GAD negative. Considering glial cells also express 5-HT_{1A} receptors (Azmitia et al., 1996), future studies are required to directly characterize 5-HT_{1A} receptors mRNA expression level in excitatory neurons with excitatory markers.

Even though we found enhancing 5-HT_{1A} signaling by NLX-101 is beneficial in ameliorating auditory hyperactivity and improving auditory temporal processing in *Fmr1*

KO mice, it does not immediately suggest that the reduced serotonin modulation is the cause of the abnormal sensory processing in FXS. It is probable that reduced serotonin modulation occurs because of lack of FMRP, and itself is not the causation of altered sensory processing. Yet, abnormal sensory processing can be ameliorated by restoring such modulation via administering serotonin receptor agonists.

Overall, my work implied that serotonin modulation may be disrupted in *Fmr1* KO mice. However, to further confirm such correlation, the following future directions should be considered. Firstly, so far there is no evidence showing expression of 5-HT_{1A} receptors is directly under regulation of FMRP. It needs to be confirmed whether subunits of 5-HT_{1A} receptors are under regulation of FMRP directly or indirectly. Secondly, future work needs to examine if 5-HT_{1A} receptors efficacy in vivo is altered in *Fmr1* KO mice. Thirdly, serotonin release was found increased in the cortex during seizures (Deng et al., 2024). Therefore, it is interesting for future studies to explore if serotonin release in AC and/ or IC is altered in *Fmr1* KO mice in response to AGS stimulation. Lastly, Future work should investigate whether there are specific brain regions that are targeted by NLX-101 to show benefits in normalizing auditory processing in *Fmr1* KO mice.

References

Azmitia, E. C., Gannon, P. J., Kheck, N. M., & Whitaker-Azmitia, P. M. (1996). *Cellular Localization of the 5-HTIA Receptor in Primate Brain Neurons and Glial Cells*.

Deng, F., Wan, J., Li, G., Dong, H., Xia, X., Wang, Y., Li, X., Zhuang, C., Zheng, Y., Liu, L., Yan, Y., Feng, J., Zhao, Y., Xie, H., & Li, Y. (2024). Improved green and red GRAB sensors for monitoring spatiotemporal serotonin release in vivo. *Nature Methods*, *21*(4), 692–702. https://doi.org/10.1038/s41592-024-02188-8

Gross, C., Zhuang, X., Stark, K., Ramboz, S., Oosting, R., Kirby, L., Santarelli, L., Beck, S., & Hen, R. (2002). Serotonin1A receptor acts during development to establish normal anxiety-like behaviour in the adult. *Nature*, *416*(6879), 396–400. https://doi.org/10.1038/416396a

Haigh, S. M. (2018). Variable sensory perception in autism. *European Journal of Neuroscience*, *47*(6), 602–609. https://doi.org/10.1111/ejn.13601

Hurley, L. M. (2007). Activation of the serotonin 1A receptor alters the temporal characteristics of auditory responses in the inferior colliculus. *Brain Research*, *1181*, 21–29. https://doi.org/10.1016/j.brainres.2007.08.053